5. Results at CLTP

The stress intensities and associated stress ratios resulting from the Rev. 4 acoustic/hydrodynamic loads [3] with associated biases and uncertainties factored in, are presented below. The bias due to finite frequency discretization and uncertainty associated with the finite element model itself, are also factored in. In the following sections the highest maximum and alternating stress intensities are presented to indicate which points on the dryer experience significant stress concentration and/or modal response (Section 5.1). The lowest stress ratios obtained by comparing the stresses against allowable values, accounting for stress type (maximum and alternating) and location (on or away from a weld), are also reported (Section 5.2). Finally the frequency dependence of the stresses at nodes experiencing the lowest stress ratios is depicted in the form of accumulative PSDs (Section 5.3).

In each section results are presented both at nominal conditions (no frequency shift) and with frequency shift included. Unless specified otherwise, frequency shifts are generally performed at 2.5% increments. The tabulated stresses and stress ratios are obtained using a 'blanking' procedure that is designed to prevent reporting a large number of high stress nodes from essentially the same location on the structure. In the case of stress intensities this procedure is as follows. The relevant stress intensities are first computed at every node and then nodes sorted according to stress level. The highest stress node is noted and all neighboring nodes within 10 inches of the highest stress node and its symmetric images (i.e., reflections across the x=0 and y=0 planes) are "blanked" (i.e., excluded from the search for subsequent high stress locations). Of the remaining nodes, the next highest stress node is identified and its neighbors (closer than 10 inches) blanked. The third highest stress node is similarly located and the search continued in this fashion until all nodes are either blanked or have stresses less than half the highest value on the structure. For stress ratios, an analogous blanking procedure is applied. Thus the lowest stress ratio of a particular type in a 10" neighborhood and its symmetric images is identified and all other nodes in these regions excluded from listing in the table. Of the remaining nodes, the one with the lowest stress ratio is reported and its neighboring points similarly excluded, and so on until all nodes are either blanked or have a stress ratio higher than 4.

The measured CLTP strain gage signals contain significant contributions from non-acoustic sources such as sensor noise, MSL turbulence and pipe bending vibration that contribute to the hoop strain measurements. The ACM analysis does not distinguish between the acoustic and non-acoustic fluctuations in the MSL signals that could lead to sizeable, but fictitious acoustic loads and resulting stresses on the dryer. One way to remove these fictitious loads is to collect data with the system maintained at operating pressure (1000 psi) and temperature, but low (less than 20% of CLTP) flow. By operating the recirculation pumps at this condition, the background plant noise and vibrations remain present. At these conditions the acoustic loads are known to be negligible so that collected data, referred to as the 1000# data, originate entirely from non-acoustic sources such as sensor noise and mechanical vibrations. This information is valuable since it allows one to now distinguish between the acoustic and non-acoustic content in the CLTP signal and therefore modify the CLTP loads so that only the acoustic component is retained. For consistency, the 1000# strain gage signals are filtered in the same manner as the CLTP data and are fed into the ACM model to obtain the monopole and dipole signals at the MSL inlets. Since there is negligible flow, these signals are fictitious, i.e., the hoop strains

measured by the strain gages are not due to pressure fluctuations, but rather due to noise. However, under the supposition that these signals are acoustic in origin the hypothetical stresses due to these signals can nevertheless be computed.

The contribution of background noise in the Browns Ferry Unit 2 steam dryer was quantified by taking strain gage measurements at 5% power. Measurements taken for the BFN2 unit at increasing power levels indicate that the 5% signal measurements provide a conservative estimate of the noise at zero power [24]. At this level there are no significant acoustic sources. To compensate for the non-acoustic noise source represented in the 1000# data, the CLTP MSL inlet pressure signals are modified according to [24]:

$$P(f) = P_0(f) * \max\left[0.5, 1 - \frac{\bar{N}(f)}{\bar{P}_0(f)}\right] \tag{8}$$

where f is the frequency (in Hz), $P_0(f)$ is the MSL inlet pressure (monopole or dipole) at CLTP conditions before correction, P(f) is the corresponding post-correction pressure and $\bar{N}(f)$ and $\bar{P}_0(f)$ are averaged pressure amplitudes associated with the 1000# data and CLTP data respectively. Specifically,

$$\bar{P}_0(f) = \frac{1}{2}\int_{f-1}^{f+1} |P_0(f)|\, df \tag{9}$$

where $|P_0(f)|$ denotes the absolute value of the complex quantity. Hence $\bar{P}_0(f)$ is the average amplitude of the CLTP pressure in the ±1 Hz interval about frequency, f. The same definition, but using the 1000# pressure signal, is used for $\bar{N}(f)$. Note that this modification leaves the phase information in the original CLTP signal unchanged.

The applied load includes all biases and uncertainties for both the ACM (summarized in [3]) and the FEM. For the latter there are three main contributors to the bias and uncertainty. The first is an uncertainty (25.26%) that accounts for modeling idealizations (e.g., vane bank mass model), geometrical approximations and other discrepancies between the modeled and actual dryer such as neglecting of weld mass and stiffness in the FEA. The second contributor is a bias (9.53% - note that this has been increased from the 5.72% value previously used in [5]) accounting for discretization errors associated with using a finite size mesh, upon computed stresses. The third contributor is also a bias and compensates for the use of a finite discretization schedule in the construction of the unit solutions. The frequencies are spaced such that at 1% damping the maximum (worst case) error in a resonance peak is 5%. The average error for this frequency schedule is 1.72%.

5.1 General Stress Distribution and High Stress Locations

The maximum stress intensities obtained by post-processing the ANSYS stress histories for CLTP at nominal frequency and with frequency shift operating conditions are listed in Table 7. Contour plots of the stress intensities over the steam dryer structure are shown on Figure 11 (nominal frequency) and Figure 12 (maximum stress over all nine frequency shifts including

nominal). The figures are oriented to emphasize the high stress regions. Note that these stress intensities *do not* account for weld factors but include end-to-end bias and uncertainty and incorporate results from submodeling (see Section 4.5). Further, it should be noted that since the allowable stresses vary with location, stress intensities do not necessarily correspond to regions of primary structural concern. Instead, structural evaluation is more accurately made in terms of the stress ratios which compare the computed stresses to allowable levels with due account made for stress type and weld factors and also account for stress corrections obtained using high-detail solid element submodels. Comparisons on the basis of stress ratios are made in Section 5.2.

The maximum stress intensities in most areas are low (less than 500 psi, or 5% of the most conservative critical stress). For the membrane stresses (Pm) the high stress regions tend to occur at: (i) the restraint locations for the upper support ring and (ii) the upper edges of the closure plates. The first location is a very localized stress location and is believed to be significantly overestimated as a 'hot-spot' in the FEA. It experiences high stresses since the entire weight of the structure is transmitted through relatively small pads to the external structure. This stress is dominated by the static component. The closure plates experience high stresses since they restrain any motion of the adjacent vane banks. Another location with Pm>3000 psi is the junction between the bottom edge of the inner hood, hood support and middle base plate. Frequency shifting does not significantly alter the high Pm stress locations, again due to the dominance of the static (deadweight) load.

The membrane + bending stress (Pm+Pb) distributions evidence a stronger modal response. Stress concentrations are observed at several locations coinciding with welds. The first pair of highest stress locations is the same as where for the highest membrane stresses and lies near the dryer supports. Note that these stresses occur in solid elements where no distinction is made between the membrane and bending stresses (this distinction is only appropriate for thin members such as shell and beam elements). The next set of locations (exemplified by the 3rd and 4th entries in Table 7a) involves the closure plate connections to the hoods or vane bank end plates. These stresses also appear to be dominated by the static component since alternating stresses are comparatively low. The drain channel/skirt weld shows up as the 5th entry in Table 7a and the 4th entry in Table 7b. These stresses contain a strong alternating stress contribution as discussed below. Other locations where Pm+Pb stresses exceed the 4000 psi level include the bottom corners of the outer hood (involving a weld) and the middle plate which has a dominant unsteady stress component.

The alternating stress distributions in Figure 11 and Figure 12 indicate that these stresses are below 500 psi over most of the dryer. The submerged skirt, though not exposed to direct acoustic forcing, evidences a modal response due to coupling with the upper steam dryer structure subjected to acoustic loads. The highest alternating stress intensities occur on the large middle plate spanning the dryer at its center section where it is restrained by the tie bars. The restraint consists of groove that slips over the plate surface, but does not involve a weld. Other nodes appearing in the Table 7b include: (i) the tie bar connecting the outer and middle hoods where it lands on the outer hood top cover plate and; (ii) the top of the weld joining the steam dam and the gusset. The latter location becomes limiting at EPU and reflects the fact that the entire steam dam exhibits a strong response as seen in the plots. Although bending stresses are relatively high, the stresses transmitted through the weld are much smaller. This is because the

gusset carries a comparatively small moment and thus essentially rides along steam dam but does not transmit a significant bending stress to it. This is confirmed with 3D modeling (Appendix A) where the stress lines in the steam dam remain parallel to the steam dam surface rather than flowing through the weld. Other locations with alternating stress intensities above 1500 psi when all frequency shifts are considered include: the USR/seismic block connection, the front edge of the new gusset base where it meets the outer hood, the bottoms of the skirt/drain channel welds and tops of the closure plates where they join to the hoods or vane banks.

Finally, for reference the highest stress intensities at any frequency shift for the locations in Table 7b are recomputed using the CLTP loads without noise removal and reported in Table 7c. For these entries. the alternating stress changes obtained with noise retained are less than 12.4%.

Table 7a. Locations with highest predicted stress intensities at CLTP conditions at zero frequency shift. Signal noise has been removed using 5% power data.

Stress Category	Location	Weld	Location (in)(a)			node(b)	Stress Intensities (psi)		
			x	y	z		Pm	Pm+Pb	S_{alt}
Pm	Upper Support Ring (USR)/Seismic Block/Support Part	No	122.1	-10	-9.5	122998	7399	7399	1521
"	USR part/Support/Support Part	No	7	122.3	-9.5	123070	6274	6274	1141
"	Top Cover Inner Hood/Middle Closure Plate/Inner Hood	Yes	31.5	108.4	88.9	100230	5536	6121	751
"	Top Cover Middle Hood/Outer Closure Plate/Middle Hood	Yes	-62.5	85	88.9	100958	3804	4236	1392
"	Splice Bar/USR Part	Yes	-2.2	-119	0	123237	3746	3746	275
Pm+Pb	USR/Seismic Block/Support Part	No	122.1	-10	-9.5	122998	7399	7399	1521
"	USR part/Support/Support Part	No	7	122.3	-9.5	123070	6274	6274	1141
"	Top Cover Inner Hood/Middle Closure Plate/Inner Hood	Yes	-31.5	-108.4	88.9	101498	5381	6206	693
"	Top Cover Middle Hood/Outer Closure Plate/Middle Hood	Yes	-62.5	85	88.9	100958	3804	4236	1392
"	Submerged Drain Channel/Skirt	Yes	91	-76.7	-98.5	97969	271	4093	678
S_{alt}	Mid Plate/Tie Bar	No	0	-3	88.9	102956	411	2939	2250
"	Mid Plate/Tie Bar	No	0	-56.8	88.9	99311	734	3089	2246
"	Dam Plate/New Gusset(e)	Yes	77	31.4	104.4	92392	242	1849	1652
"	Dam Plate/New Gusset	Yes	77	58.2	101.4	104386	125	1665	1625
"	Old Hood Overlap/Gusset Pad Thin	Yes	93.5	58	88.9	92981	184	2205	1625

Notes for Table 7 and Table 8.

(a) Spatial coordinates are in a reference frame whose origin is located at the intersection of the steam dryer centerline and the plane containing the base plates (this plane also contains the top of the upper support ring and the bottom edges of the hoods). The y-axis is parallel to the hoods, the x-axis is normal to the hoods pointing from MSL C/D to MSL A/B, and the z-axis is vertical, positive up.

(b) Node numbers are retained for further reference.

(c) In accordance with [23], the nominal stress intensities at the drain channel/skirt junction are multiplied by 0.58.

(d) In accordance with [23], the nominal stress intensities at the inner hood/hood support/middle base plate junction are multiplied by 0.79.

(e) In accordance with Appendix A, the nominal stress intensities at the top of the steam dam/new gusset weld are multiplied by 0.82.

Table 7b. Locations with highest predicted stress intensities taken over all frequency shifts at CLTP conditions. Signal noise has been removed using 5% power data.

Stress Category	Location	Weld	Location (in)[a]			node[b]	Stress Intensities (psi)			% Freq. Shift
			x	y	z		Pm	Pm+Pb	S_{alt}	
Pm	USR/Seismic Block/Support Part	No	122.1	-10	-9.5	122998	7520	7520	1850	5
"	USR part/Support/Support Part	No	7	122.3	-9.5	123070	6522	6522	1390	-2.5
"	Top Cover Inner Hood/Middle Closure Plate/Inner Hood	Yes	31.5	108.4	88.9	100230	5826	6458	1026	5
"	Top Cover Middle Hood/Outer Closure Plate/Middle Hood	Yes	62.5	-85	88.9	106443	3876	4189	1628	2.5
"	Splice Bar/USR Part	Yes	-2.2	-119	0	123237	3861	3861	383	7.5
Pm+Pb	USR/Seismic Block/Support Part	No	122.1	-10	-9.5	122998	7520	7520	1850	5
"	USR part/Support/Support Part	No	7	122.3	-9.5	123070	6522	6522	1390	-2.5
"	Top Cover Inner Hood/Middle Closure Plate/Inner Hood	Yes	31.5	108.4	88.9	100230	5826	6458	1026	5
"	Submerged Drain Channel/Skirt	Yes	91	-76.7	-98.5	97969	309	4683	1359	-7.5
"	Submerged Drain Channel/Skirt[c]	Yes	91	-76.7	-100.5	98197	871	4267	1261	10
S_{alt}	Mid Plate/Tie Bar	No	0	-3	88.9	102956	673	3937	3254	2.5
"	Mid Plate/Tie Bar	No	0	-56.8	88.9	99311	807	3294	2393	10
"	Top Cover Middle Hood/Middle Hood/Tie Bar	Yes	-62.5	-25.2	88.9	101376	1007	2165	2029	-7.5
"	USR/Seismic Block/Support Part	No	122.1	-10	-9.5	122998	7520	7520	1850	5
"	Dam Plate/New Gusset[e]	Yes	77	31.4	104.4	92392	262	1986	1836	2.5

See Table 7a for notes (a)-(e).

Table 7c. Highest stress intensities at any frequency shift for the nodes listed in Table 7b computed using the unfiltered CLTP loads (i.e., signal noise has *not* been removed).

Stress Category	Location	Weld	Location (in)[a]			node[b]	Stress Intensities (psi)			% Freq. Shift
			x	y	z		Pm	Pm+Pb	S_{alt}	
Pm	USR/Seismic Block/Support Part	No	122.1	-10	-9.5	122998	7587	7587	1956	10
"	USR part/Support/Support Part	No	7	122.3	-9.5	123070	6550	6550	1447	-2.5
"	Top Cover Inner Hood/Middle Closure Plate/Inner Hood	Yes	31.5	108.4	88.9	100230	5960	6620	1193	10
"	Top Cover Middle Hood/Outer Closure Plate/Middle Hood	Yes	62.5	-85	88.9	106443	4217	4495	1964	2.5
"	Splice Bar/USR Part	Yes	-2.2	-119	0	123237	3878	3878	401	7.5
Pm+Pb	USR/Seismic Block/Support Part	No	122.1	-10	-9.5	122998	7587	7587	1956	10
"	USR part/Support/Support Part	No	7	122.3	-9.5	123070	6550	6550	1447	-2.5
"	Top Cover Inner Hood/Middle Closure Plate/Inner Hood	Yes	31.5	108.4	88.9	100230	5960	6620	1193	10
"	Submerged Drain Channel/Skirt	Yes	91	-76.7	-98.5	97969	328	4853	1507	-7.5
"	Submerged Drain Channel/Skirt[c]	Yes	91	-76.7	-100.5	98197	936	4344	1369	10
S_{alt}	Mid Plate/Tie Bar	No	0	-3	88.9	102956	764	4442	3655	-10
"	Mid Plate/Tie Bar	No	0	-56.8	88.9	99311	858	3561	2670	10
"	Top Cover Middle Hood/Middle Hood/Tie Bar	Yes	-62.5	-25.2	88.9	101376	1037	2383	2259	-7.5
"	USR/Seismic Block/Support Part	No	122.1	-10	-9.5	122998	7587	7587	1956	5
"	Dam Plate/New Gusset[e]	Yes	77	31.4	104.4	92392	239	1778	1659	2.5

See Table 7a for notes (a)-(e).

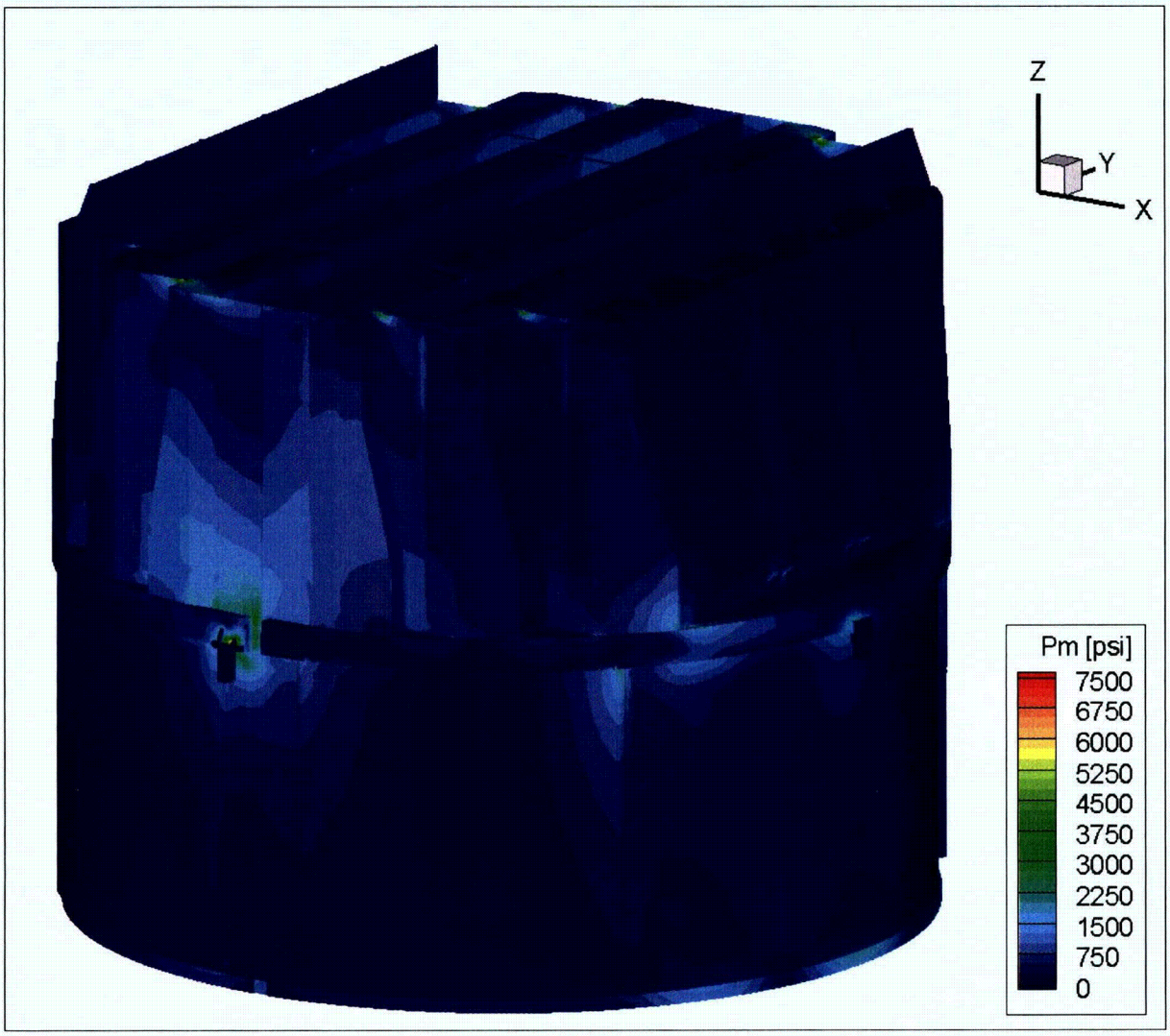

Figure 11a. Contour plot of maximum membrane stress intensity, Pm, for CLTP load. The maximum stress intensity is 7399 psi. First view.

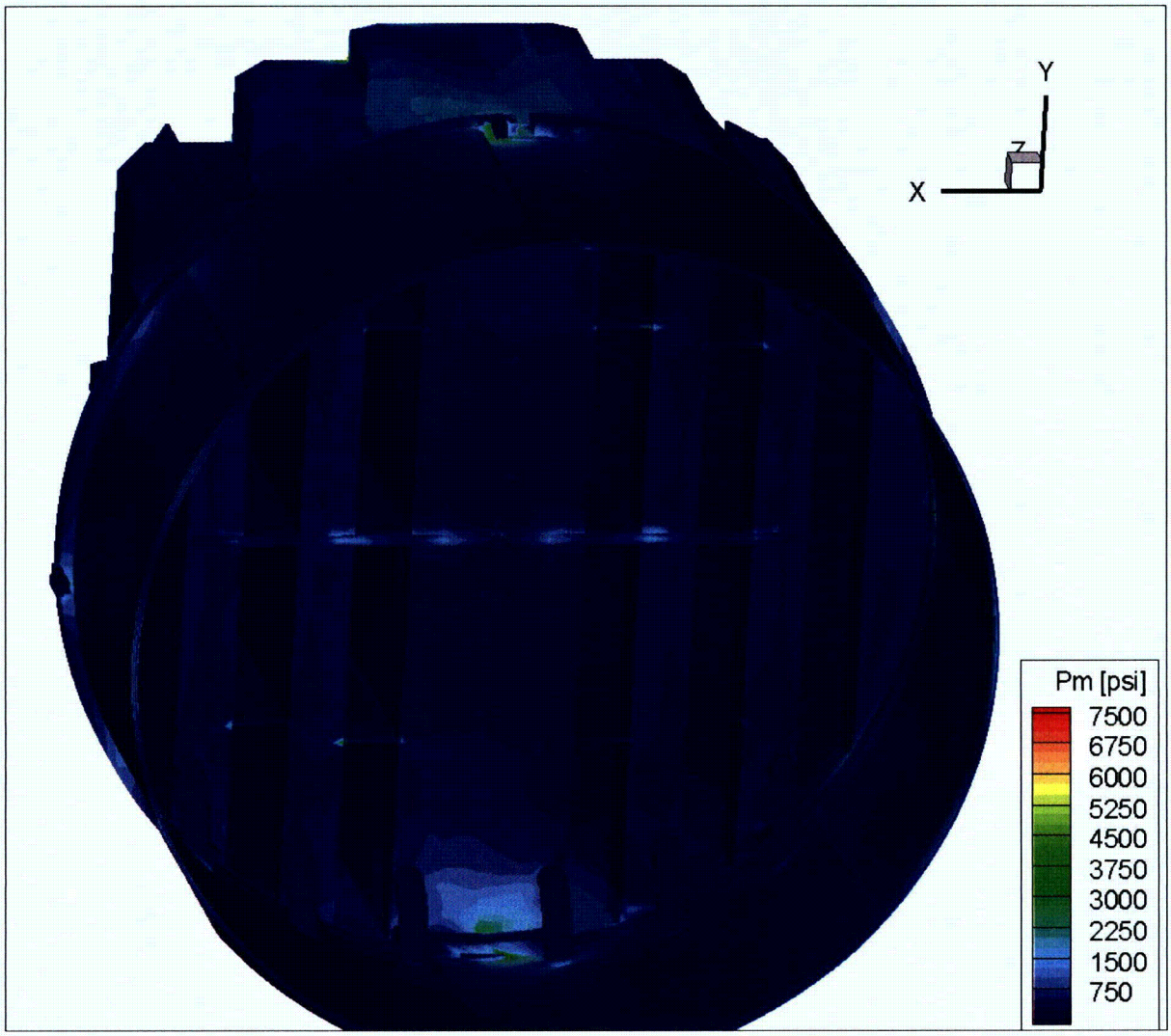

Figure 11b. Contour plot of maximum membrane stress intensity, Pm, for CLTP load. Second view from below.

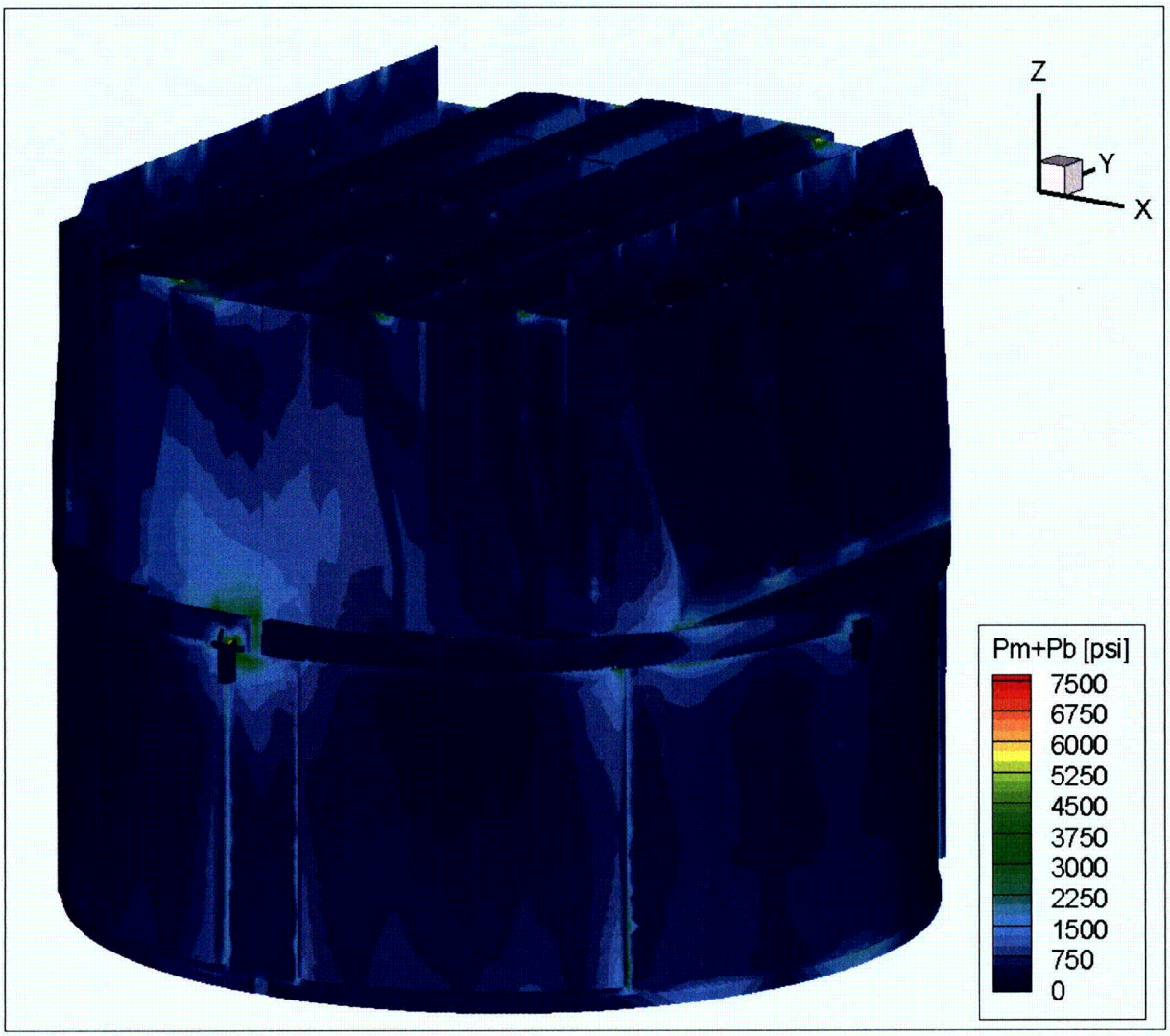

Figure 11c. Contour plot of maximum membrane+bending stress intensity, Pm+Pb, for CLTP load. The maximum stress intensity is 7399 psi. First view.

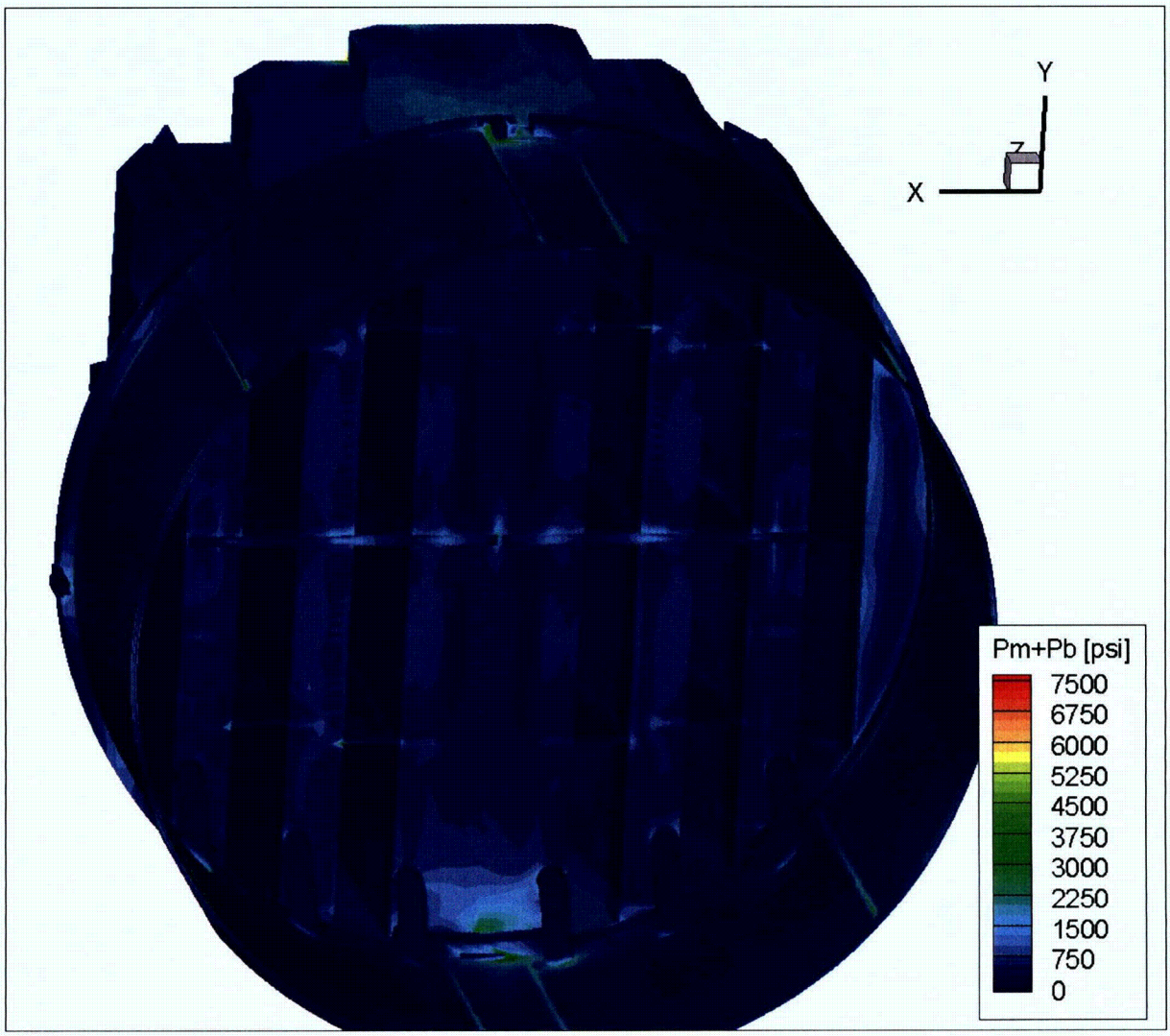

Figure 11d. Contour plot of maximum membrane+bending stress intensity, Pm+Pb, for CLTP load. Second view from below.

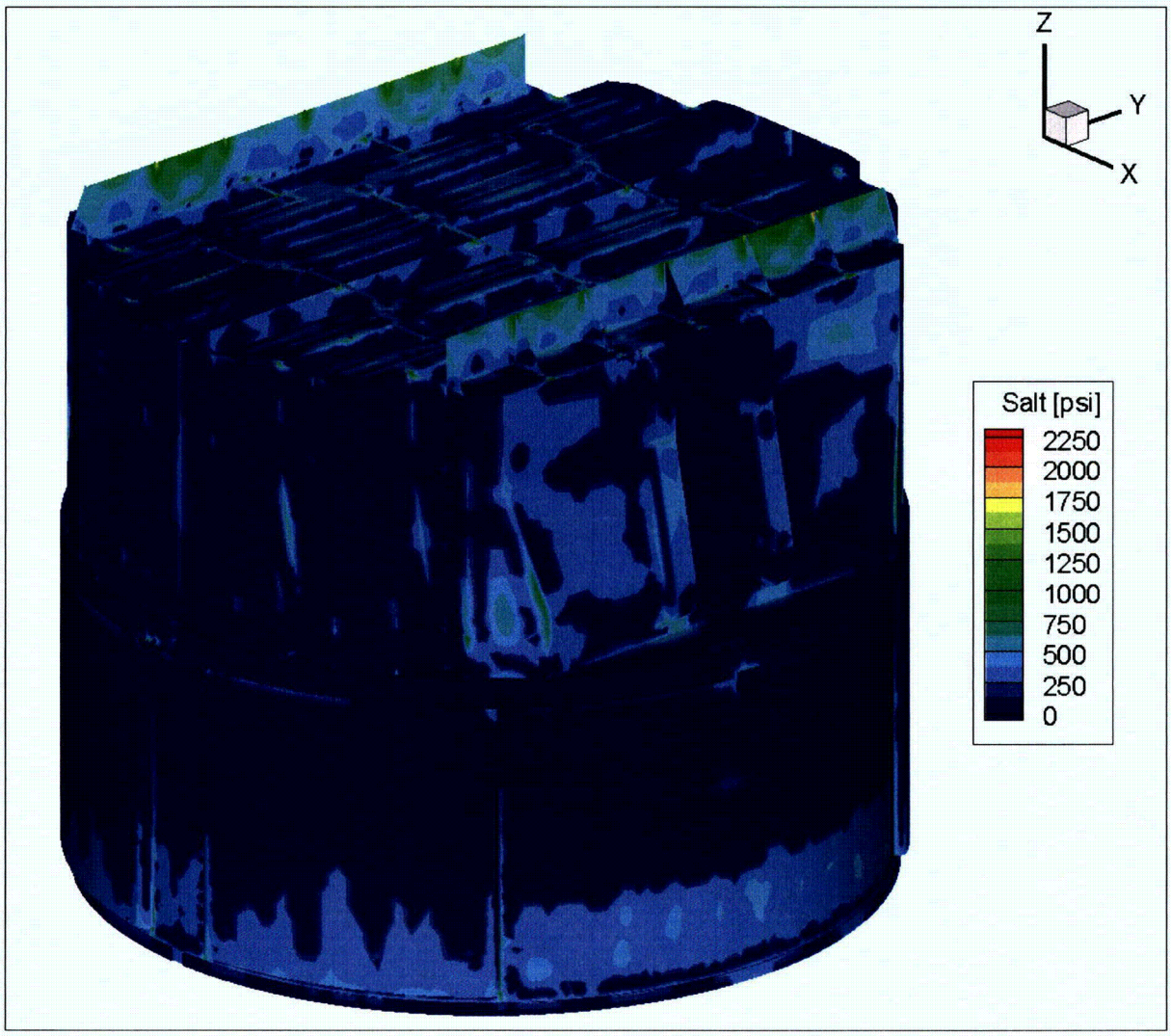

Figure 11e. Contour plot of alternating stress intensity, S_{alt}, for CLTP load. The maximum alternating stress intensity is 2250 psi.

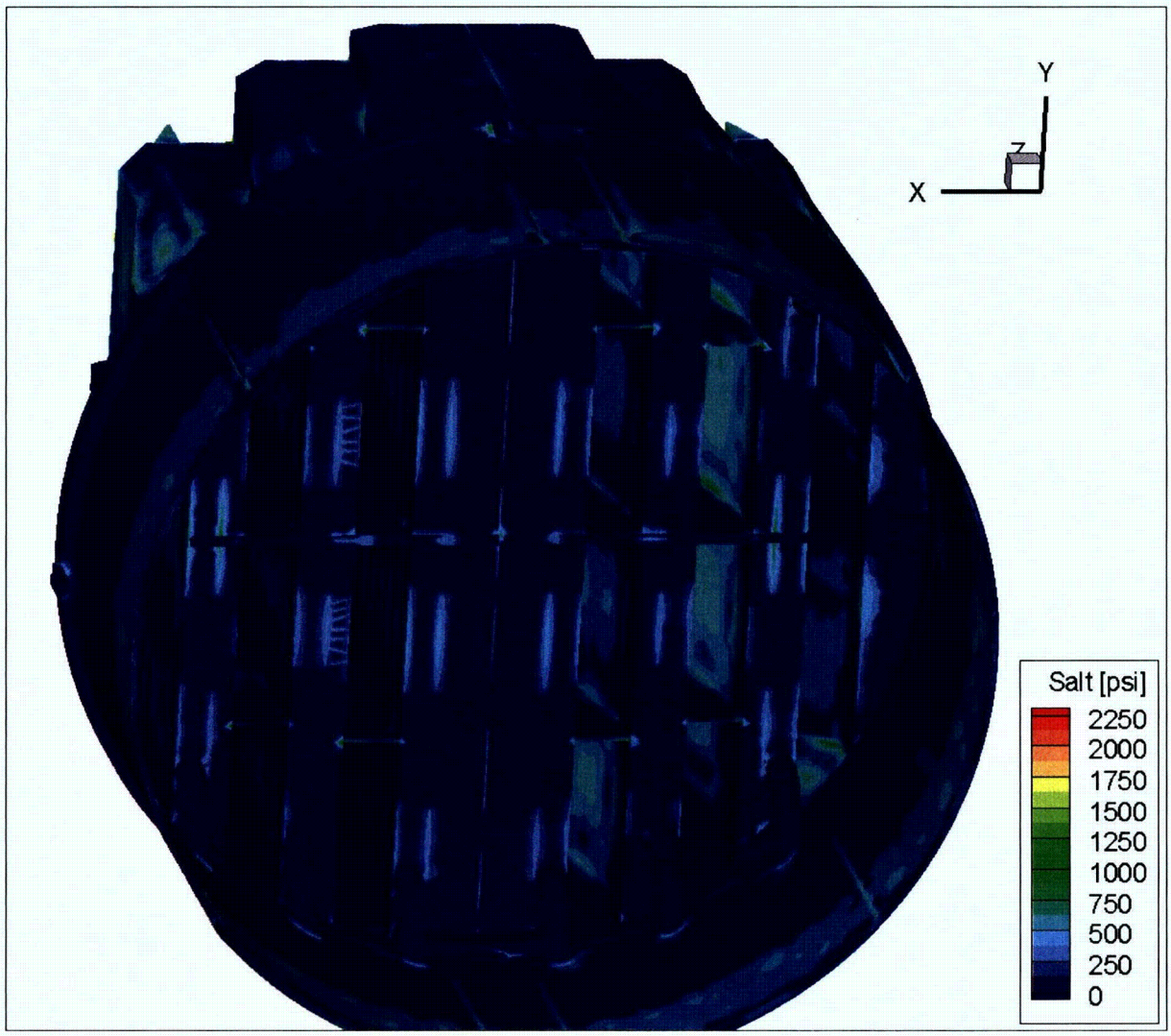

Figure 11f. Contour plot of alternating stress intensity, S_{alt}, for CLTP load. Second view from below.

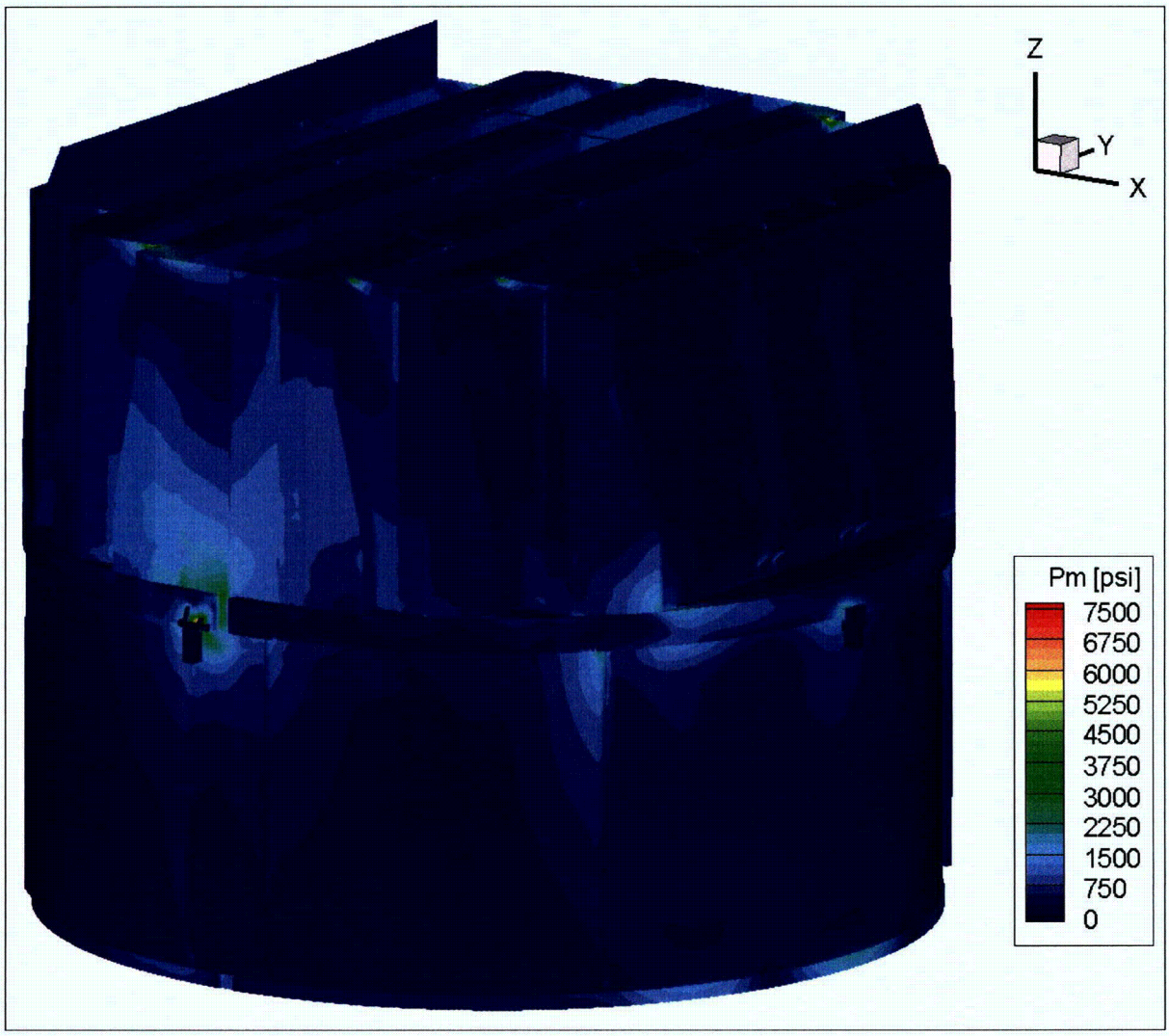

Figure 12a. Contour plot of maximum membrane stress intensity, Pm, for CLTP operation with frequency shifts. The recorded stress at a node is the maximum value taken over all frequency shifts. The maximum stress intensity is 7520 psi.

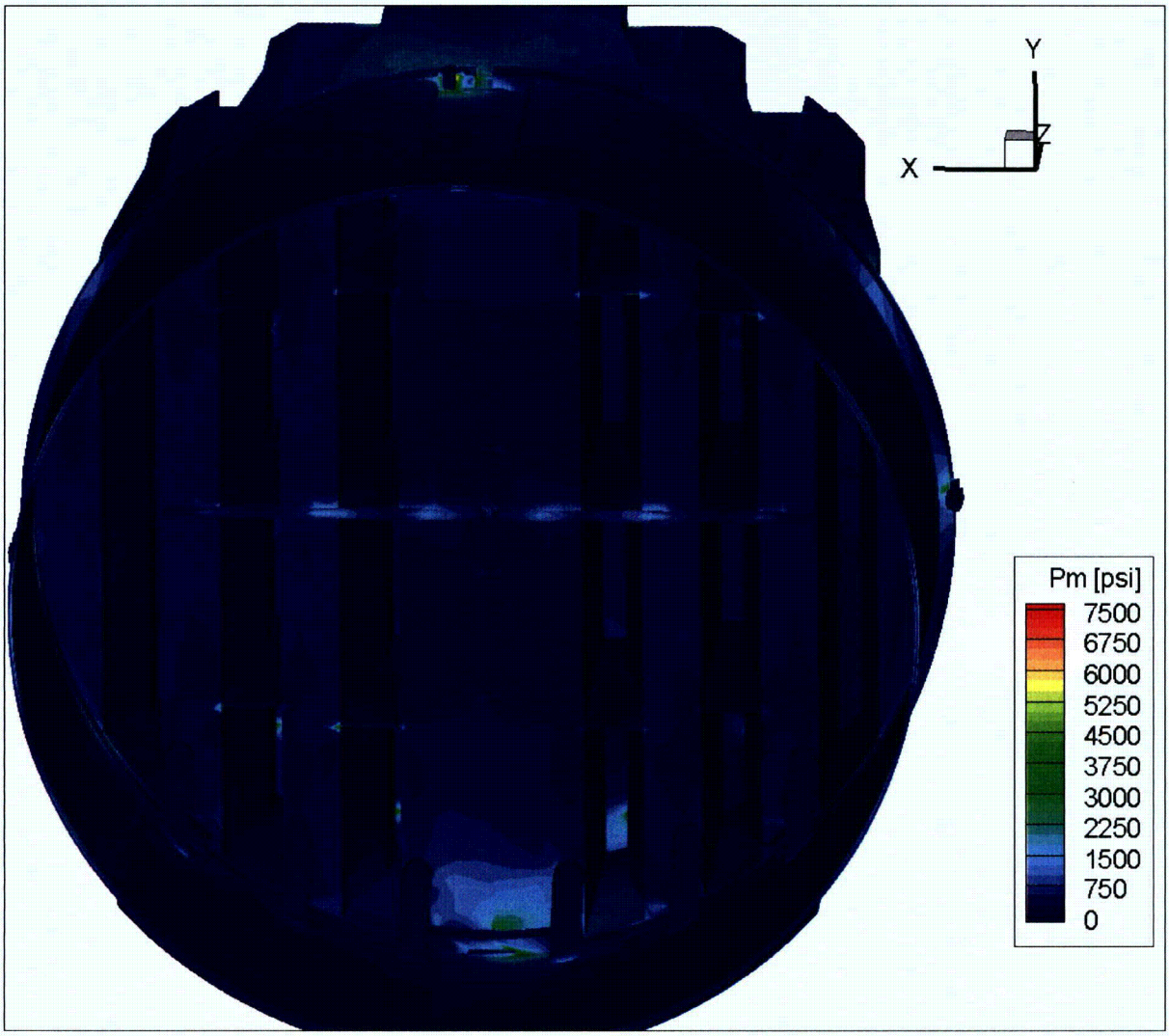

Figure 12b. Contour plot of maximum membrane stress intensity, Pm, for CLTP operation with frequency shifts. The recorded stress at a node is the maximum value taken over all frequency shifts. Second view from below.

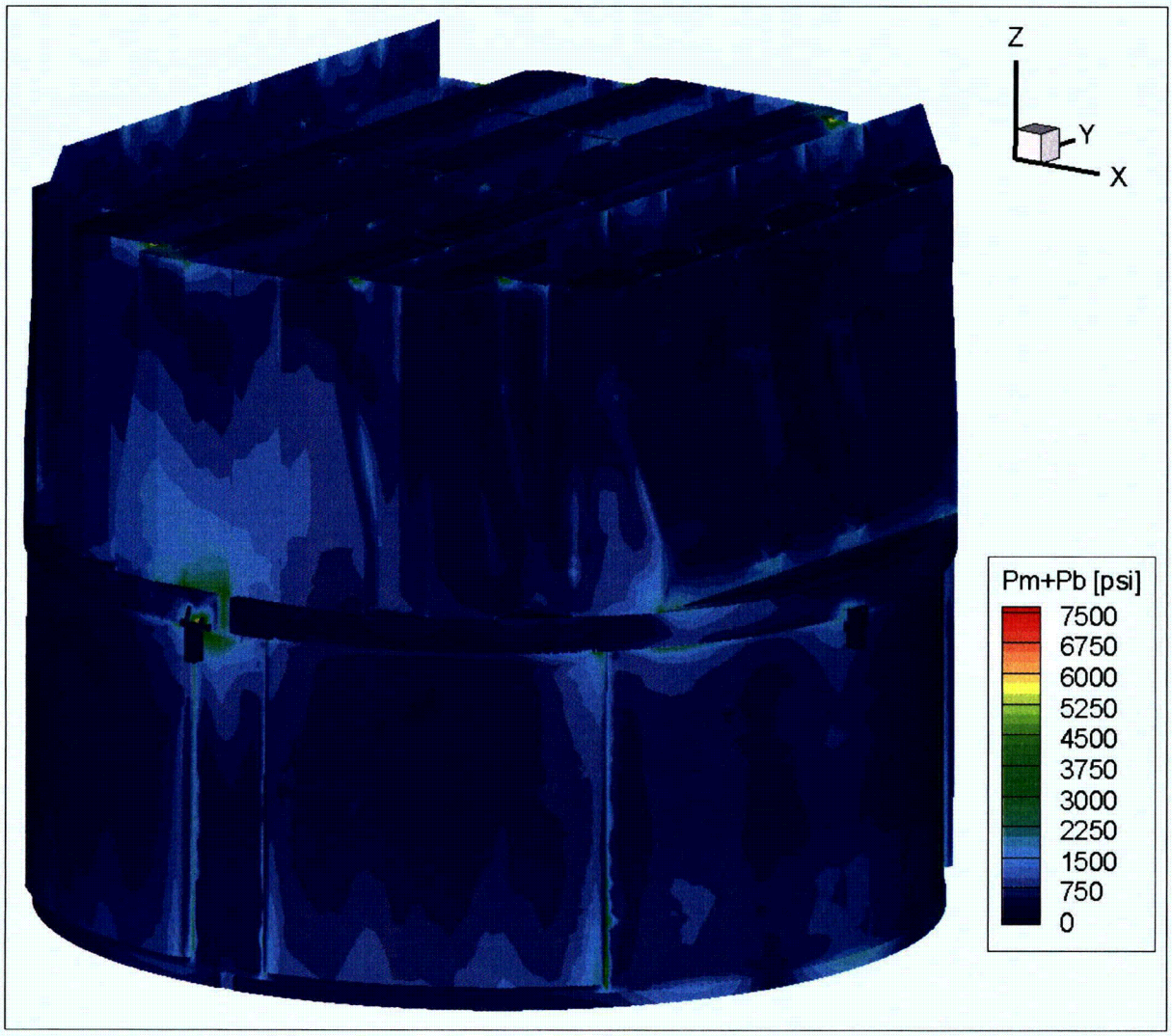

Figure 12c. Contour plot of maximum membrane+bending stress intensity, Pm+Pb, for CLTP operation with frequency shifts. The recorded stress at a node is the maximum value taken over all frequency shifts. The maximum stress intensity is 7520 psi. First view.

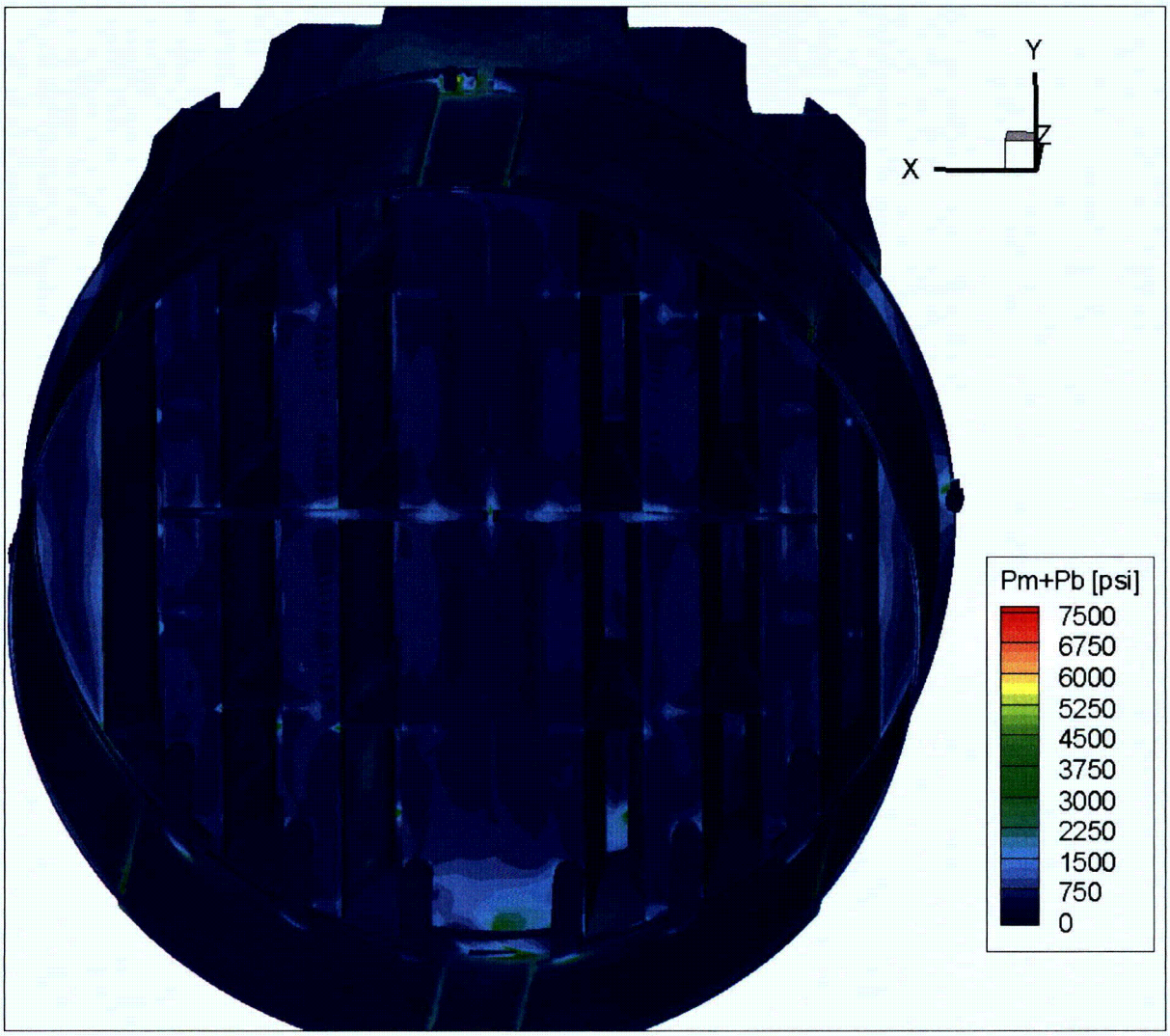

Figure 12d. Contour plot of maximum membrane+bending stress intensity, Pm+Pb, for CLTP operation with frequency shifts. This second view from beneath reveals high stress and modal response of interior hood supports.

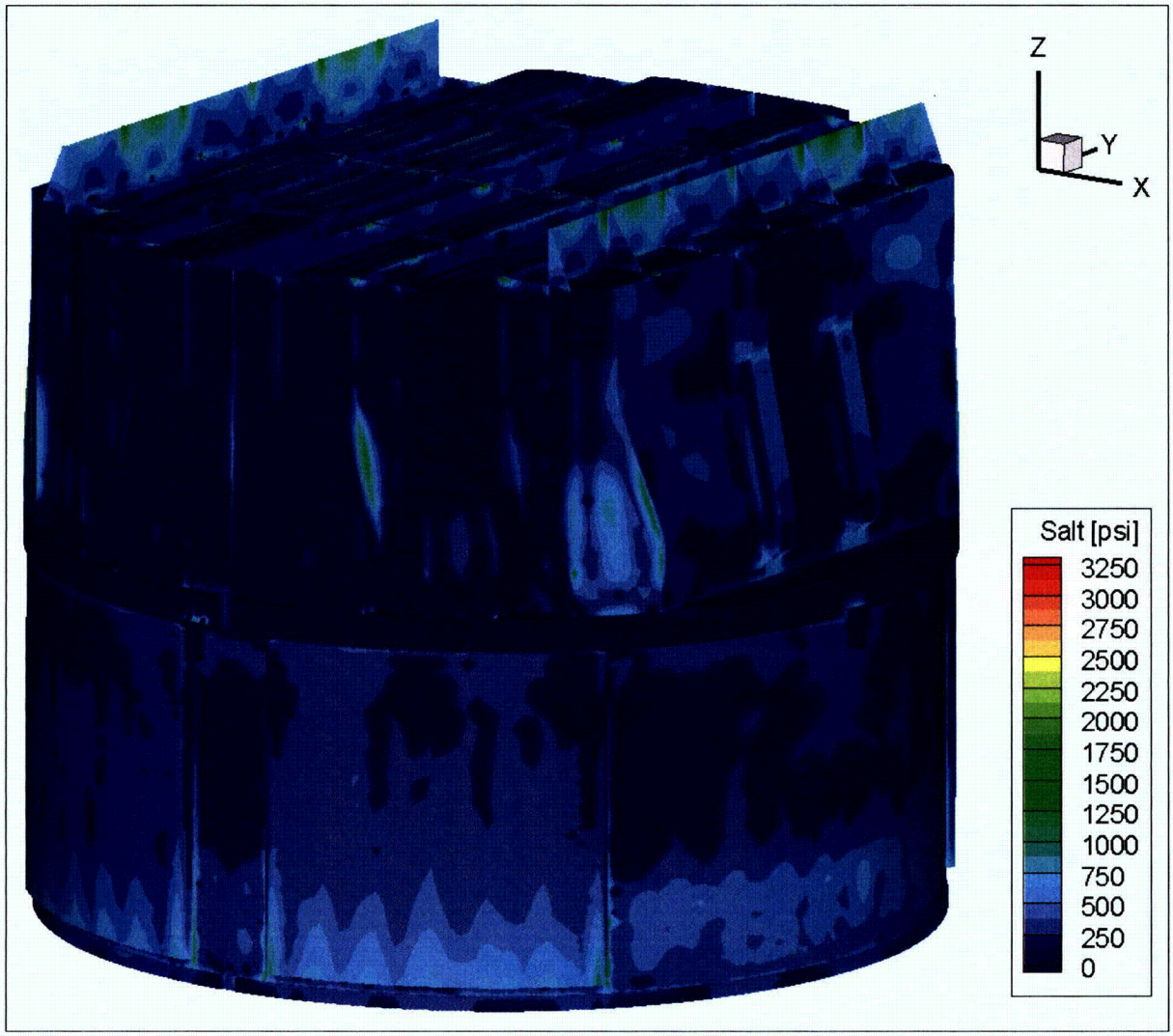

Figure 12e. Contour plot of alternating stress intensity, S_{alt}, for CLTP operation with frequency shifts. The recorded stress at a node is the maximum value taken over all frequency shifts. The maximum alternating stress intensity is 3254 psi.

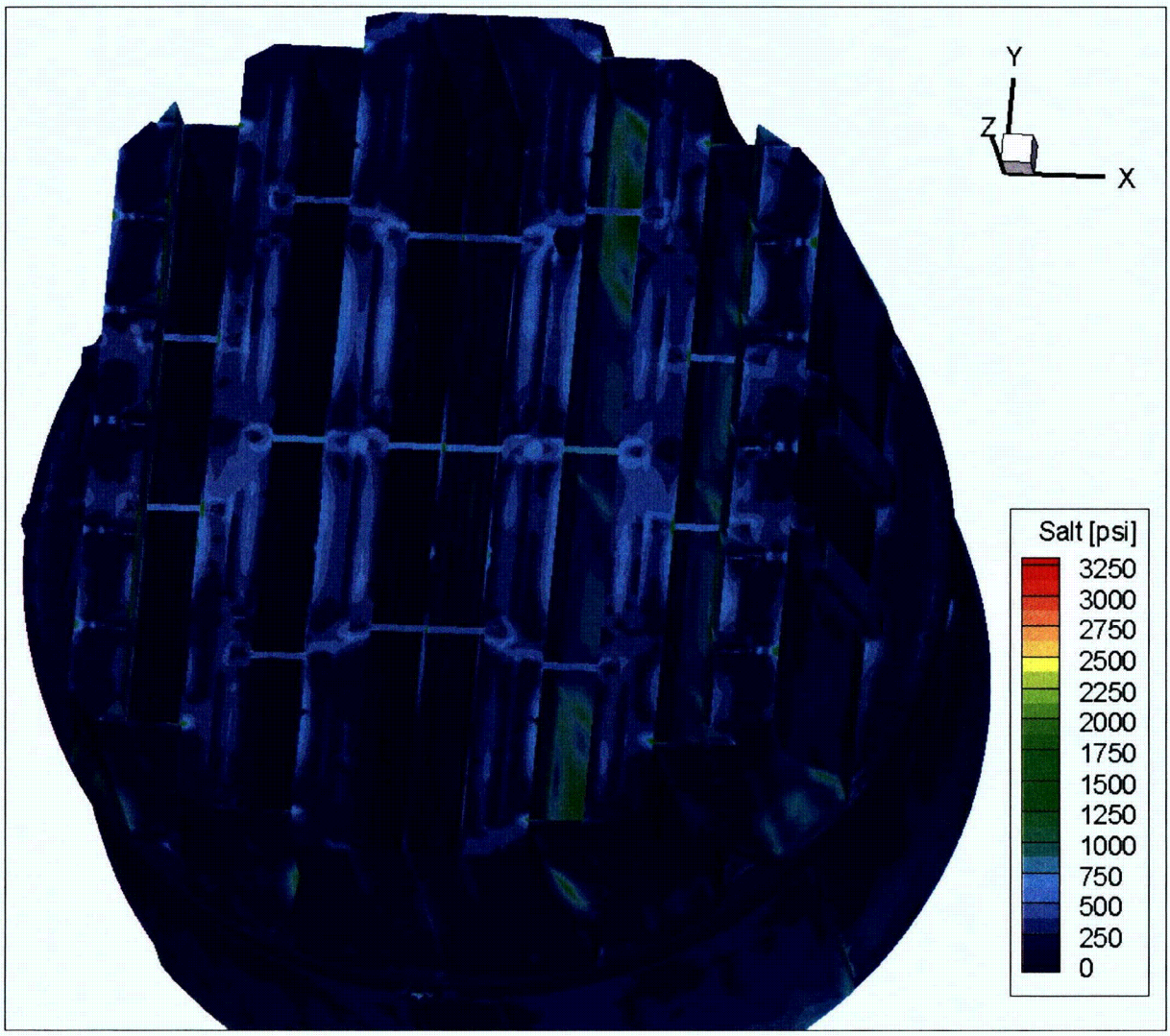

Figure 12f. Contour plot of alternating stress intensity, S_{alt}, for CLTP operation with frequency shifts. The recorded stress at a node is the maximum value taken over all frequency shifts. Second view from top.

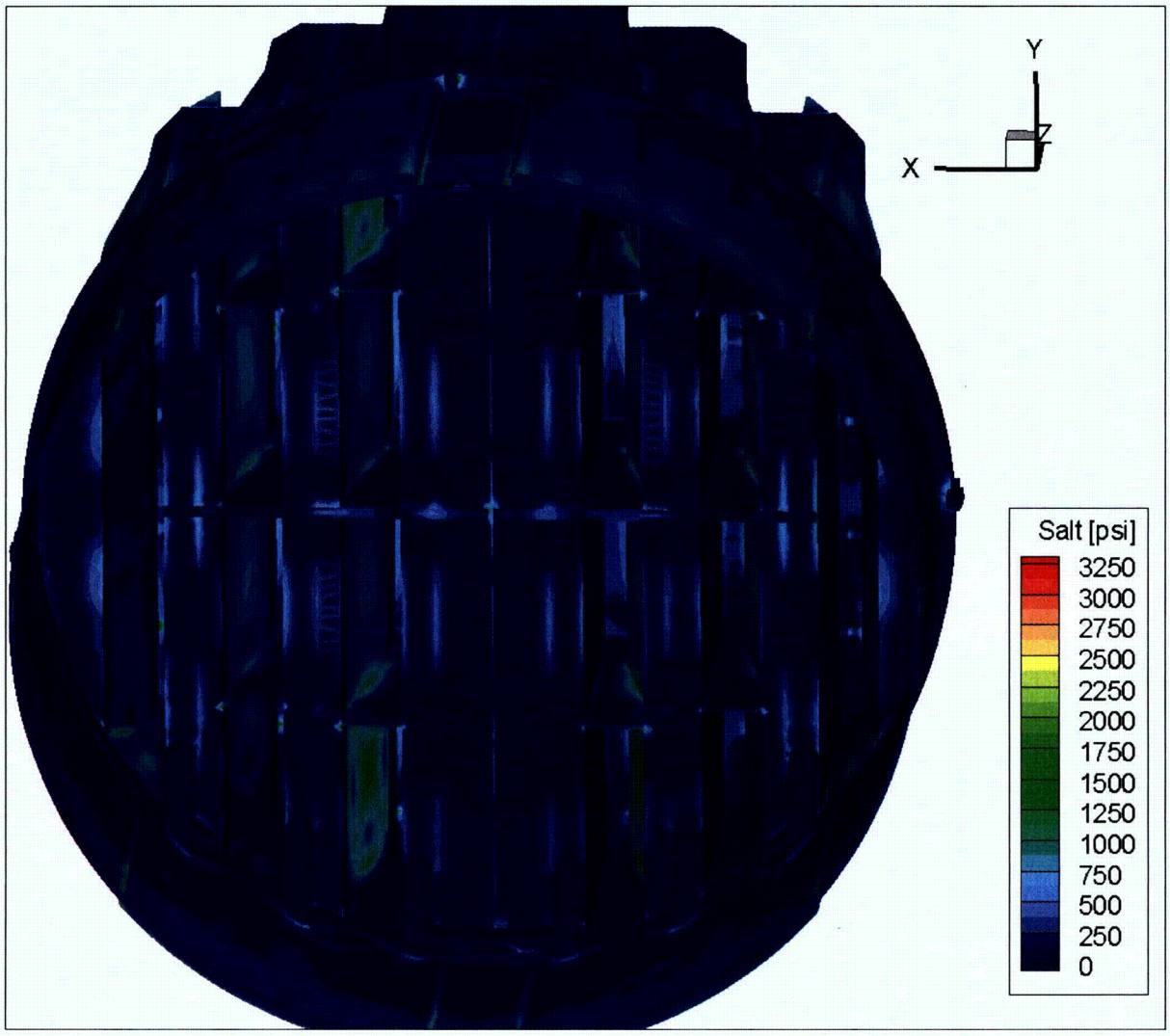

Figure 12g. Contour plot of alternating stress intensity, S_{alt}, for CLTP operation with frequency shifts. The recorded stress at a node is the maximum value taken over all frequency shifts. Third view from below.

5.2 Load Combinations and Allowable Stress Intensities

The stress ratios computed for CLTP at nominal frequency and with frequency shifting are listed in Table 8. The stress ratios are grouped according to type (SR-P for maximum membrane and membrane+bending stress, SR-a for alternating stress) and location (away from welds or on a weld). The tabulated nodes are also depicted in Figure 13 (no frequency shift) and Figure 14 (all frequency shifts included). The plots corresponding to maximum stress intensities depict all nodes with stress ratios SR-P≤4, whereas the plots of alternating stress ratios display all nodes with SR-a≤4 or, in some cases, SR-a≤5 as indicated.

For CLTP operation at nominal frequency the minimum alternating stress ratio is SR-a=4.16, and occurs on the weld joining the top of the steam dam/gusset weld. When all frequency shifts are included the minimum alternating stress reduces by 23% to SR-a=3.39 and occurs where the tie bar connecting the outer and middle vane banks lands on the middle hood. The leading alternating stress locations in Table 8b generally occur on: (i) the weld connecting the steam dam to one of its support gussets; (ii) the bottom of the weld joining the drain channel to the skirt; (iii) the end of a tie bar connecting the middle and outer vane banks; (iv) the top of a closure plate. The 4th and 6th nodes in the table correspond to nodes whose computed stresses have been revised to reflect the results from detailed submodeling analysis in [23] and Appendix A. The minimum stress ratio due to maximum stress intensity at no frequency shift is SR-P=1.68 and occurs on the middle closure plate connecting to the inner hood; it reduces to 1.60 when all frequency shifts are included. All of these locations lie on welds.

Compared to previous stress analysis of the BFN2 steam dryer [5], the addition of the modified tie bars with widened and tapered ends has eliminated virtually all of the high stress areas previously associated with old tie bar bases resulting in stress ratios SR-a>3.39 for the welds on the ends of these tie bars. Moreover replacing the existing outer hood with one that is 1 in thick and supported by outer channels rather than interior supports results in substantially lower stresses overall.

Finally, the highest stress intensities (and lowest stress ratios) at any frequency shift for the locations in Table 8b are recomputed using the CLTP loads <u>without</u> noise removal and reported in Table 8c. For alternating stresses at welds, the alternating stress intensities change by less than 13.1% at all locations except the last one (location 8, node 106443) which increases by 20.6%. All alternating stress ratios at these locations remain above SR-a=3 when noise is retained and all frequency shifts are considered.

In summary, the lowest alternating stress ratio occurs where the tie bar connecting the outer and middle vane banks lands on the middle hood. Its value, SR-a=3.39 at the -7.5% frequency shift indicates that stresses are well below allowable levels. The lowest stress ratio associated with a maximum stress is SR-P=1.60. This value is dominated by the static component and is only weakly altered by acoustic loads. Since acoustic loads scale roughly with the square of the steam flow, it is reasonable to anticipate that under EPU conditions where the square of the steam flow increases by 35% the limiting stress ratio would reduce from 3.39 to 3.39/1.35=2.51, which given that the applied loads already account for all end-to-end biases and uncertainties, still contains ample margin for sustained EPU operation.

Table 8a. Locations with minimum stress ratios for CLTP conditions with no frequency shift. Signal noise is removed using 5% power data. Stress ratios are grouped according to stress type (maximum – SR-P; or alternating – SR-a) and location (away from a weld or at a weld). Bold text indicates minimum stress ratio of any type on the structure. Locations are depicted in Figure 13.

Stress Ratio	Weld	Location	Location (in.) (a)			node(b)	Stress Intensity (psi)			Stress Ratio	
			x	y	z		Pm	Pm+Pb	S_{alt}	SR-P	SR-a
SR-P	No	1. USR/Seismic Block/Support Part	122.1	-10	-9.5	122998	7399	7399	1521	2.28	8.13
"	"	2. USR part/Support/Support Part	7	122.3	-9.5	123070	6274	6274	1141	2.69	10.83
"	"	3. Middle Closure Plate	33.9	108.4	88.9	7238	4936	5206	631	3.42	19.6
SR-a	No	*NONE SR-a > 5 at all non weld nodes*									
SR-P	**Yes**	**1. Top Cover Inner Hood/Middle Closure Plate/Inner Hood**	**31.5**	**108.4**	**88.9**	**100230**	**5536**	**6121**	**751**	**1.68**	**9.14**
"	"	2. USR part/Support/Support Part	8.5	122.2	-9.5	123072	3884	3884	520	2.39	13.2
"	"	3. Upper Support Ring/Seismic Block	-122.1	10.3	-9.5	122767	3807	3807	766	2.44	8.96
"	"	4. Top Cover Middle Hood/Outer Closure Plate/Middle Hood	-62.5	85	88.9	100958	3804	4236	1392	2.44	4.94
"	"	5. Splice Bar/USR Part	-2.2	-119	0	123237	3746	3746	275	2.48	25
"	"	6. Middle Base Plate/Hood Support/Inner Hood(d)	39.8	-59.8	0	96024	3390	3398	1279	2.74	5.37
"	"	7. Submerged Drain Channel/Skirt	91	-76.7	-98.5	97969	271	4093	678	3.41	10.13
SR-a	Yes	1. Dam Plate/New Gusset	77	31.4	104.4	92392	242	1849	1652	7.54	4.16
"	"	2. Dam Plate/New Gusset	77	58.2	101.4	104386	125	1665	1625	8.37	4.23
"	"	3. Old Hood Overlap/Gusset Pad Thin	93.5	58	88.9	92981	184	2205	1625	6.32	4.23
"	"	4. Dam Plate/New Gusset(e)	77	58.2	104.4	104715	154	1640	1593	8.5	4.31
"	"	5. Top Cover Middle Hood/Middle Hood/Tie Bar	-62.5	-25.2	88.9	101376	894	1482	1437	9.41	4.78

See Table 7a for notes (a)-(e).

Table 8b. Locations with minimum stress ratios at CLTP conditions with frequency shifts. Signal noise is removed using 5% power data. Stress ratios at every node are recorded as the lowest stress ratio identified during the frequency shifts. Stress ratios are grouped according to stress type (maximum – SR-P; or alternating – SR-a) and location (away from a weld or at a weld). Bold text indicates minimum stress ratio of any type on the structure. Locations are depicted in Figure 14.

Stress Ratio	Weld	Location	Location (in.) (a)			node(b)	Stress Intensity (psi)			Stress Ratio		% Freq. Shift
			x	y	z		Pm	Pm+Pb	S_{alt}	SR-P	SR-a	
SR-P	No	1. USR/Seismic Block/Support Part	122.1	-10	-9.5	122998	7520	7520	1850	2.25	6.68	5
"	"	2. USR part/Support/Support Part	7	122.3	-9.5	123070	6522	6522	1390	2.59	8.9	-2.5
"	"	3. Middle Closure Plate	33.9	108.4	88.9	7238	5194	5458	871	3.25	14.2	5
SR-a	No	1. Mid Plate/Tie Bar	0	-3	88.9	102956	673	3937	3254	6.44	3.8	2.5
SR-P	**Yes**	**1. Top Cover Inner Hood/Middle Closure Plate/Inner Hood**	**31.5**	**108.4**	**88.9**	**100230**	**5826**	**6458**	**1026**	**1.60**	**6.69**	**5**
"	"	2. USR part/Support/Support Part	8.5	122.2	-9.5	123072	4044	4044	644	2.3	10.67	7.5
"	"	3. USR/Seismic Block	-122.1	10.3	-9.5	122767	3906	3906	876	2.38	7.84	-7.5
"	"	4. Top Cover Middle Hood/Outer Closure Plate/Middle Hood	62.5	-85	88.9	106443	3876	4189	1628	2.4	4.22	2.5
"	"	5. Splice Bar/USR Part	-2.2	-119	0	123237	3861	3861	383	2.41	17.95	7.5
"	"	6. Middle Base Plate/Hood Support/Inner Hood(d)	39.8	-59.8	0	96024	3553	3601	1476	2.62	4.65	-10
"	"	7. Submerged Drain Channel/Skirt	91	-76.7	-98.5	97969	309	4683	1359	2.98	5.05	-7.5
"	"	8. Submerged Drain Channel/Skirt(c)	91	-76.7	-100.5	98197	871	4267	1261	3.27	5.45	10

See Table 7a for notes (a)-(e).

Table 8b (cont.). Locations with minimum stress ratios at CLTP conditions with frequency shifts. Signal noise is removed using 5% power data. Stress ratios at every node are recorded as the lowest stress ratio identified during the frequency shifts. Stress ratios are grouped according to stress type (maximum – SR-P; or alternating – SR-a) and location (away from a weld or at a weld). Bold text indicates minimum stress ratio of any type on the structure. Locations are depicted in Figure 14.

Stress Ratio	Weld	Location	Location (in.) (a)			node(b)	Stress Intensity (psi)			Stress Ratio		% Freq. Shift
			x	y	z		Pm	Pm+Pb	S_{alt}	SR-P	SR-a	
SR-a	Yes	1. Top Cover Middle Hood/Middle Hood/Tie Bar	-62.5	-25.2	88.9	101376	1007	2165	2029	6.44	3.39	-7.5
"	"	2. Dam Plate/New Gusset	77	31.4	104.4	92392	262	1986	1836	7.02	3.74	2.5
"	"	3. Dam Plate/New Gusset	77	58.2	101.4	104386	129	1813	1770	7.69	3.88	2.5
"	"	4. Dam Plate/New Gusset(e)	77	58.2	104.4	104715	157	1799	1741	7.75	3.95	2.5
"	"	5. Old Hood Overlap/Top Cover Outer Hood/Thin Gusset Pad	93.5	57.5	88.9	92842	241	2343	1739	5.95	3.95	5
"	"	6. Submerged Drain Channel/Skirt(c)	-11.5	118.4	-100.5	104136	631	3151	1690	4.42	4.06	-10
"	"	7. Top Thick Plate/Dam Plate/Tie Bar/Top Cover Outer Bank	77	-23.2	88.9	93568	1360	2043	1637	6.82	4.20	-10
"	"	8. Top Cover Middle Hood/Outer Closure Plate/Middle Hood	62.5	-85	88.9	106443	3876	4189	1628	2.4	4.22	2.5

See Table 7a for notes (a)-(e).

Table 8c. Minimum stress ratios at any frequency shift for the nodes listed in Table 8b computed using the unfiltered CLTP loads (i.e., signal noise has *not* been removed). Locations are depicted in Figure 14.

Stress Ratio	Weld	Location	Location (in.) (a)			node(b)	Stress Intensity (psi)			Stress Ratio		% Freq. Shift
			x	y	z		Pm	Pm+Pb	S_{alt}	SR-P	SR-a	
SR-P	No	1. USR/Seismic Block/Support Part	122.1	-10	-9.5	122998	7587	7587	1956	2.23	6.32	10
"	"	2. USR part/Support/Support Part	7	122.3	-9.5	123070	6550	6550	1447	2.58	8.55	-2.5
"	"	3. Middle Closure Plate	33.9	108.4	88.9	7238	5310	5573	989	3.18	12.50	5
SR-a	No	1. Mid Plate/Tie Bar	0	-3	88.9	102956	5960	4442	3655	5.71	3.38	-10
SR-P	**Yes**	**1. Top Cover Inner Hood/Middle Closure Plate/Inner Hood**	**31.5**	**108.4**	**88.9**	**100230**	**5960**	**6620**	**1193**	**1.56**	**5.76**	**10**
"	"	2. USR part/Support/Support Part	8.5	122.2	-9.5	123072	4060	4060	676	2.29	10.16	7.5
"	"	3. USR/Seismic Block	-122.1	10.3	-9.5	122767	3954	3954	948	2.35	7.24	-7.5
"	"	4. Top Cover Middle Hood/Outer Closure Plate/Middle Hood	62.5	-85	88.9	106443	4217	4495	1964	2.20	3.50	2.5
"	"	5. Splice Bar/USR Part	-2.2	-119	0	123237	3878	3878	401	2.40	17.15	7.5
"	"	6. Middle Base Plate/Hood Support/Inner Hood(d)	39.8	-59.8	0	96024	3605	3786	1782	2.58	3.85	7.5
"	"	7. Submerged Drain Channel/Skirt	91	-76.7	-98.5	97969	328	4853	1507	2.87	4.56	-7.5
"	"	8. Submerged Drain Channel/Skirt(c)	91	-76.7	-100.5	98197	936	4344	1369	3.21	5.02	10

See Table 7a for notes (a)-(e).

Table 8c (cont.). Minimum stress ratios at any frequency shift for the nodes listed in Table 8b computed using the unfiltered CLTP loads (i.e., signal noise has *not* been removed). Locations are depicted in Figure 14.

Stress Ratio	Weld	Location	Location (in.) (a)			node(b)	Stress Intensity (psi)			Stress Ratio		% Freq. Shift
			x	y	z		Pm	Pm+Pb	S_{alt}	SR-P	SR-a	
SR-a	Yes	1. Top Cover Middle Hood/Middle Hood/Shell Tie Bar	-62.5	-25.2	88.9	101376	1037	2383	2259	5.85	3.04	-7.5
"	"	2. Dam Plate/New Gusset	77	31.4	104.4	92392	291	2168	2024	6.43	3.39	2.5
"	"	3. Dam Plate/New Gusset	77	58.2	101.4	104386	147	1974	1943	7.06	3.54	2.5
"	"	4. Dam Plate/New Gusset(e)	77	58.2	104.4	104715	169	1964	1915	7.10	3.59	2.5
"	"	5. Old Hood Overlap/Top Cover Outer Hood/Thin Gusset Pad	93.5	57.5	88.9	92842	251	2501	1912	5.58	3.59	5
"	"	6. Submerged Drain Channel/Skirt(c)	-11.5	118.4	-100.5	104136	716	3332	1910	4.18	3.60	-10
"	"	7. Top Thick Plate/Dam Plate/Tie Bar/Top Cover Outer Bank	77	-23.2	88.9	93568	1427	2210	1788	6.31	3.84	-10
"	"	8. Top Cover Middle Hood/Outer Closure Plate/Middle Hood	62.5	-85	88.9	106443	4217	4495	1964	2.20	3.50	2.5

See Table 7a for notes (a)-(e).

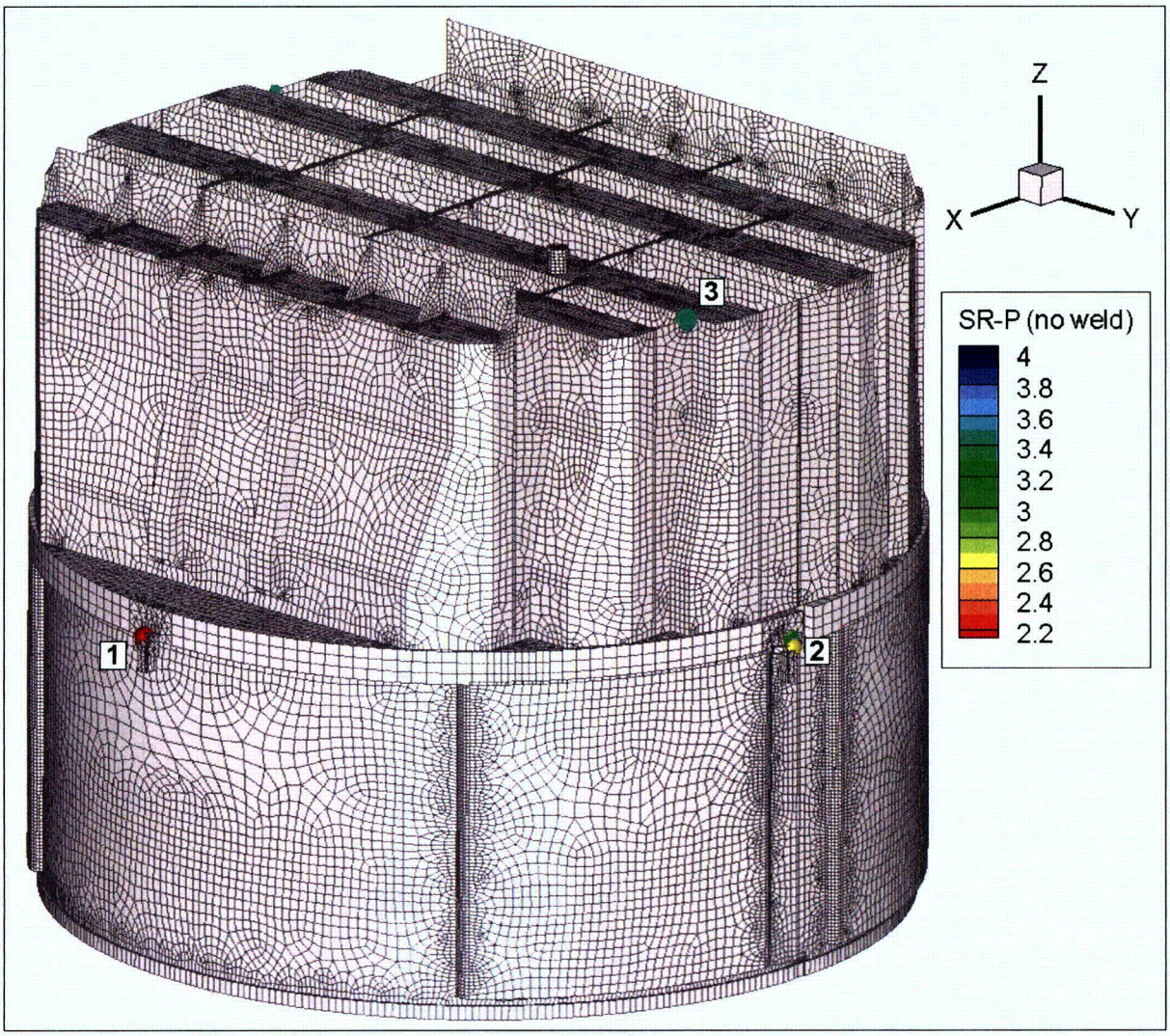

Figure 13a. Locations of smallest maximum stress ratios, SR-P≤4, at non-welds for nominal CLTP operation. Numbers refers to the enumerated locations for SR-P values at non-welds in Table 8a.

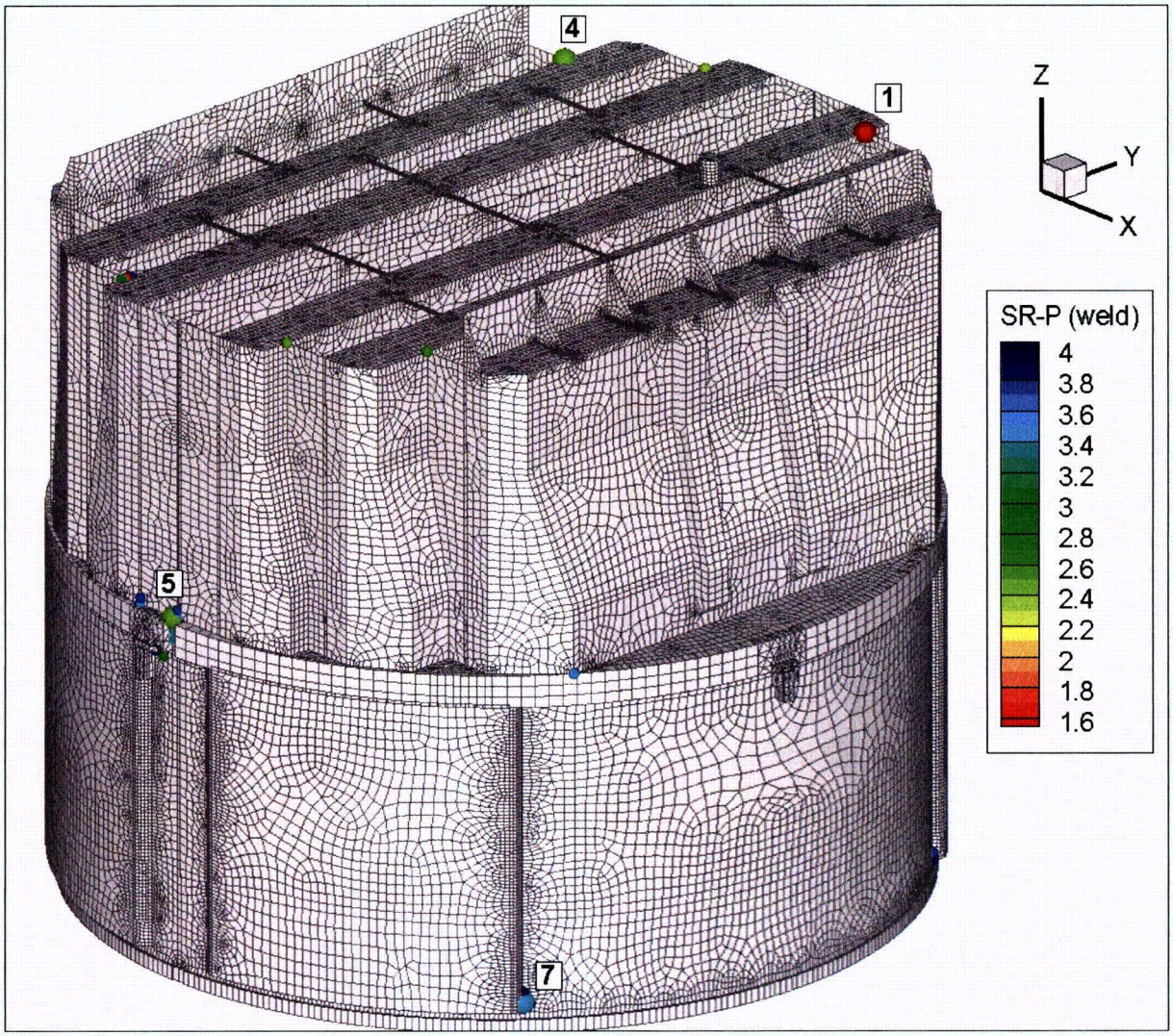

Figure 13b. Locations of smallest maximum stress ratios, SR-P≤4, at welds for nominal CLTP operation. Numbers refer to the enumerated locations for SR-P values at welds in Table 8a. Second view showing locations 1, 4, 5 and 7.

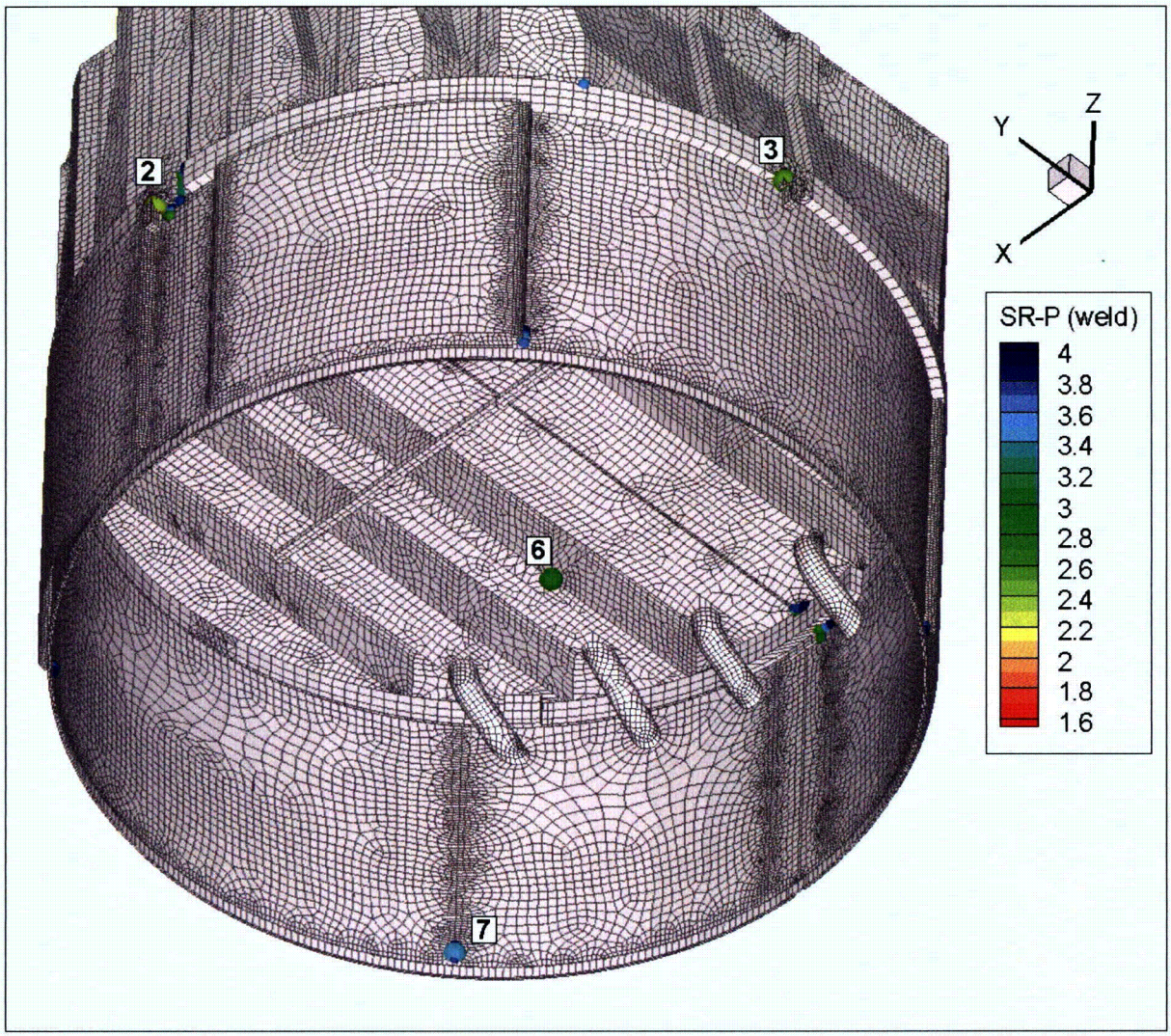

Figure 13c. Locations of smallest maximum stress ratios, SR-P≤4, at welds for nominal CLTP operation. Numbers refer to the enumerated locations for SR-P values at welds in Table 8a. Second view showing locations 2, 3, 6 and 7.

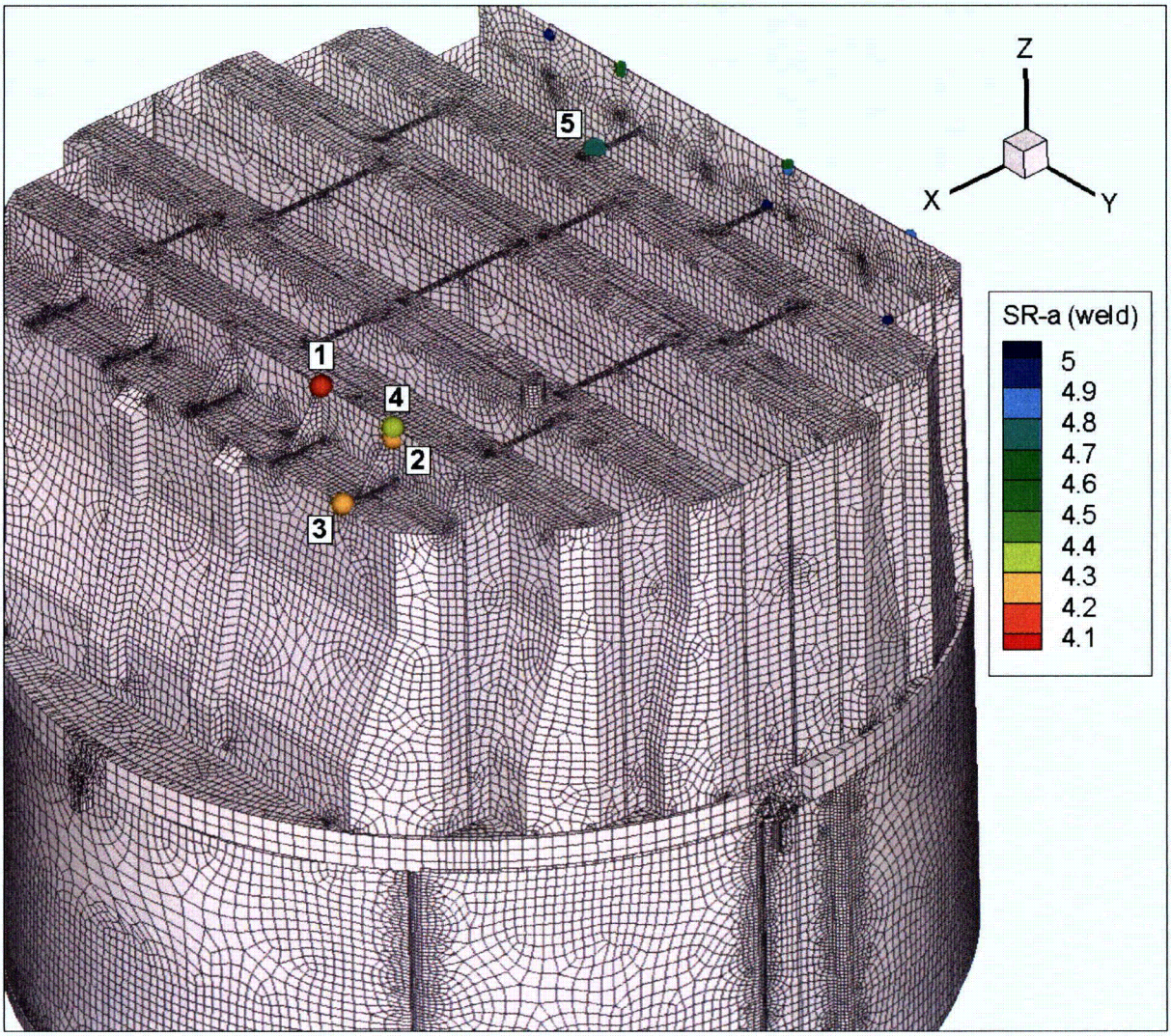

Figure 13d. Locations of minimum alternating stress ratios, SR-a≤5, at welds for nominal CLTP operation. Numbers refer to the enumerated locations for SR-a values at welds in Table 8a.

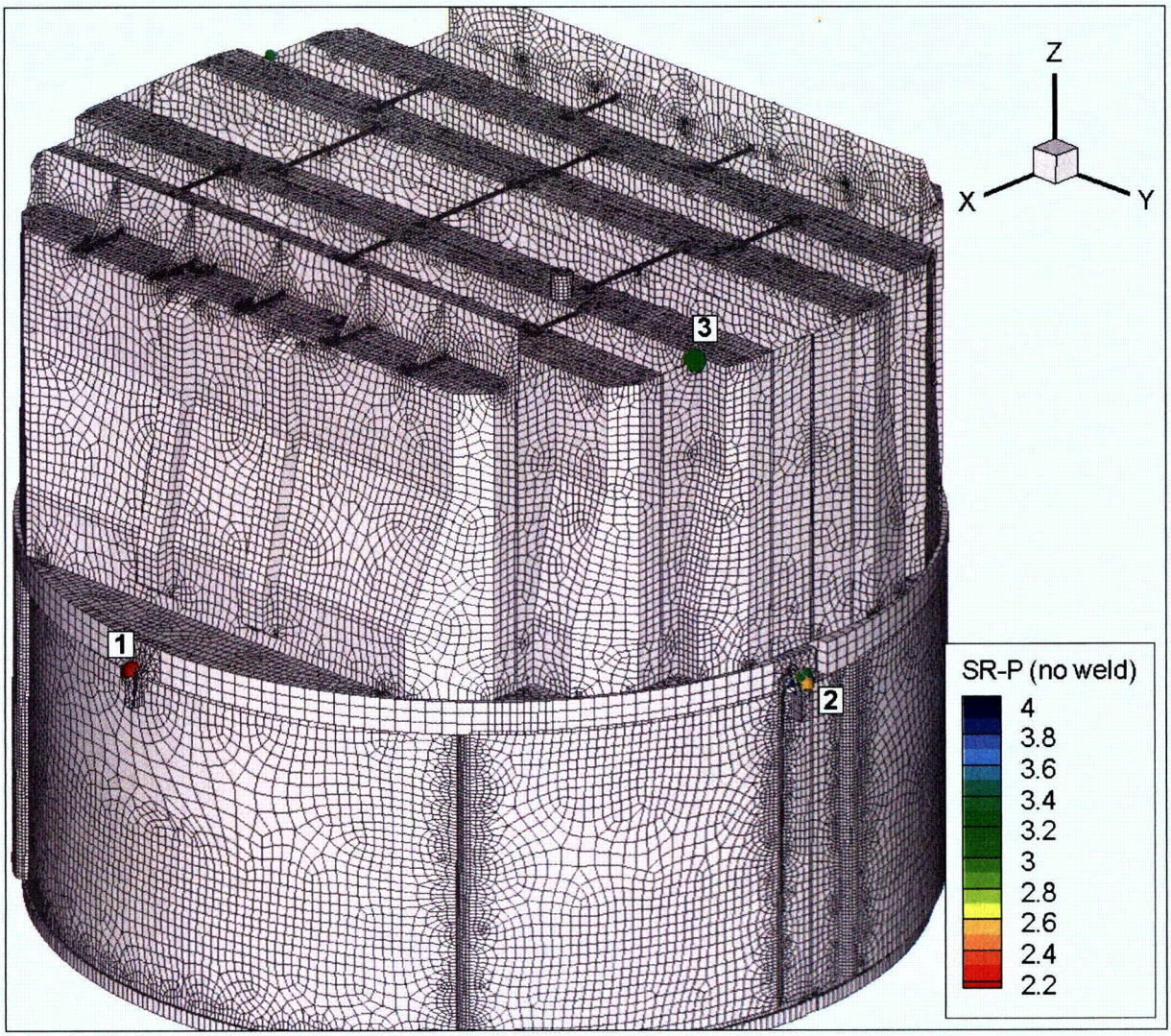

Figure 14a. Locations of minimum stress ratios, SR-P≤4, associated with maximum stress intensities at non-welds for CLTP operation with frequency shifts. The recorded stress ratio is the minimum value taken over all frequency shifts. The numbers refers to the enumerated location for SR-P values at non-welds in Table 8b.

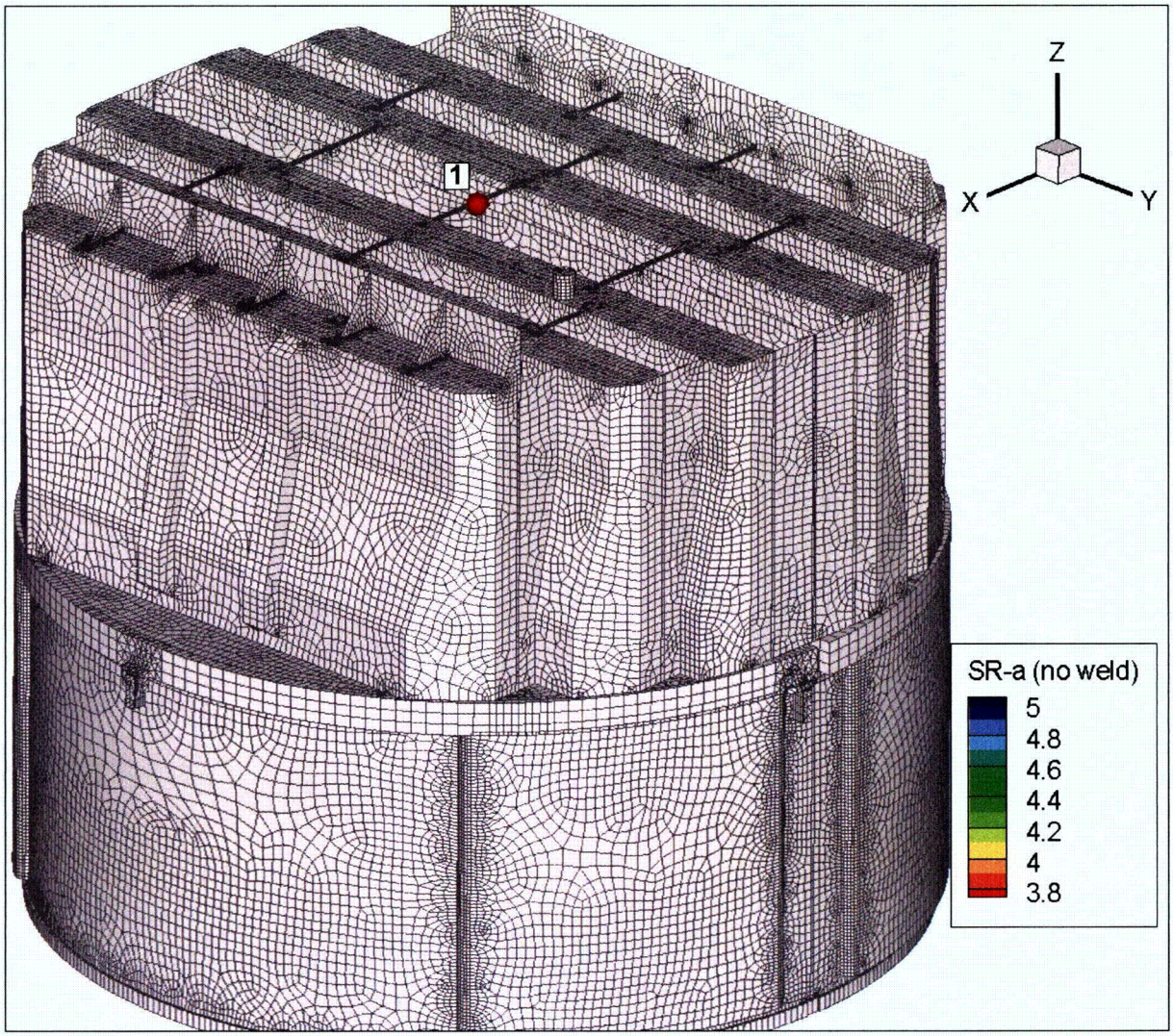

Figure 14b. Locations of minimum alternating stress ratios, SR-a≤5, at non-welds for CLTP operation with frequency shifts. The recorded stress ratio at a node is the minimum value taken over all frequency shifts. Numbers refer to the enumerated locations for SR-a values at welds in Table 8b.

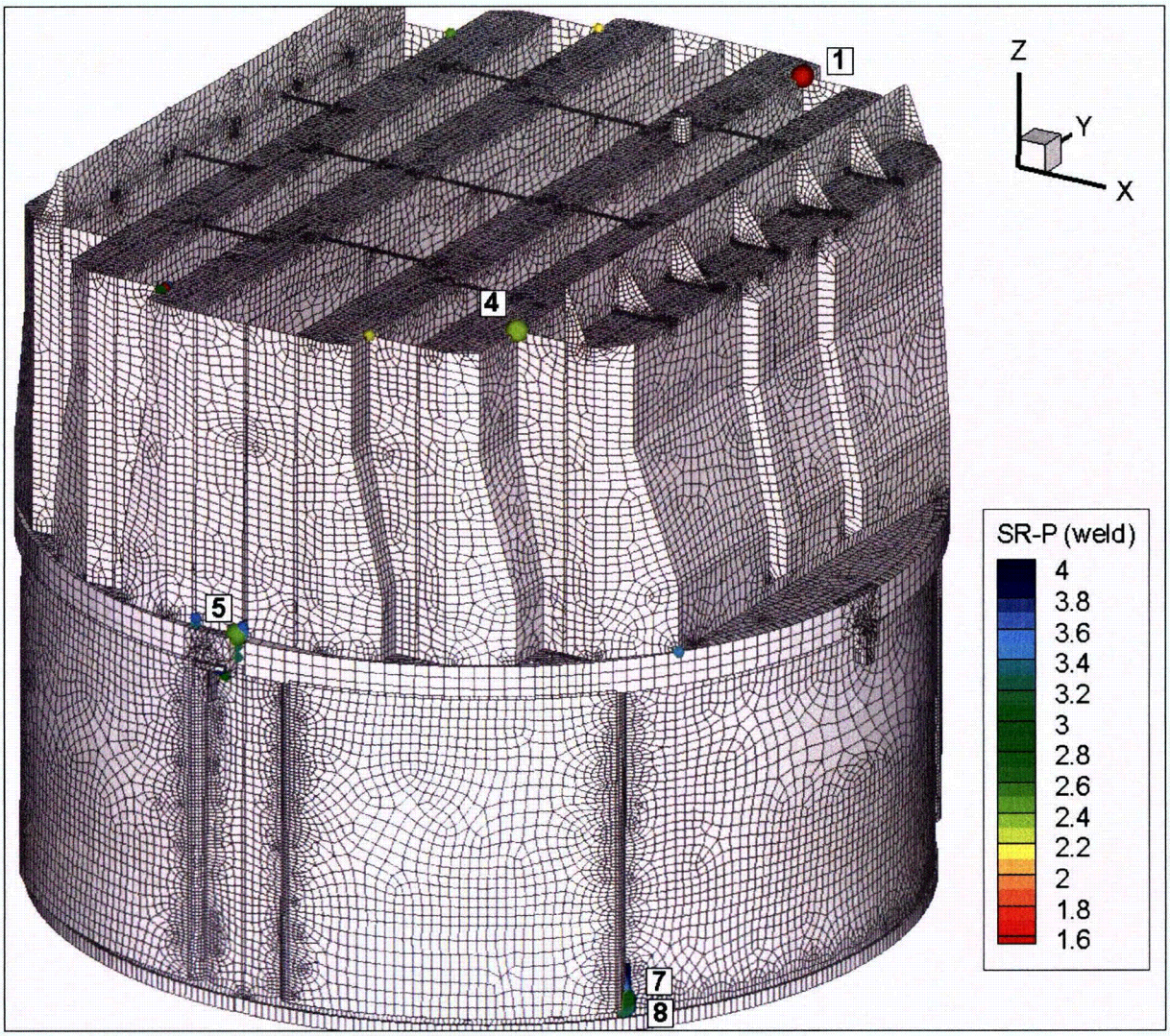

Figure 14c. Locations of minimum stress ratios, SR-P≤4, associated with maximum stress intensities at welds for CLTP operation with frequency shifts. The recorded stress ratio at a node is the minimum value taken over all frequency shifts. Numbers refer to the enumerated locations for SR-P values at welds in Table 8b. This view shows locations 1, 4, 5, 7 and 8.

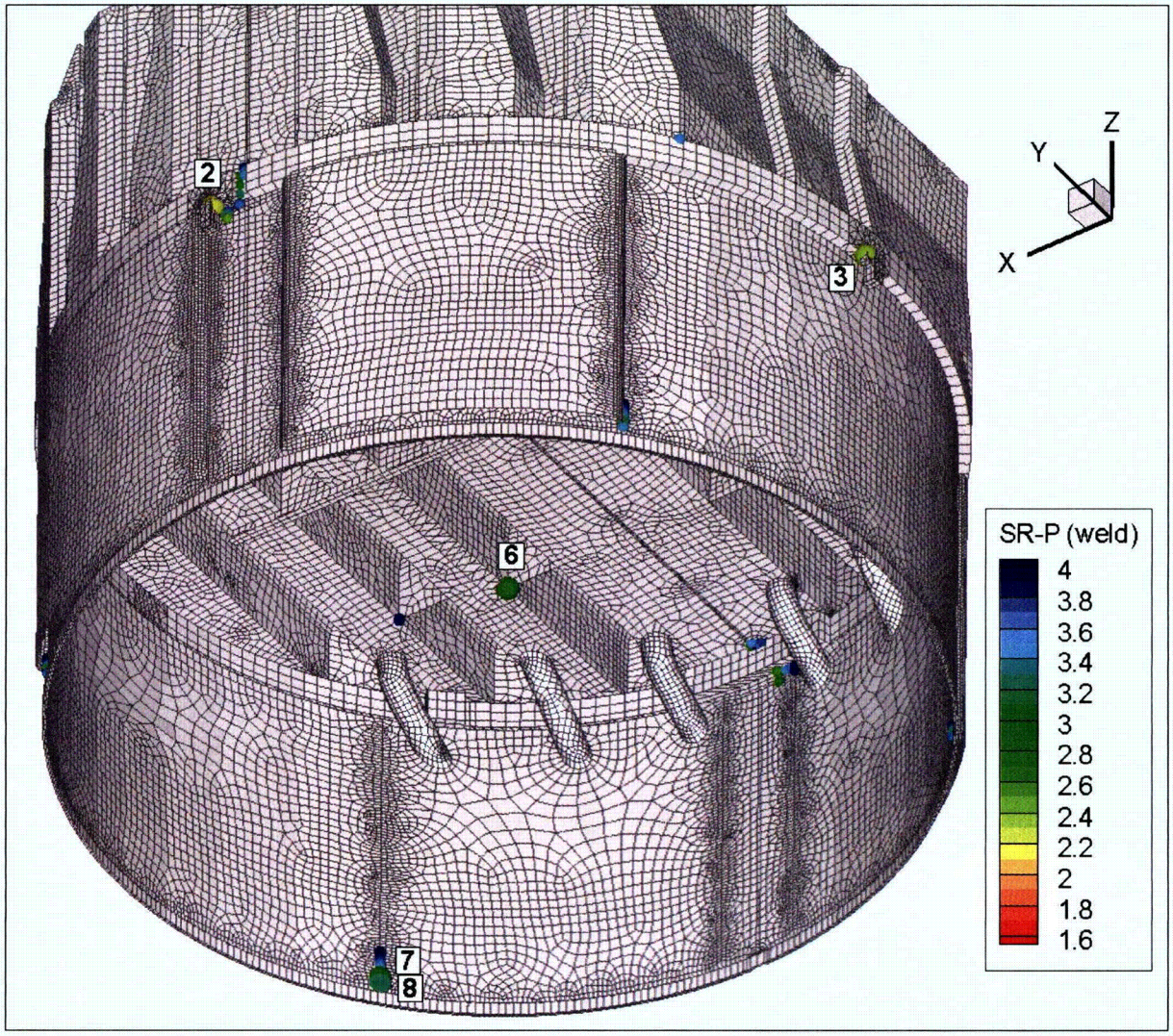

Figure 14d. Locations of minimum stress ratios, SR-P≤4, associated with maximum stress intensities at welds for CLTP operation with frequency shifts. The recorded stress ratio at a node is the minimum value taken over all frequency shifts. Numbers refer to the enumerated locations for SR-P values at welds in Table 8b. This view shows locations 2, 3 and 6-8.

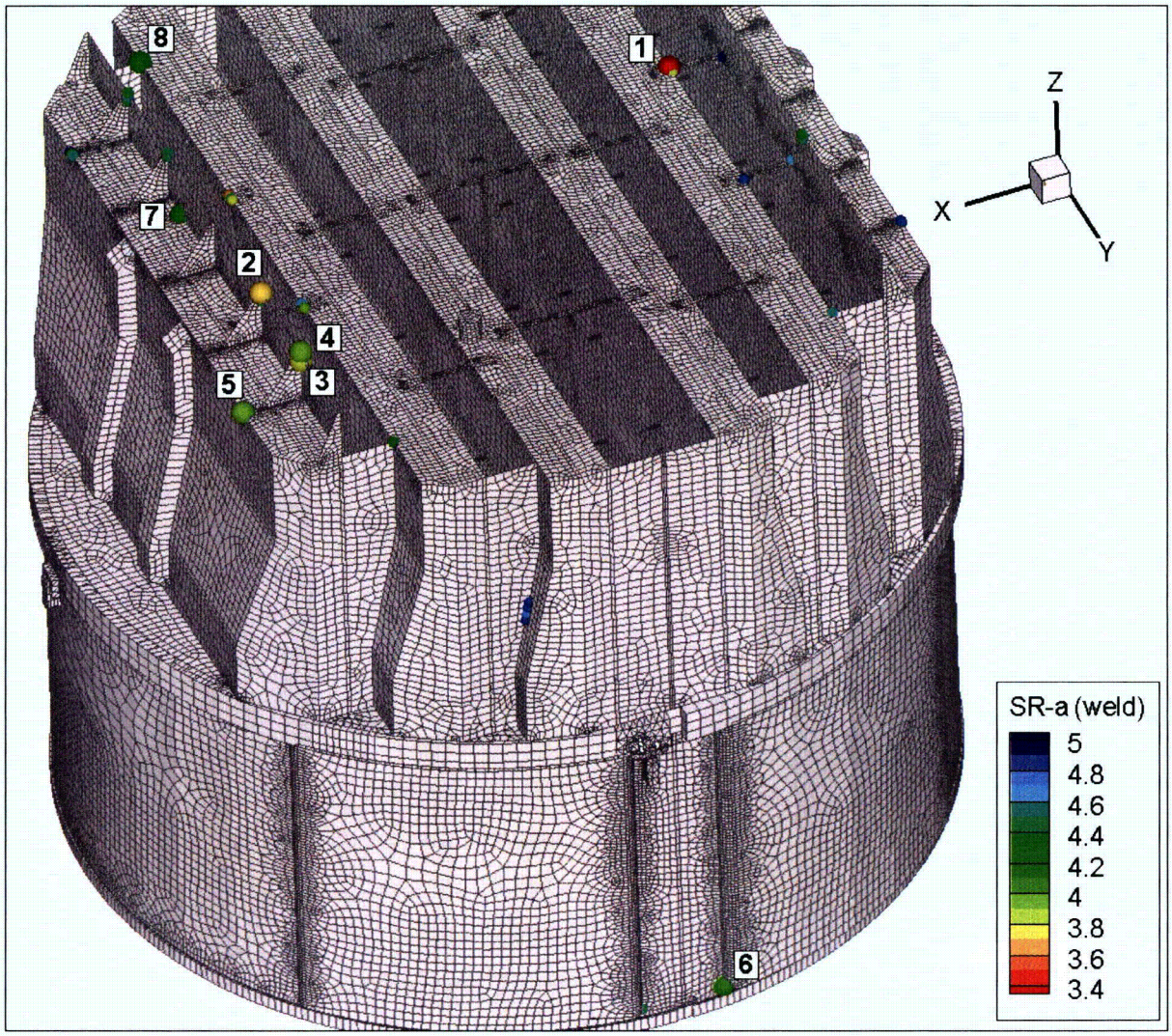

Figure 14e. Locations of minimum alternating stress ratios, SR-a≤5, at welds for CLTP operation with frequency shifts. The recorded stress ratio at a node is the minimum value taken over all frequency shifts. Numbers refer to the enumerated locations for SR-a values at welds in Table 8b. This view shows locations 1- 8.

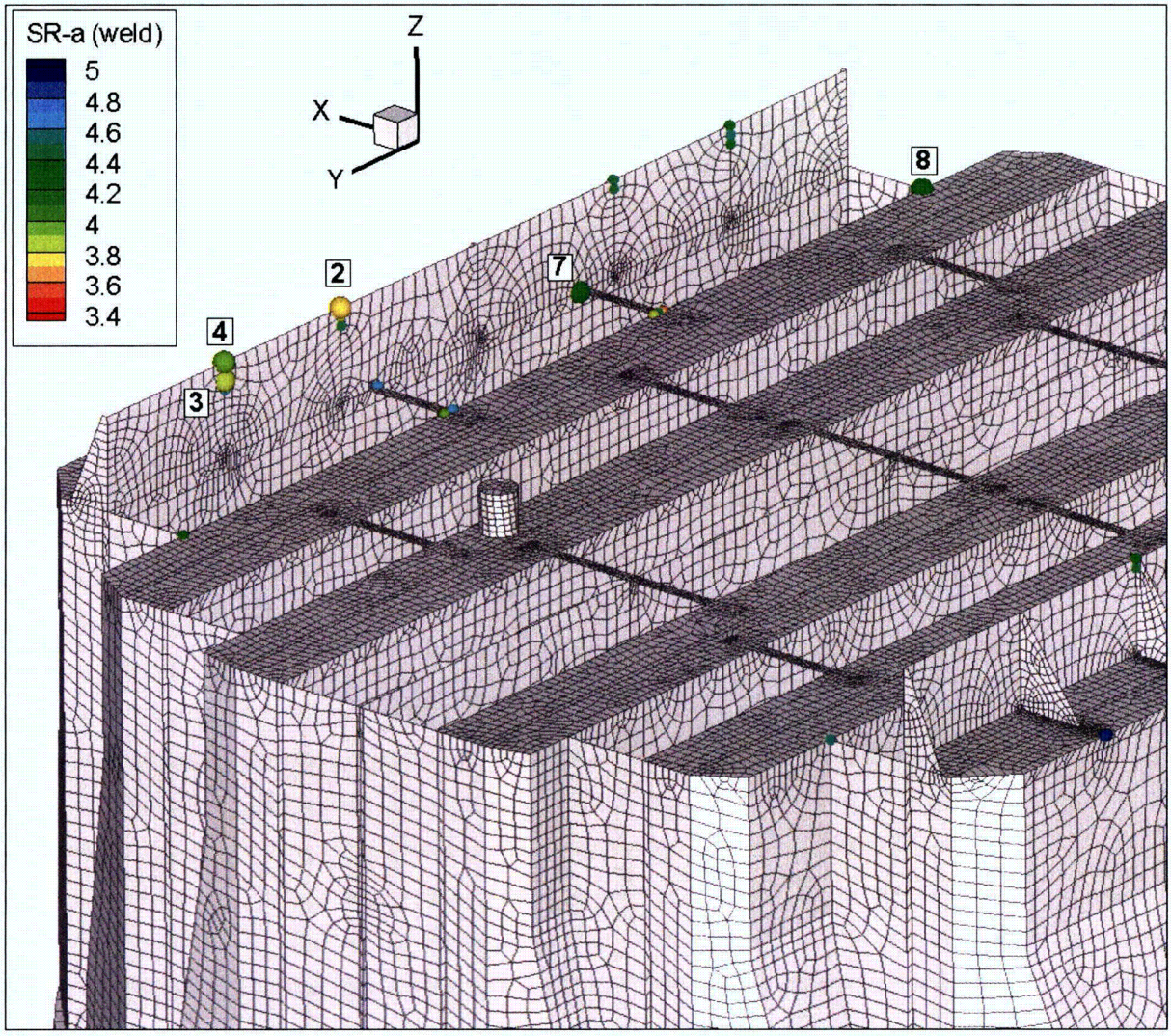

Figure 14f. Locations of minimum alternating stress ratios, SR-a≤5, at welds for CLTP operation with frequency shifts. The recorded stress ratio at a node is the minimum value taken over all frequency shifts. Numbers refer to the enumerated locations for SR-a values at welds in Table 8b. Second view showing locations 2-4 and 7-8.

5.3 Frequency Content

The frequency contribution to the stresses can be investigated by examining the power spectral density (PSD) curves and accumulative PSDs for selected nodes having low alternating stress ratios. The accumulative PSDs are computed directly from the Fourier coefficients as

$$\Sigma(\omega_n) = \sqrt{\sum_{k=1}^{n} |\tilde{\sigma}(\omega_k)|^2}$$

where $\tilde{\sigma}(\omega_k)$ is the complex stress harmonic at frequency, ω_k. Accumulative PSD plots are useful for determining the frequency components and frequency ranges that make the largest contributions to the fluctuating stress. Unlike PSD plots, no "binning" or smoothing of frequency components is needed to obtain smooth curves. Steep step-like rises in $\Sigma(\omega)$ indicate the presence of a strong component at a discrete frequency whereas gradual increases in the curve imply significant content over a broader frequency range. From Parsival's theorem, equality between $\Sigma(\omega_N)$ (where N is the total number of frequency components) and the RMS of the stress signal in the time domain is established.

The selected nodes are the first three and the sixth locations having the lowest alternating stress ratios (at a weld) in Table 8b. These are:

Node 101376 – this node has the lowest alternating stress ratio and is located on the weld where the tie bar connecting the middle and outer vane banks lands on the middle hood. The associated PSDs are shown in Figure 15a.

Node 92392 - located at the top of the weld connecting the steam dam to the support gusset. The associated PSDs are shown in Figure 15b.

Node 104386 – also located on the weld connecting a support gusset to the steam dam. The 4th and 5th entries having the lowest alternating stress ratios in Table 8b are similar. The associated PSDs are shown in Figure 15c.

Node 104136 –located at bottom of the skirt/drain channel weld. The associated PSDs are shown in Figure 15d.

In each case, since there are six stress components and up to three different section locations for shells (the top, mid and bottom surfaces), there is a total of 18 stress histories per component. Moreover, at junctions there are at least two components that meet at the junction. The particular stress component that is plotted is chosen as follows. First, the component and section location (top/mid/bottom) is taken as the one that has the highest alternating stress. This narrows the selection to six components. Of these, the component having the highest Root Mean Square (RMS) is selected.

For the limiting stress location, the dominant frequency peak is centered at 79.6 Hz. Since it occurs at the -7.5% shift, the corresponding frequency in the non-shifted signal is 85.6 Hz. Comparing the shifted and non-shifted stress PSDs (and accumulative PSDs) it is clear that peaks (or step increases) are shifted and amplified. This is indicative of a strong peak in the load signal being applied to the structure. This is in contrast to the case when stress peaks increase but do

not shift which is indicative of a broad spectrum load with less pronounced peaks being imposed upon the structure. The next two locations both involve the steam dam and have a pronounced peak at 112 Hz which corresponds to 109.3 Hz in the non-shifted signal. This is in the range where the onset of SRV resonance is anticipated so one expects the steam dam to be an important component in the EPU response as is confirmed in Section 6. The last node has two peaks at 57.9 Hz and 49.3 Hz (64.3 Hz and 54.8 Hz respectively in the non-shifted signal). In all cases the accumulative stress PSDs are flat above 150 Hz suggesting that the signals at high frequencies are not significant stresses contributors.

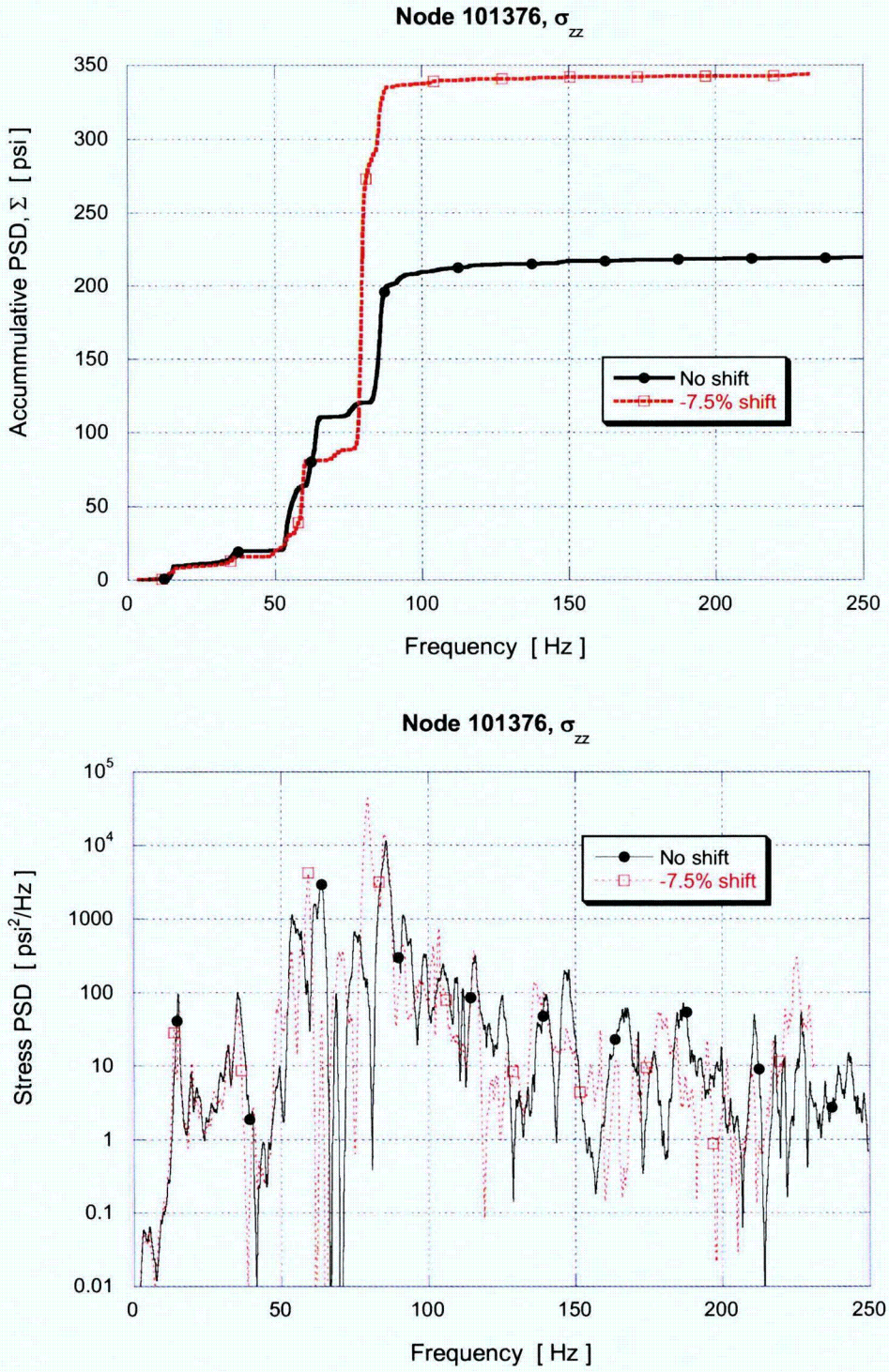

Figure 15a. Accumulative PSD and PSD curves of the σ_{ZZ} stress response at node 101376.

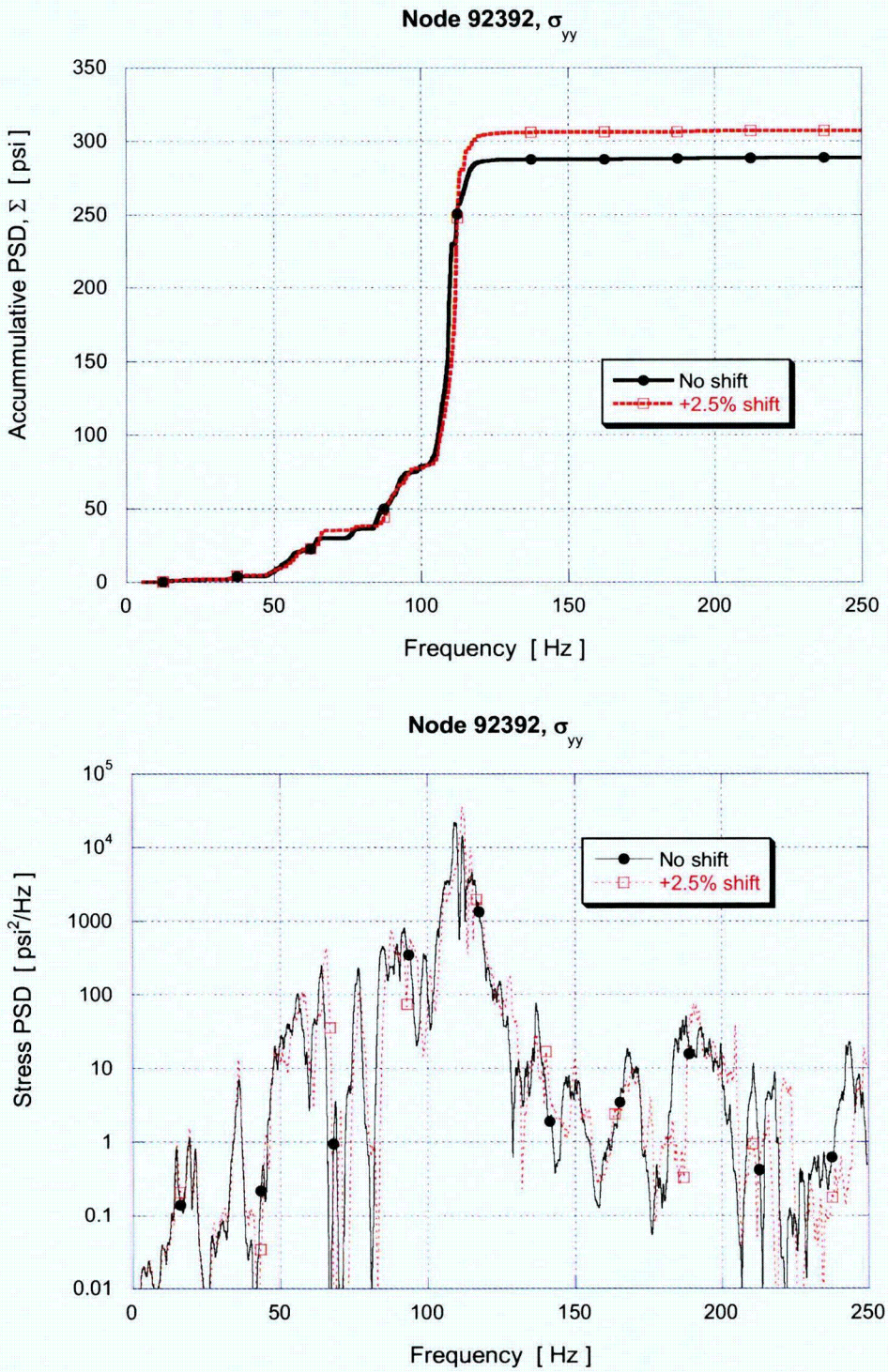

Figure 15b. Accumulative PSD and PSD of the σ_{yy} stress response at node 92392.

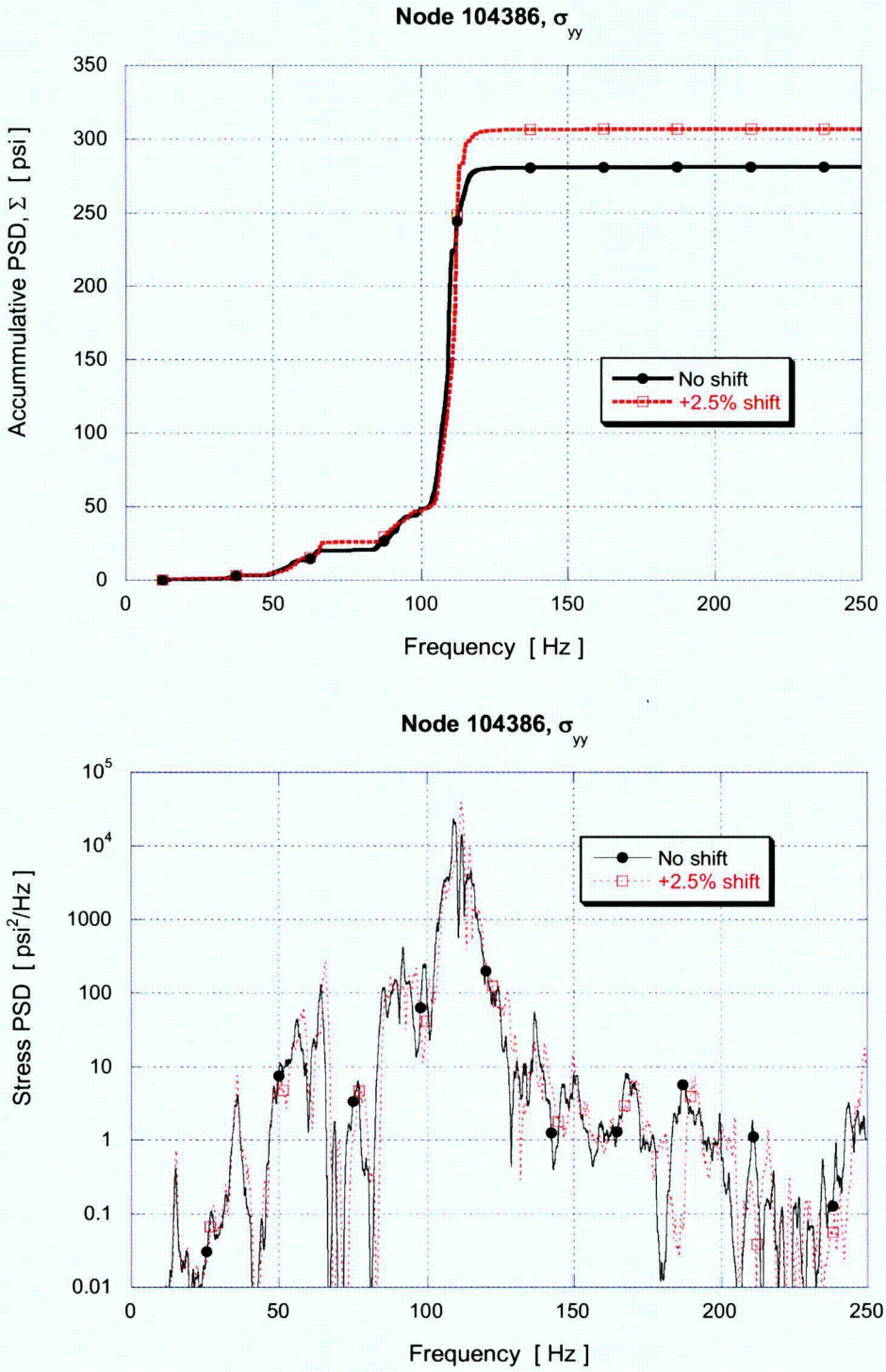

Figure 15c. Accumulative PSD and PSD of the σ_{yy} stress response at node 104386.

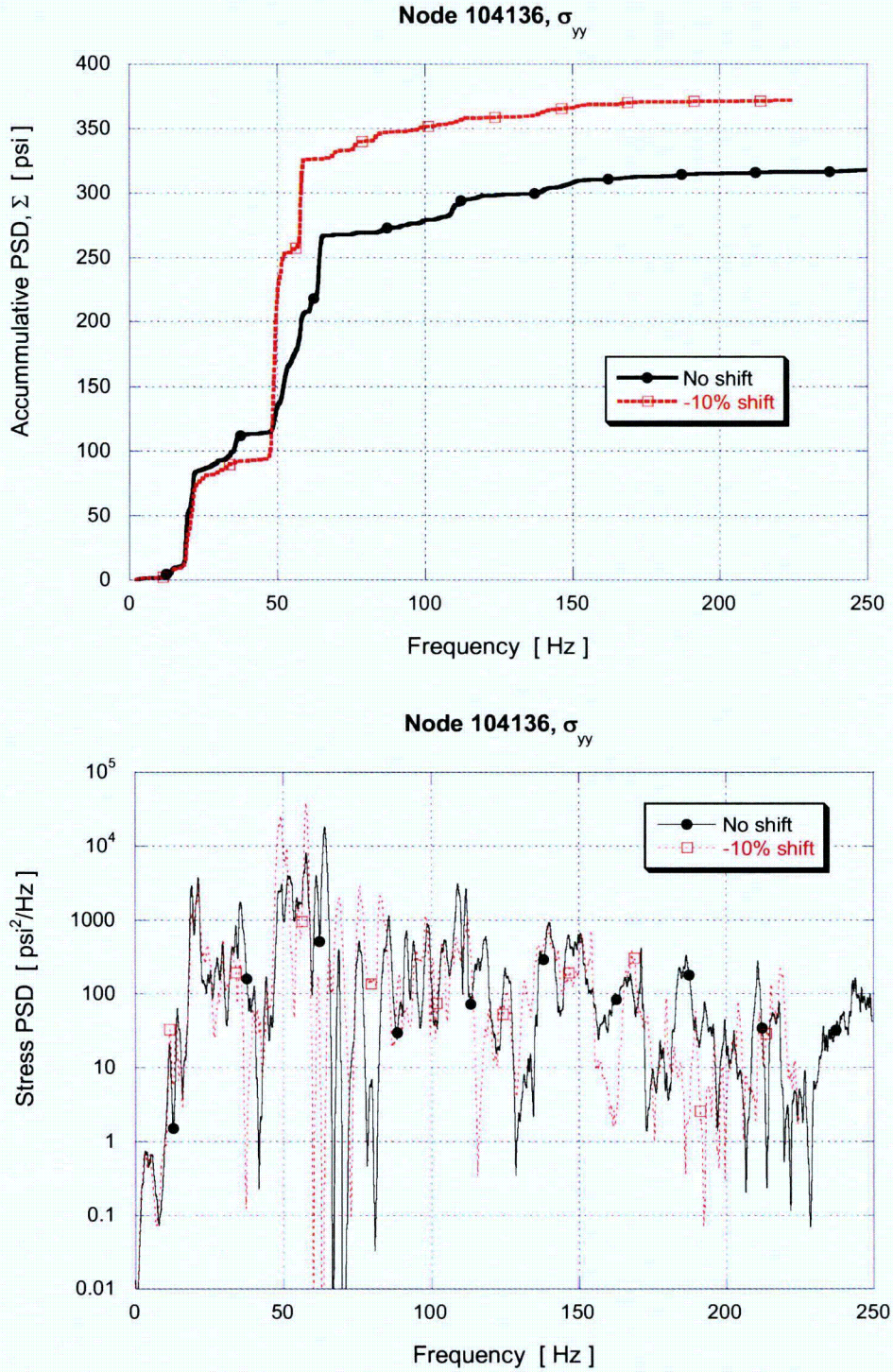

Figure 15d. Accumulative PSD and PSD of the σ_{yy} stress response at node 104136.

6. Results at Predicted EPU Using Bump Up Factors

[[

(3)]]

6.1 Load Combinations and Allowable Stress Intensities at EPU

[[

(3)]]

[[

(3)]]

Table 9a. Locations with minimum stress ratios for estimated EPU conditions with no frequency shift. Signal noise is removed using 5% power data. Stress ratios are grouped according to stress type (maximum – SR-P; or alternating – SR-a) and location (away from a weld or at a weld). Bold text indicates minimum stress ratio of any type on the structure. Locations are depicted in Figure 16.

Stress Ratio	Weld	Location	Location (in.) (a)			node(b)	Stress Intensity (psi)			Stress Ratio	
			x	y	z		Pm	Pm+Pb	S_{alt}	SR-P	SR-a
SR-P	No	1. USR/Seismic Block/Support Part	122.1	-10	-9.5	122998	7925	7925	2061	2.13	6.00
"	"	2. USR part/Support/Support Part	7	122.3	-9.5	123070	6630	6630	1532	2.55	8.07
"	"	3. Middle Closure Plate	33.9	108.4	88.9	7238	5183	5463	894	3.26	13.82
SR-a	No	1. Mid PlateTie Bar	0	-3	88.9	102956	555	3740	3053	6.78	4.05
"	"	2. Mid Plate/Tie Bar	0	-56.8	88.9	99311	856	3922	3029	6.46	4.08
"	"	3. Dam Plate	-77	-46	104.4	81218	204	2640	2498	9.60	4.95
SR-P	**Yes**	**1. Top Cover Inner Hood/Middle Closure Plate/Inner Hood**	**31.5**	**108.4**	**88.9**	**100230**	**5823**	**6408**	**1055**	**1.60**	**6.51**
"	"	2. Top Cover Middle Hood/Outer Closure Plate/Middle Hood	-62.5	85	88.9	100958	4412	4954	2106	2.11	3.26
"	"	3. USR/Seismic Block	-122.1	10.3	-9.5	122767	4061	4061	1031	2.29	6.67
"	"	4. Middle Base Plate/Hood Support/Inner Hood(d)	39.8	-59.8	0	96024	4027	4043	1932	2.31	3.55
"	"	5. USR part/Support/Support Part	8.5	122.2	-9.5	123072	3996	3996	700	2.33	9.81
"	"	6. Splice Bar/USR Part	-2.2	-119	0	123237	3856	3856	378	2.41	18.17
"	"	7. Submerged Drain Channel /Skirt	91	-76.7	-98.5	97969	330	4419	978	3.16	7.02
"	"	8. Middle Base Plate/Hood Support/Middle Hood	70.8	-54.6	0	104413	2923	3024	1691	3.18	4.06
"	"	9. Submerged Drain Channel/Skirt(c)	-91	76.7	-100.5	104054	934	4169	1329	3.34	5.17

See Table 7a for notes (a)-(e).

Table 9a (cont.). Locations with minimum stress ratios for estimated EPU conditions with no frequency shift. Signal noise is removed using 5% power data. Stress ratios are grouped according to stress type (maximum – SR-P; or alternating – SR-a) and location (away from a weld or at a weld). Bold text indicates minimum stress ratio of any type on the structure. Locations are depicted in Figure 16.

Stress Ratio	Weld	Location	Location (in.) (a)			node(b)	Stress Intensity (psi)			Stress Ratio	
			x	y	z		Pm	Pm+Pb	S_{alt}	SR-P	SR-a
SR-a	Yes	1. Dam Plate/New Gusset	-77	-31.4	102.9	91887	278	2928	2753	4.76	2.50
"	"	2. Dam Plate/New Gusset	-77	-58.2	101.4	99698	161	2806	2751	4.97	2.50
"	"	3. Old Hood Overlap/Gusset Pad Thin	-93.5	58.5	88.9	110292	267	3731	2727	3.74	2.52
"	"	4. Dam Plate/New Gusset(e)	-77	58.2	104.4	94763	192	2796	2697	4.99	2.55
"	"	5. Top Cover Middle Hood/Outer Closure Plate/Middle Hood	-62.5	-85	88.9	100498	2620	2844	2203	3.55	3.12
"	"	6. Top Cover Middle Hood/Middle Hood/Tie Bar	-62.5	-25.2	88.9	101376	1081	2008	1964	6.94	3.50
"	"	7. Middle Base Plate/Hood Support/Middle Hood	70.8	54.6	0	105680	1882	2105	1949	4.94	3.52
"	"	8. Top Thick Plate/Dam Plate/Tie Bar/Top Cover Outer Hood	-77	23.2	88.9	102630	1487	2265	1938	6.16	3.54
"	"	9. Middle Base Plate/Hood Support/Inner Hood(d)	39.8	-59.8	0	96024	4027	4043	1932	2.31	3.55
"	"	10. Dam Plate/New Gusset	77	0	104.4	91724	302	2090	1932	6.67	3.56
"	"	11. Mid Bottom Perf Exit/Mid Top Perf Exit/Tie Bar	-77	9.6	62.9	108386	474	1845	1822	7.56	3.77
"	"	12. Submerged Drain Channel /Skirt(c)	-11.5	118.4	-100.5	104136	793	3142	1638	4.44	4.19

See Table 7a for notes (a)-(e).

Table 9b. Locations with minimum stress ratios at estimated EPU conditions with frequency shifts. Signal noise is removed using 5% power data. Stress ratios at every node are recorded as the lowest stress ratio identified during the frequency shifts. Stress ratios are grouped according to stress type (maximum – SR-P; or alternating – SR-a) and location (away from a weld or at a weld). Bold text indicates minimum stress ratio of any type on the structure. Locations are depicted in Figure 17.

Stress Ratio	Weld	Location	Location (in.) (a)			node(b)	Stress Intensity (psi)			Stress Ratio		% Freq. Shift
			x	y	z		Pm	Pm+Pb	S_{alt}	SR-P	SR-a	
SR-P	No	1. USR/Seismic Block/Support Part	122.1	-10	-9.5	122998	8116	8116	2493	2.08	4.96	7.5
"	"	2. USR part/Support/Support Part	7	122.3	-9.5	123070	6986	6986	1878	2.42	6.58	-2.5
"	"	3. Middle Closure Plate	33.9	108.4	88.9	7238	5524	5799	1235	3.06	10.01	5
SR-a	No	1. Mid Plate/Tie Bar	0	-3	88.9	102956	876	5180	4463	4.89	2.77	2.5
"	"	2. Mid Plate/Tie Bar	0	-56.8	88.9	99311	950	4362	3401	5.81	3.64	10
"	"	3. Dam Plate	77	46	104.4	81791	228	2686	2573	9.44	4.81	2.5
SR-P	**Yes**	**1. Top Cover Inner Hood/Middle Closure Plate/Inner Hood**	**31.5**	**108.4**	**88.9**	**100230**	**6197**	**6822**	**1443**	**1.50**	**4.76**	**5**
"	"	2. Top Cover Middle Hood/Outer Closure Plate/Middle Hood	-62.5	85	88.9	100958	4617	5049	2249	2.01	3.05	5
"	"	3. USR/Seismic Block	-122.1	10.3	-9.5	122767	4224	4224	1188	2.20	5.78	-7.5
"	"	4. Middle Base Plate/Hood Support/Inner Hood(d)	39.8	-59.8	0	96024	4222	4348	2262	2.20	3.04	2.5
"	"	5. USR part/Support/Support Part	8.5	122.2	-9.5	123072	4217	4217	870	2.20	7.89	7.5
"	"	6. Splice Bar/USR Part	-2.2	-119	0	123237	4003	4003	519	2.32	13.23	7.5
"	"	7. Submerged Drain Channel/Skirt	91	-76.7	-98.5	97969	363	5151	1797	2.71	3.82	-7.5
"	"	8. Submerged Drain Channel/Skirt(c)	91	-76.7	-100.5	98197	1063	4819	1778	2.89	3.86	10
"	"	9. Middle Base Plate/Hood Support/Middle Hood	70.8	-54.6	0	104413	3159	3384	2161	2.94	3.18	2.5
"	"	10. Inner Side Panel Overlap/Vane Bank/Inner Closure Plate/Inner Cover Plate	-15	-118.9	0	101458	2673	4351	667	3.20	10.29	10

See Table 7a for notes (a)-(e).

Table 9b (cont.). Locations with minimum stress ratios at estimated EPU conditions with frequency shifts. Signal noise is removed using 5% power data. Stress ratios at every node are recorded as the lowest stress ratio identified during the frequency shifts. Stress ratios are grouped according to stress type (maximum – SR-P; or alternating – SR-a) and location (away from a weld or at a weld). Bold text indicates minimum stress ratio of any type on the structure. Locations are depicted in Figure 17.

Stress Ratio	Weld	Location	Location (in.) (a)			node(b)	Stress Intensity (psi)			Stress Ratio		% Freq. Shift
			x	y	z		Pm	Pm+Pb	S_{alt}	SR-P	SR-a	
SR-a	Yes	1. Dam Plate/New Gusset	77	31.4	104.4	92392	323	3327	3174	4.19	2.16	2.5
"	"	2. Old Hood Overlap/Gusset Pad Thin	93.5	58	88.9	92981	345	3765	3140	3.7	2.19	5
"	"	3. Dam Plate/New Gusset	77	58.2	101.4	104386	193	3172	3128	4.39	2.2	5
"	"	4. Dam Plate/New Gusset(e)	77	58.2	104.4	104715	221	3124	3075	4.46	2.23	5
"	"	5. Top Cover Middle Hood/Middle Hood/Tie Bar	-62.5	-25.2	88.9	101376	1212	2949	2802	4.73	2.45	-7.5
"	"	6. Top Cover Middle Hood/Outer Closure Plate/Middle Hood	62.5	85	88.9	102706	3015	3284	2475	3.08	2.78	7.5
"	"	7.Submerged Drain Channel/Skirt(c)	-11.5	118.4	-100.5	104136	894	3778	2286	3.69	3	-10
"	"	8. Middle Base Plate/Hood Support/Middle Hood	70.8	54.6	0	105680	2171	2315	2271	4.28	3.02	2.5
"	"	9. Middle Base Plate/Hood Support/Inner Hood(d)	39.8	-59.8	0	96024	4222	4348	2262	2.2	3.04	5
"	"	10. Top Thick Plate/Dam Plate/Tie Bar/Top Cover Outer Bank	77	-23.2	88.9	93568	1586	2679	2239	5.2	3.07	-10
"	"	11. Middle Closure Plate/Inner Hood	35.8	108.4	38	109095	761	2176	1998	6.41	3.44	10
"	"	12. Dam Plate/New Gusset	77	0	104.4	91724	327	2090	1932	6.67	3.56	0

See Table 7a for notes (a)-(e).

Table 9c. Minimum stress ratios at any frequency shift for the nodes listed in Table 8b computed using the unfiltered EPU loads (i.e., signal noise has *not* been removed). Locations are depicted in Figure 17.

Stress Ratio	Weld	Location	Location (in.) (a)			node(b)	Stress Intensity (psi)			Stress Ratio		% Freq. Shift
			x	y	z		Pm	Pm+Pb	S_{alt}	SR-P	SR-a	
SR-P	No	1. USR/Seismic Block/Support Part	122.1	-10	-9.5	122998	8209	8209	2645	2.06	4.67	7.5
"	"	2. USR part/Support/Support Part	7	122.3	-9.5	123070	7015	7015	1951	2.41	6.34	-2.5
"	"	3. Middle Closure Plate	33.9	108.4	88.9	7238	5684	5987	1397	2.97	8.85	5
"	"	4. Mid Plate/Tie Bar	0	-3	88.9	102956	1020	5798	4944	4.37	2.50	-10
SR-a	No	1. Mid Plate/Tie Bar	0	-3	88.9	102956	1020	5798	4944	4.37	2.50	-10
"	"	2. Mid Plate/Tie Bar	0	-56.8	88.9	99311	1019	4656	3706	5.44	3.34	10
"	"	3. Dam Plate	77	46	104.4	81791	262	2942	2816	8.62	4.39	2.5
SR-P	**Yes**	**1. Top Cover Inner Hood/Middle Closure Plate/Inner Hood**	**31.5**	**108.4**	**88.9**	**100230**	**6376**	**7040**	**1648**	**1.46**	**4.17**	**5**
"	"	2. Top Cover Middle Hood/Outer Closure Plate/Middle Hood	-62.5	85	88.9	100958	4847	5246	2506	1.92	2.74	5
"	"	3. USR/Seismic Block	-122.1	10.3	-9.5	122767	4282	4282	1275	2.17	5.39	-7.5
"	"	4. Middle Base Plate/Hood Support/Inner Hood(d)	39.8	-59.8	0	96024	4380	4521	2506	2.12	2.74	2.5
"	"	5. USR part/Support/Support Part	8.5	122.2	-9.5	123072	4235	4235	911	2.19	7.54	7.5
"	"	6. Splice Bar/USR Part	-2.2	-119	0	123237	4017	4017	541	2.31	12.70	7.5
"	"	7. Submerged Drain Channel/Skirt	91	-76.7	-98.5	97969	386	5394	2028	2.58	3.39	-7.5
"	"	8. Submerged Drain Channel/Skirt(c)	91	-76.7	-100.5	98197	1151	4919	1915	2.83	3.59	7.5
"	"	9. Middle Base Plate/Hood Support/Middle Hood	70.8	-54.6	0	104413	3440	4359	3112	2.70	2.21	5
"	"	10. Inner Side Panel Overlap/Vane Bank/Inner Closure Plate/Inner Cover Plate	-15	-118.9	0	101458	2685	4374	686	3.19	10.01	10

See Table 7a for notes (a)-(e).

Table 9c (cont.). Minimum stress ratios at any frequency shift for the nodes listed in Table 8b computed using the unfiltered EPU loads (i.e., signal noise has *not* been removed). Locations are depicted in Figure 17.

Stress Ratio	Weld	Location	Location (in.) (a)			node(b)	Stress Intensity (psi)			Stress Ratio		% Freq. Shift
			x	y	z		Pm	Pm+Pb	S_{alt}	SR-P	SR-a	
SR-a	Yes	1. Dam Plate/New Gusset	77	31.4	104.4	92392	370	3629	3480	3.84	1.97	2.5
"	"	2. Old Hood Overlap/Gusset Pad Thin	93.5	58	88.9	92981	360	3978	3425	3.50	2.01	5
"	"	3. Dam Plate/New Gusset	77	58.2	101.4	104386	208	3383	3379	4.12	2.03	5
"	"	4. Dam Plate/New Gusset(e)	77	58.2	104.4	104715	242	3332	3331	4.18	2.06	5
"	"	5. Top Cover Middle Hood/Middle Hood/Tie Bar	-62.5	-25.2	88.9	101376	1256	3225	3097	4.32	2.22	-7.5
"	"	6. Top Cover Middle Hood/Outer Closure Plate/Middle Hood	62.5	85	88.9	102706	3198	3508	2681	2.91	2.56	7.5
"	"	7.Submerged Drain Channel/Skirt(c)	-11.5	118.4	-100.5	104136	926	3980	2561	3.50	2.68	-10
"	"	8. Middle Base Plate/Hood Support/Middle Hood	70.8	54.6	0	105680	2492	3027	2993	3.73	2.29	10
"	"	9. Middle Base Plate/Hood Support/Inner Hood(d)	39.8	-59.8	0	96024	4380	4521	2506	2.12	2.74	7.5
"	"	10. Top Thick Plate/Dam Plate/Tie Bar/Top Cover Outer Bank	77	-23.2	88.9	93568	1653	2813	2399	4.96	2.86	-10
"	"	11. Middle Closure Plate/Inner Hood	35.8	108.4	38	109095	773	2271	2086	6.14	3.29	10
"	"	12. Dam Plate/New Gusset	77	0	104.4	91724	353	2272	2075	6.14	3.31	5

See Table 7a for notes (a)-(e).

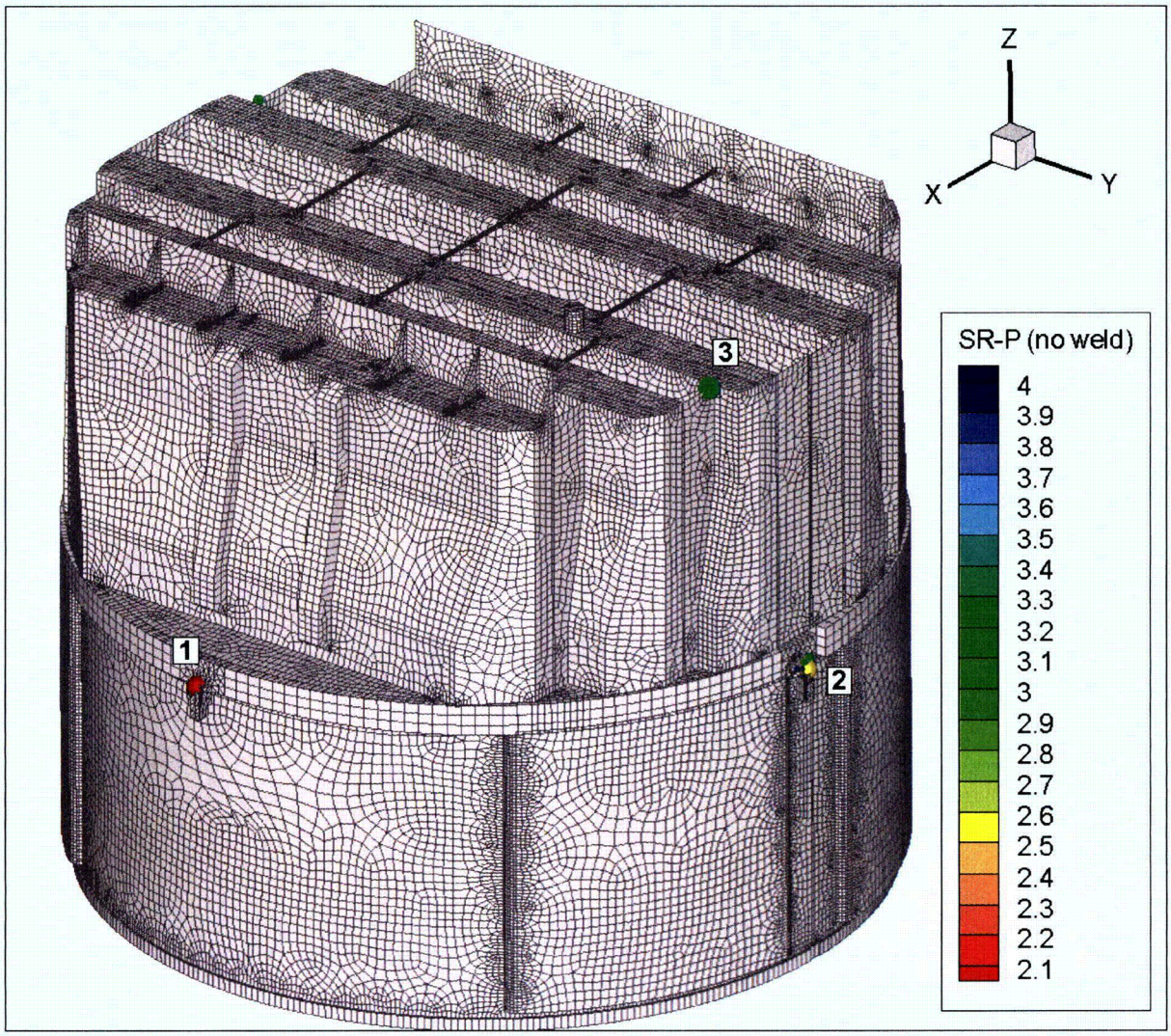

Figure 16a. Locations of smallest maximum stress ratios, SR-P≤4, at non-welds for nominal EPU operation. Numbers refers to the enumerated locations for SR-P values at non-welds in Table 9a.

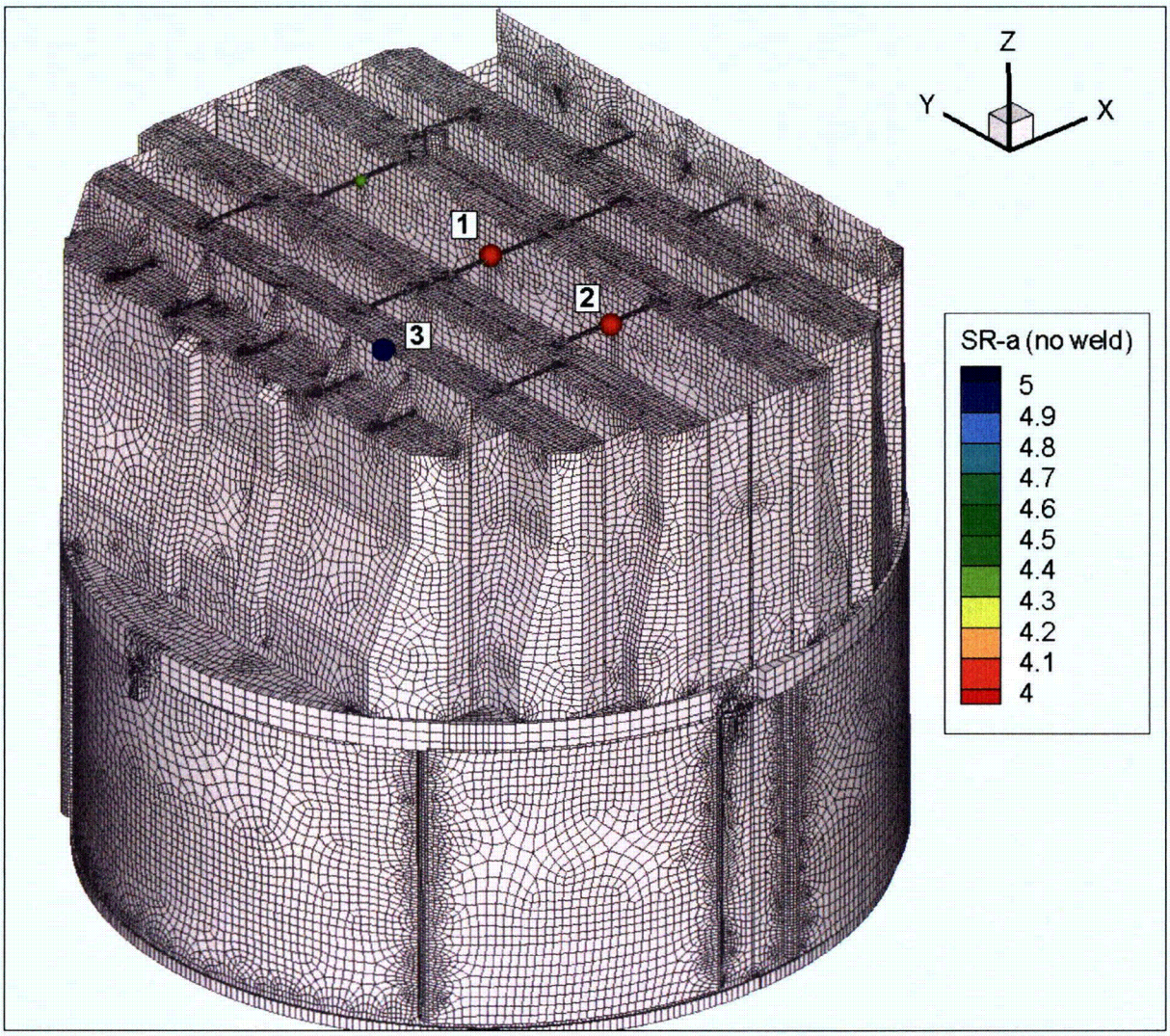

Figure 16b. Locations of smallest alternating stress ratios, SR-a≤5, at non-welds for nominal EPU operation. Numbers refers to the enumerated locations for SR-a values at non-welds in Table 9a.

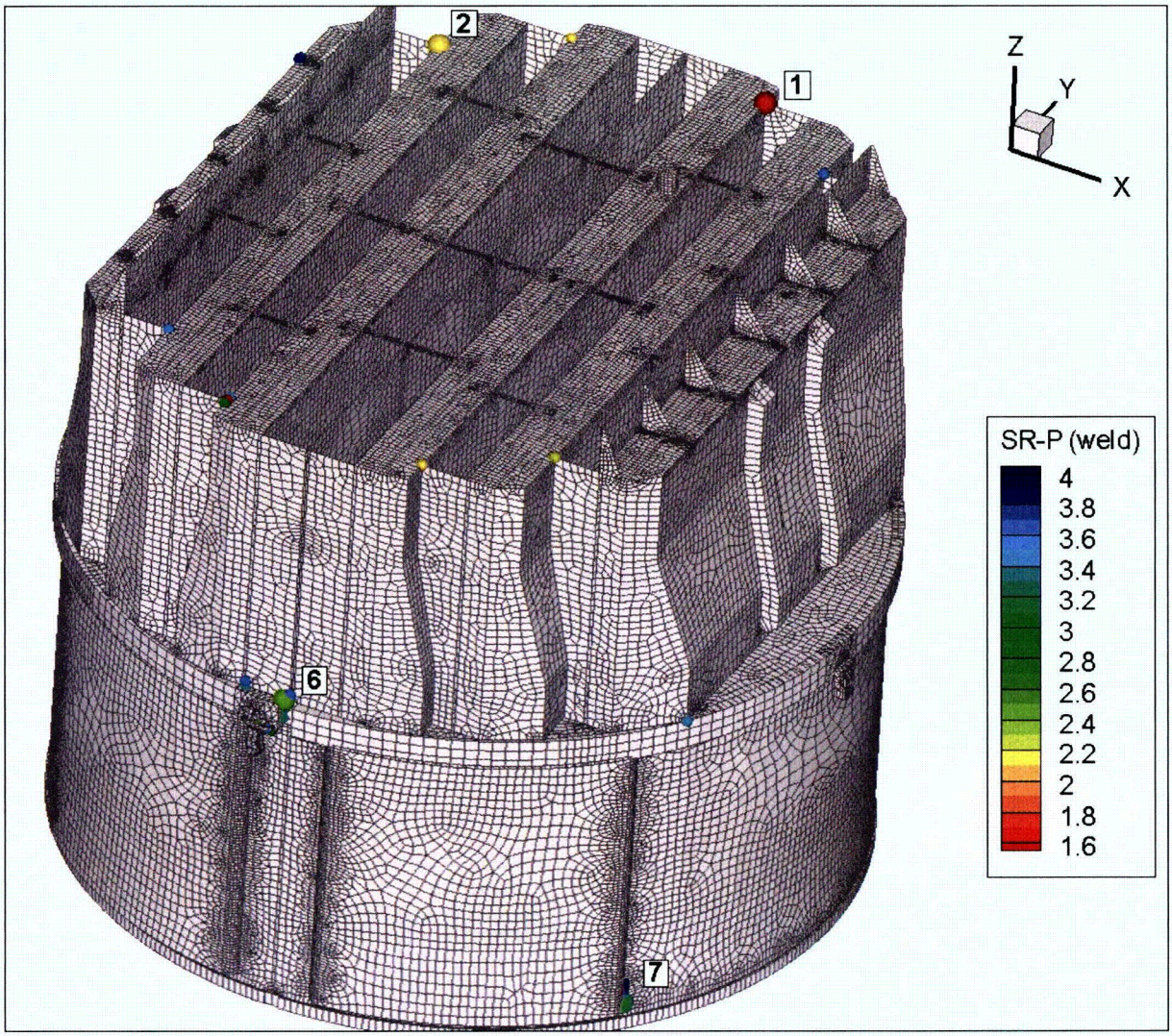

Figure 16c. Locations of smallest maximum stress ratios, SR-P≤4, at welds for nominal EPU operation. Numbers refer to the enumerated locations for SR-P values at welds in Table 9a. First view showing locations 1, 2, 6 and 7.

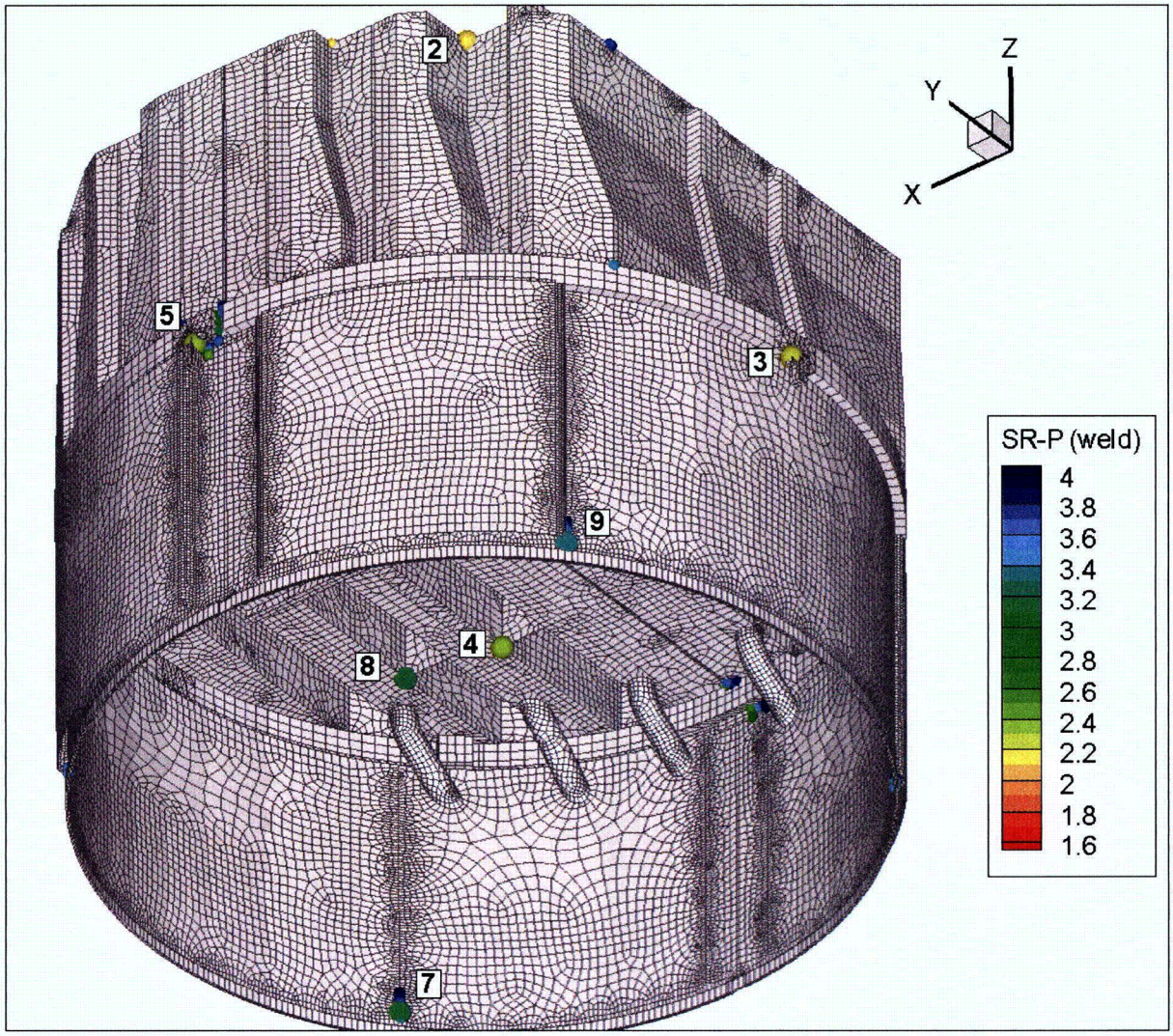

Figure 16d. Locations of smallest maximum stress ratios, SR-P≤4, at welds for nominal EPU operation. Numbers refer to the enumerated locations for SR-P values at welds in Table 9a. Second view showing locations 2-5 and 7-9..

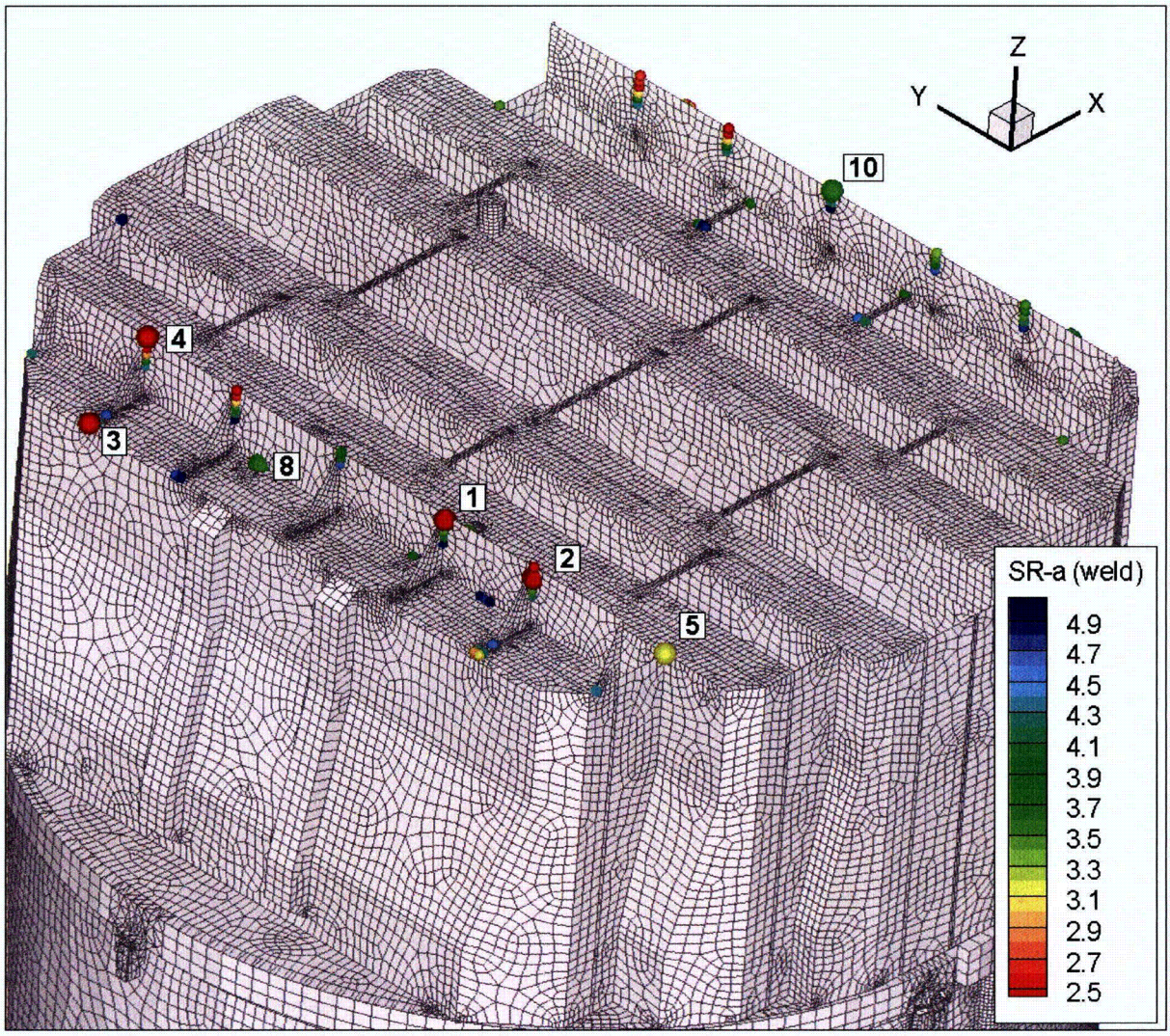

Figure 16e. Locations of minimum alternating stress ratios, SR-a≤5, at welds for nominal EPU operation. Numbers refer to the enumerated locations for SR-a values at welds in Table 9a. First view showing locations 1-5, 8 and 10.

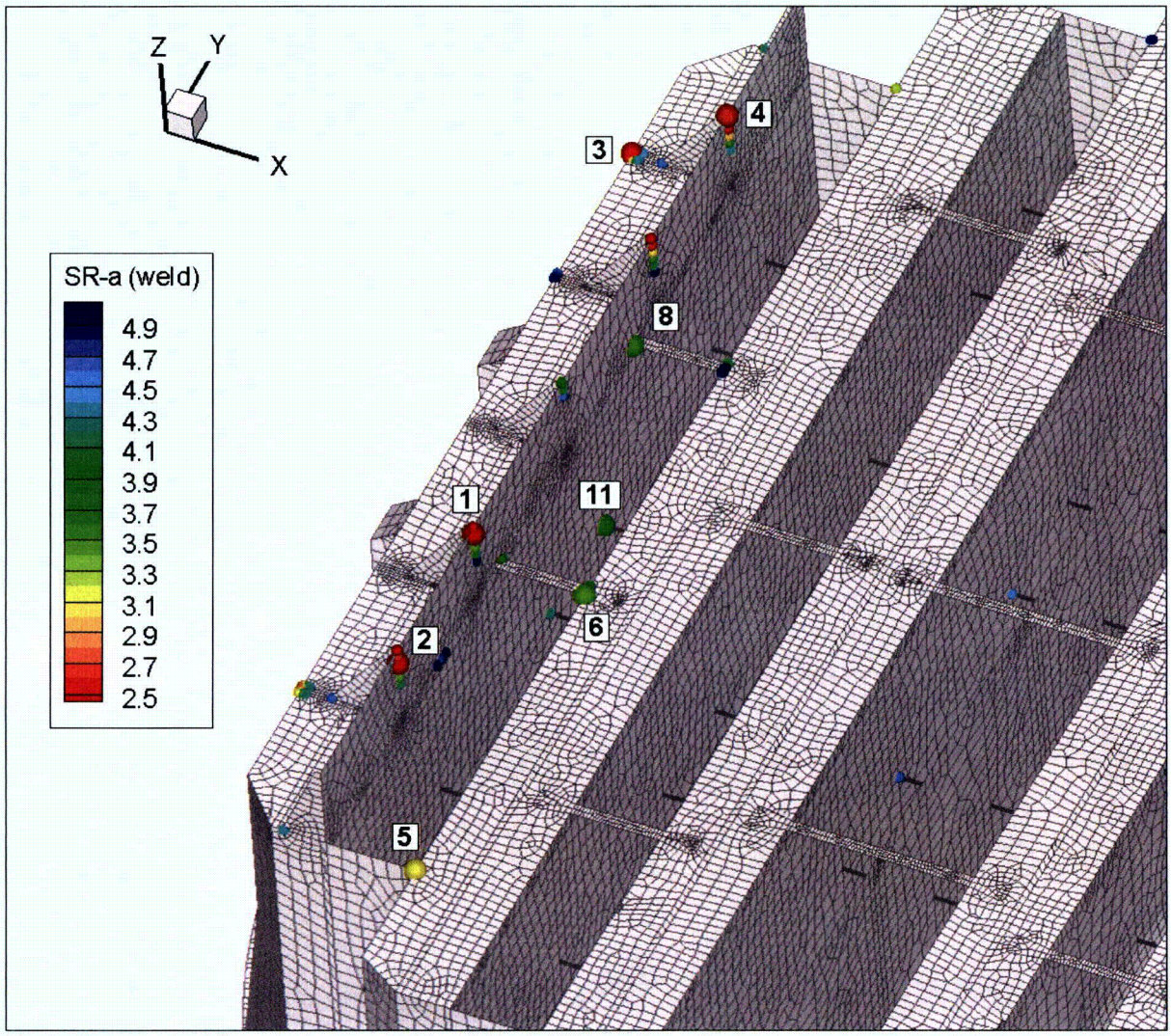

Figure 16f. Locations of minimum alternating stress ratios, SR-a≤5, at welds for nominal EPU operation. Numbers refer to the enumerated locations for SR-a values at welds in Table 9a. Second view showing locations 1-6, 8 and 11.

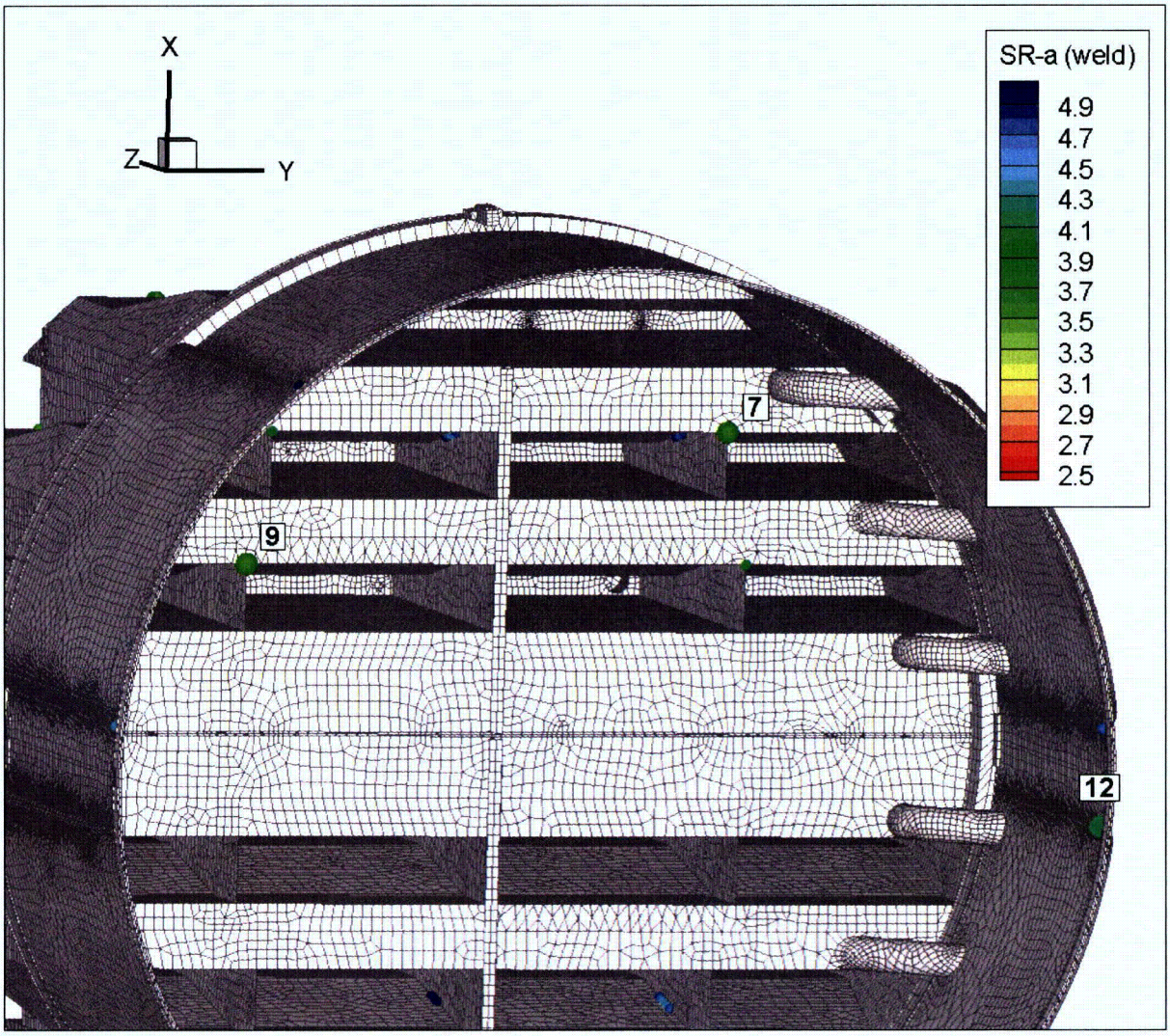

Figure 16g. Locations of minimum alternating stress ratios, SR-a≤5, at welds for nominal EPU operation. Numbers refer to the enumerated locations for SR-a values at welds in Table 9a. Third view showing locations 7, 9 and 12.

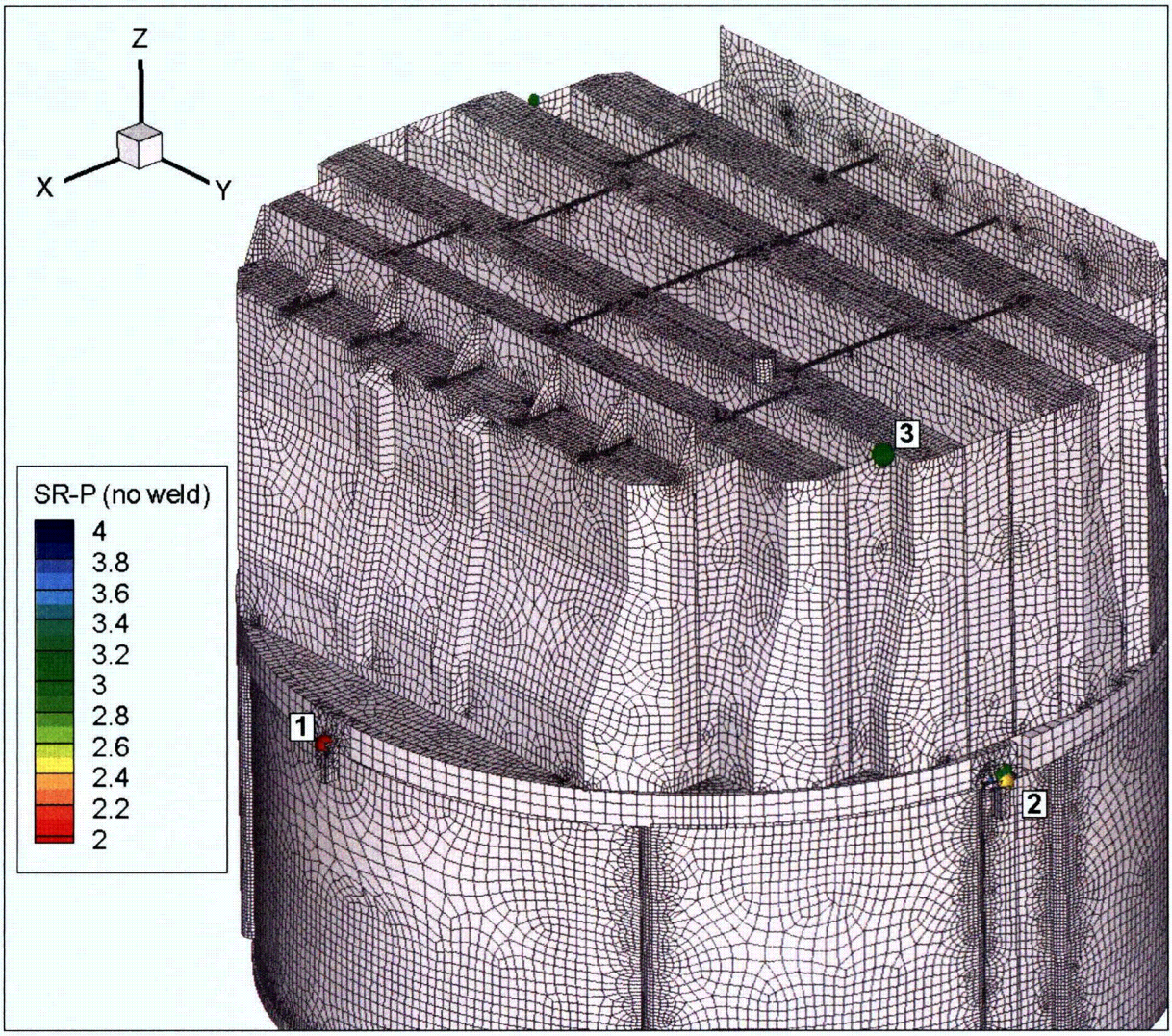

Figure 17a. Locations of minimum stress ratios, SR-P≤4, associated with maximum stress intensities at non-welds for EPU operation with frequency shifts. The recorded stress ratio is the minimum value taken over all frequency shifts. The numbers refers to the enumerated location for SR-P values at non-welds in Table 9b.

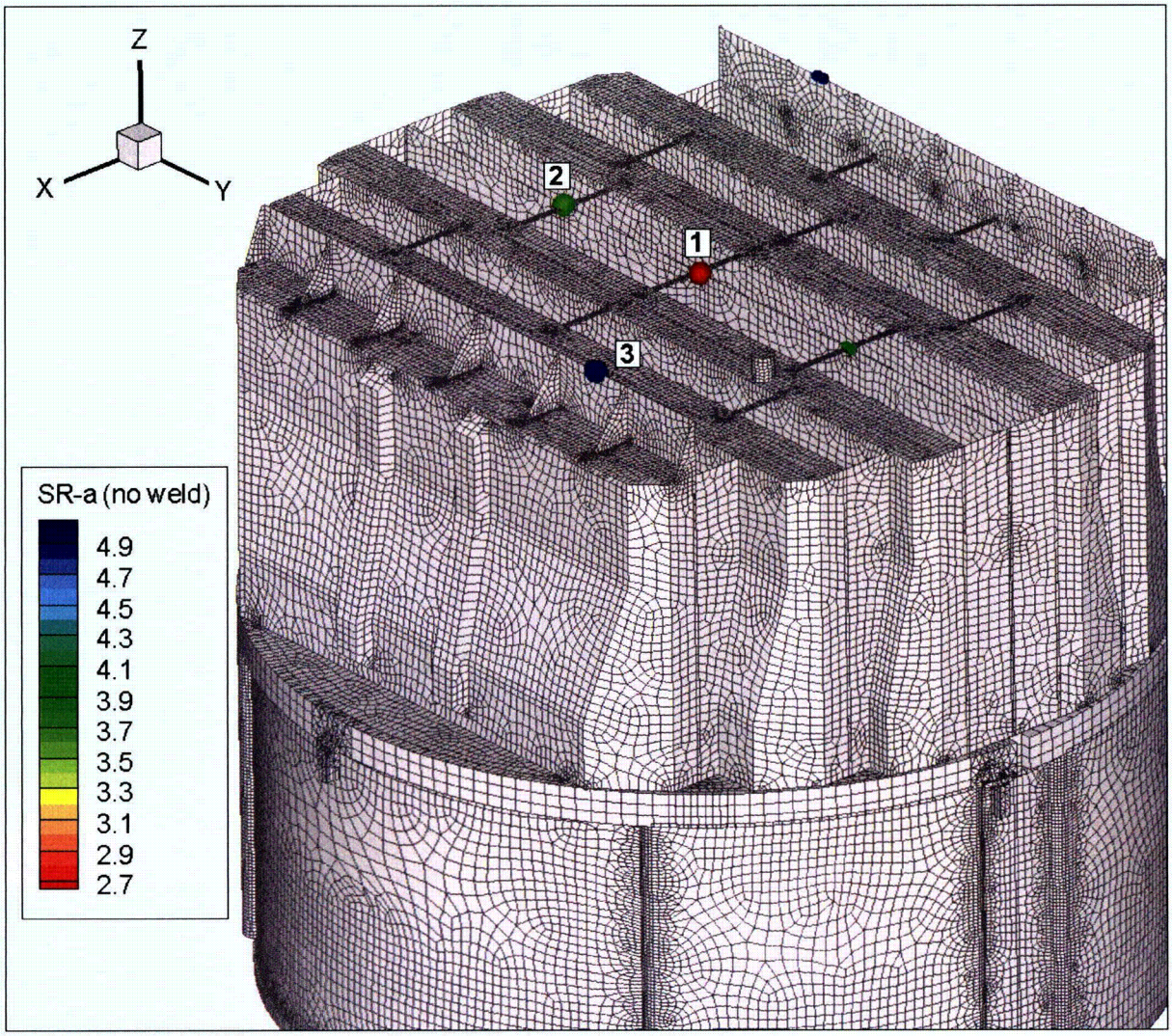

Figure 17b. Locations of smallest alternating stress ratios, SR-a≤5, at non-welds for EPU operation with frequency shifts. The recorded stress ratio is the minimum value taken over all frequency shifts. The numbers refers to the enumerated location for SR-a values at non-welds in Table 9b.

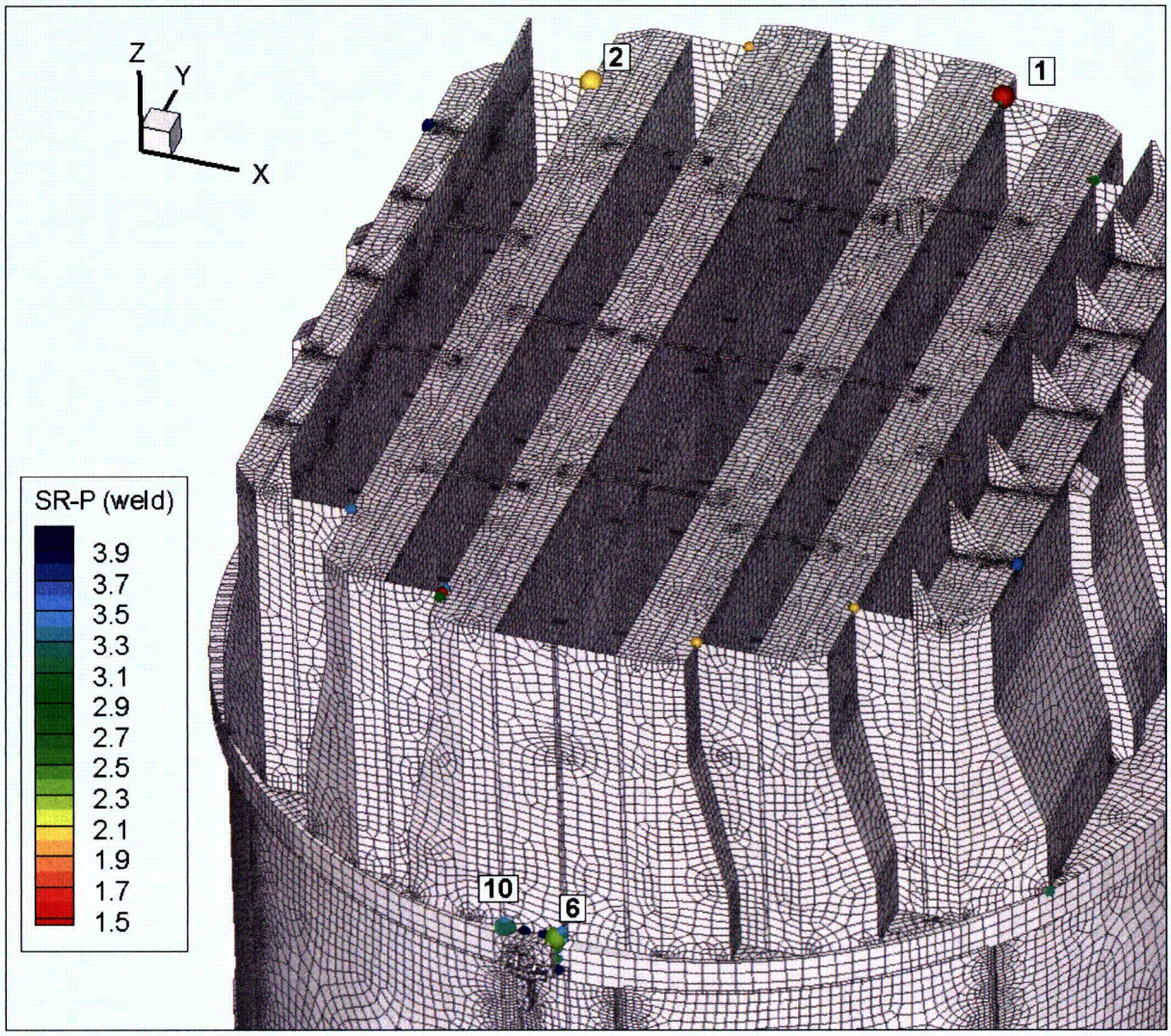

Figure 17c. Locations of minimum stress ratios, SR-P≤4, associated with maximum stress intensities at welds for EPU operation with frequency shifts. The recorded stress ratio at a node is the minimum value taken over all frequency shifts. Numbers refer to the enumerated locations for SR-P values at welds in Table 9b. This view shows locations 1, 2, 6 and 10.

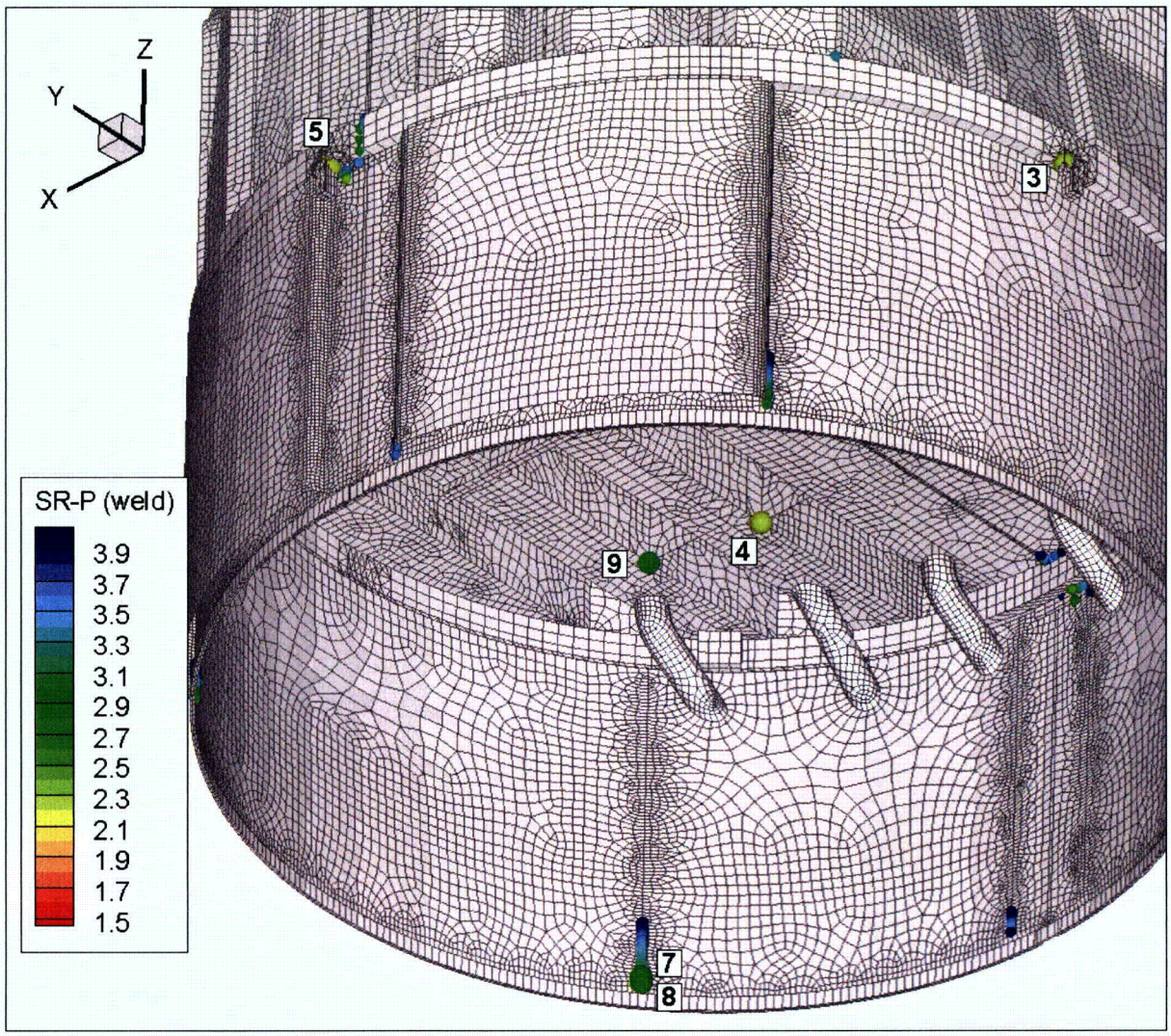

Figure 17d. Locations of minimum stress ratios, SR-P≤4, associated with maximum stress intensities at welds for EPU operation with frequency shifts. The recorded stress ratio at a node is the minimum value taken over all frequency shifts. Numbers refer to the enumerated locations for SR-P values at welds in Table 9b. This view shows locations 3-5 and 7-9.

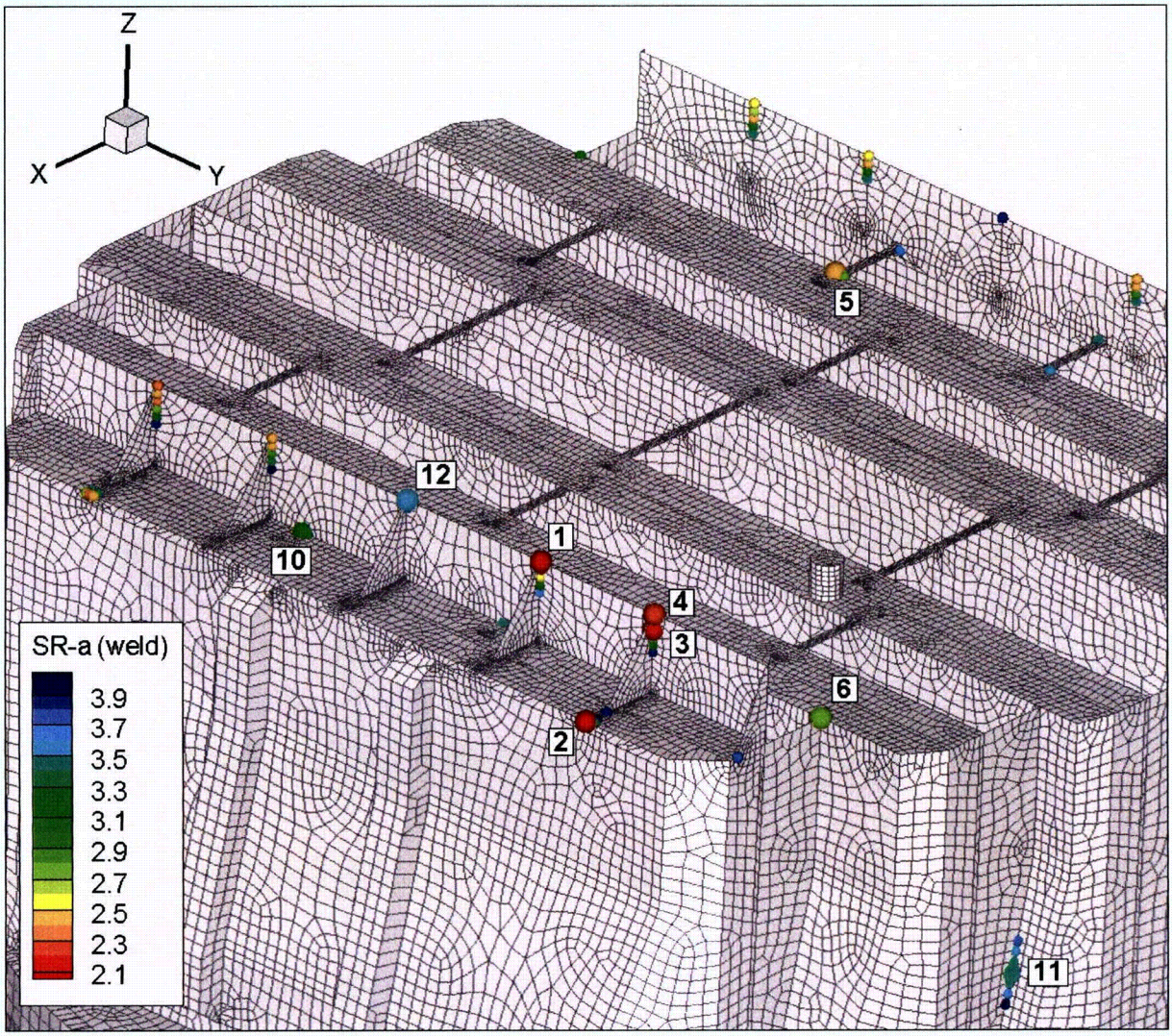

Figure 17e. Locations of minimum alternating stress ratios, SR-a≤4, at welds for EPU operation with frequency shifts. The recorded stress ratio at a node is the minimum value taken over all frequency shifts. Numbers refer to the enumerated locations for SR-a values at welds in Table 9b. This view shows locations 1-6 and 10-12.

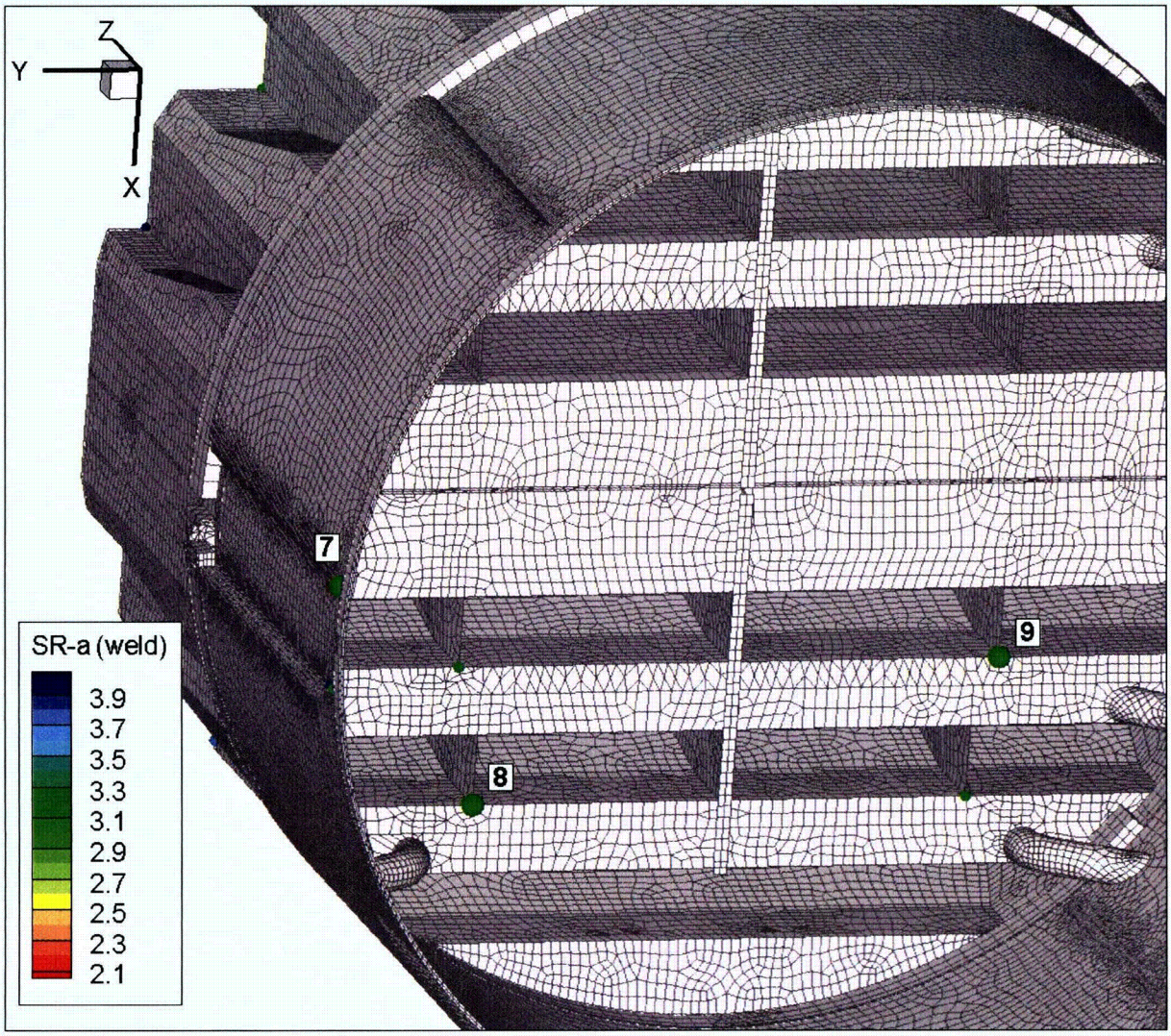

Figure 17f. Locations of minimum alternating stress ratios, SR-a≤4, at welds for EPU operation with frequency shifts. The recorded stress ratio at a node is the minimum value taken over all frequency shifts. Numbers refer to the enumerated locations for SR-a values at welds in Table 9b. This view shows locations 7-9.

6.2 Frequency Content at EPU

The same nodes whose frequency content was examined in Section 5.3 are considered here. At EPU these nodes reappear in Table 9b as the first or limiting (node 92392), third (node 104386), fifth (node 101376) and seventh (node 104136) entries in the list of lowest alternating stress ratio locations. The stress PSDs and accumulative stress PSDs are reported in Figure 18 in the same order as in Section 5.3 to facilitate comparison between the plots at CLTP and EPU.

After one accounts for the overall velocity ratio-based scaling of 1.35 (which corresponds to a factor of 1.35^2=1.82 scaling in PSDs) the stress PSDs and accumulative PSDs at CLTP and EPU conditions are very similar. This is clearly the case for the first node 101376 which was limiting at CLTP. Moreover, its alternating stress ratio at EPU is SR-a=2.45 which is close to the value expected from scaling the CLTP value, SR-a=3.39/1.35=2.51. For the second node 92392 which is limiting at EPU, the curves at CLTP and EPU are still similar, but the increase over the 109-113 Hz range is higher than the velocity ratio scaling, 1.35. Hence the increase in the peak in the stress PSD is also higher. This is ultimately reflected in the change in stress ratio from SR-a=3.74 at CLTP to SR-a=2.16 at EPU which corresponds to an increase in alternating stress intensity of 73% rather than the 35% increase resulting from a pure velocity-based scaling. Similar observations apply to the third node 104386 which also involves the steam dam. Finally, for the last node considered, node 104136 on the skirt/drain channel junction, the dominant peak lies outside the 109-113 Hz range. The alternating stress intensity at this node increases by 35% when proceeding from CLTP to EPU which is consistent with the velocity-based scaling. The PSD curve also scales by this amount except in the 109-113 Hz range where the PSD scaling are different, but, as it turns out, inconsequential with regard to the overall stress ratio.

Overall it appears that the steam dam is the component that is responsive to the 109-113 Hz signal and hence becomes the alternating stress leader at the EPU condition. The skirt and tie bars continue to be dominated by lower frequency contributions.

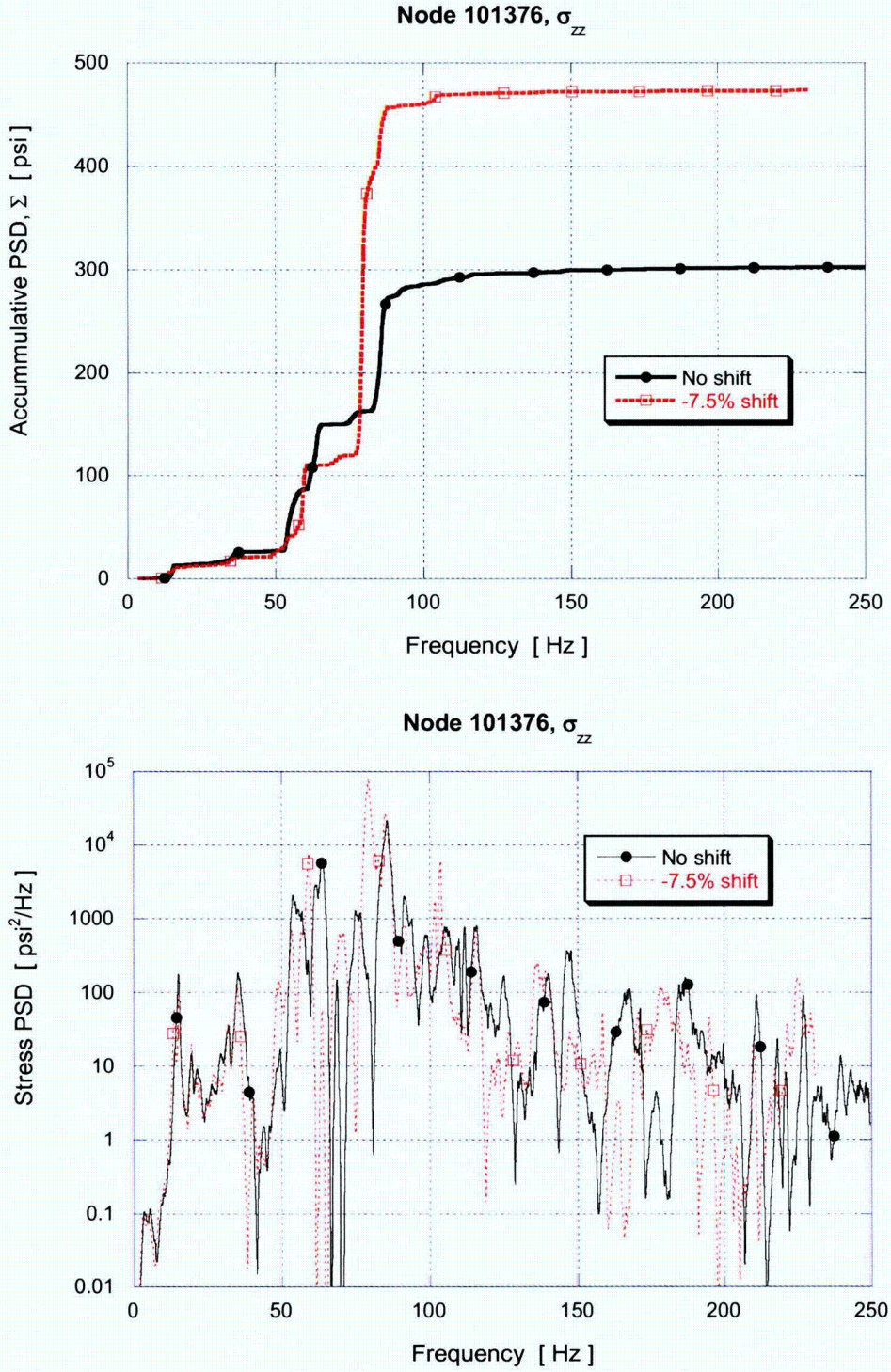

Figure 18a. Accumulative PSD and PSD of the σ_{ZZ} stress response at node 101376 at EPU.

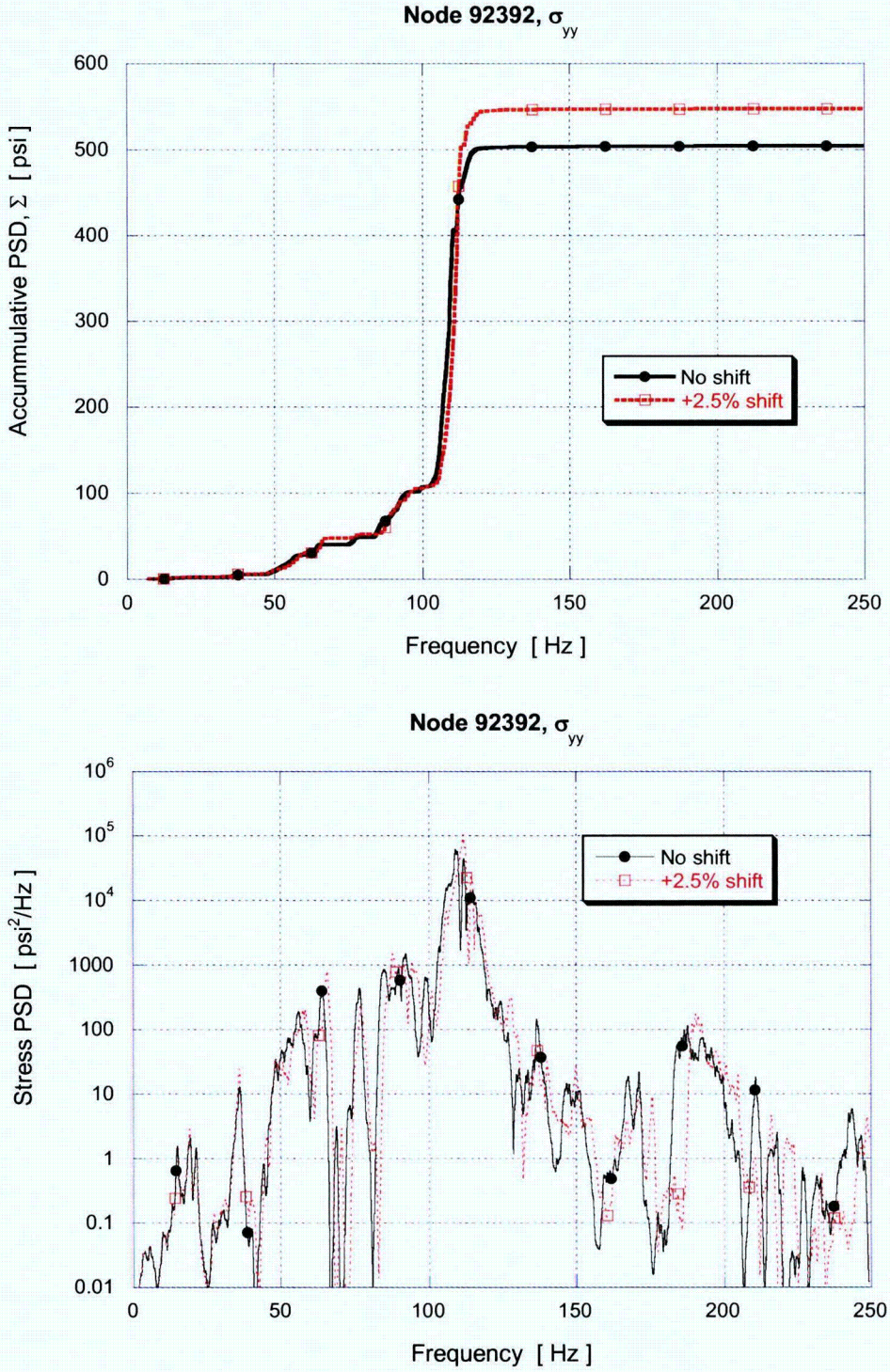

Figure 18b. Accumulative PSD and PSD of the σ_{yy} stress response at node 92392 at EPU.

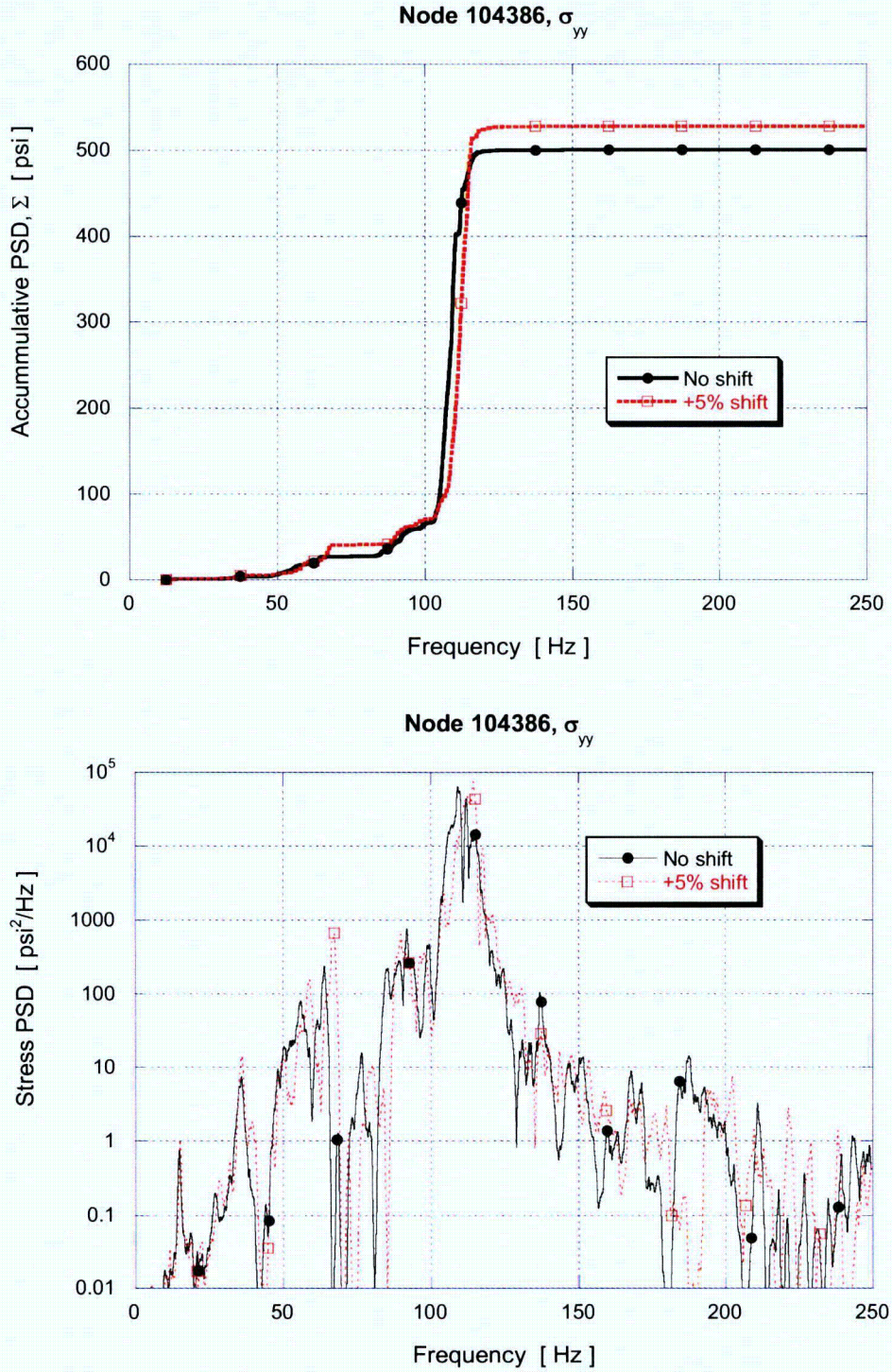

Figure 18c. Accumulative PSD and PSD of the σ_{yy} stress response at node 104386 at EPU.

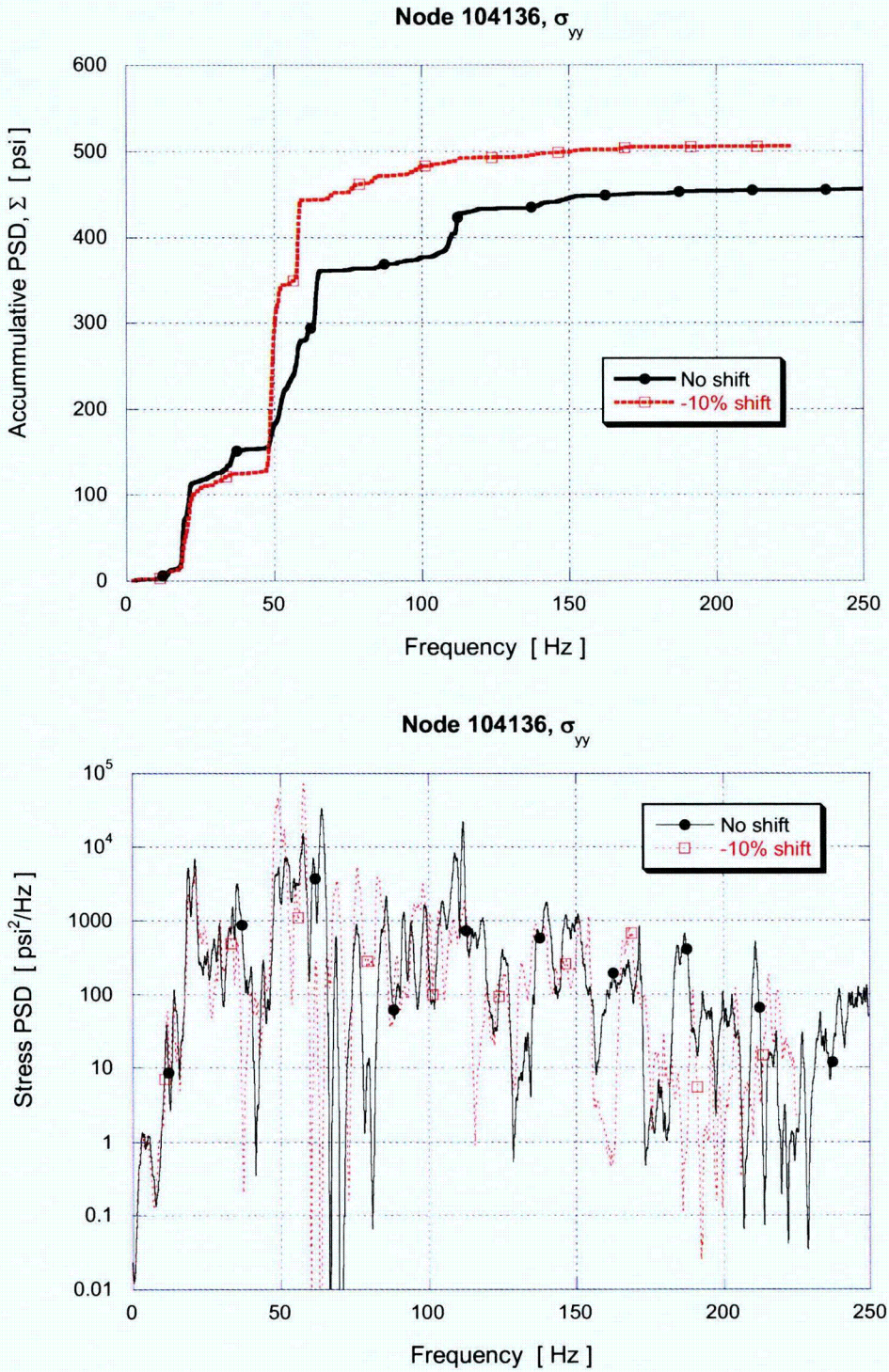

Figure 18d. Accumulative PSD and PSD of the σ_{yy} stress response at node 104136 at EPU.

7. Conclusions

A frequency-based steam dryer stress analysis has been used to calculate high stress locations and calculated / allowable stress ratios for the Browns Ferry Unit 2 steam dryer at CLTP load conditions using plant measurement data. A detailed description of the frequency-based methodology and the finite element model for the BFN2 steam dryer is presented. The CLTP loads obtained in a separate acoustic circuit model [2,3,7], including end-to-end bias and uncertainty for both the ACM and FEA, were applied to a finite element model of the steam dryer consisting mainly of the ANSYS Shell 63 elements, brick continuum elements, and beam elements. The resulting stress histories were analyzed to obtain maximum and alternating stresses at all nodes for comparison against allowable levels.

The CLTP loads are applied with compensation for background noise based on 1000# data taken at 5% power. These results are tabulated in Table 8 of this report. The minimum alternating stress ratio at nominal operation is SR-a=4.16 and the minimum alternating stress ratio taken over all frequency shifts is SR-a=3.39. The stress ratios corresponding to maximum stresses are SR-P=1.68 at nominal operation and 1.60 when all frequency shifts are considered. The results show that the new tie-bars with widened and tapered ends, and the thicker 1 in hood with external channel reinforcements replacing the interior hood supports result in significantly lower stresses.

On the basis of these CLTP plant loads, the dynamic analysis of the steam dryer shows that the combined acoustic, hydrodynamic, and gravity loads produces the following minimum stress ratios.

Frequency Shift	Minimum Stress Ratio at CLTP	
	Max. Stress, SR-P	Alternating Stress, SR-a
0% (nominal)	1.68	4.16
-10%	1.67	3.77
-7.5%	1.67	3.39
-5%	1.66	3.69
-2.5%	1.66	4.00
+2.5%	1.62	3.74
+5%	1.60	3.95
+7.5%	1.64	4.27
+10%	1.61	4.35
All shifts	1.60 – 1.68	3.39 – 4.35
Limiting	**1.60**	**3.39**

EPU stresses are estimated using two methods. The first scales the CLTP stresses by the square of the steam flow velocity ratio, $(U_{EPU}/U_{CLTP})^2=1.35$. The second method utilizes the bump up factors developed in [4] over the 100-120 Hz frequency interval and the velocity scaling (1.35) at all other frequencies. The limiting stress ratios using these methods are

summarized for each frequency shift in the table below. The limiting alternating stress ratios at any frequency shift are: 2.51 with velocity scaling (Method 1) and 2.16 when bump up factors are used over the 100-120 Hz range (Method 2). In all cases the alternating stress ratio remains above 2.0, thus qualifying the steam dryer for EPU operation with regard to stress evaluation.

Frequency Shift	Method 1	Method 2	
	Alt. Stress, SR-a	Max. Stress, SR-P	Alt. Stress, SR-a
0% (nominal)	3.08	1.60	2.50
-10%	2.80	1.59	2.78
-7.5%	2.51	1.59	2.45
-5%	2.73	1.59	2.67
-2.5%	2.97	1.57	2.88
+2.5%	2.77	1.52	2.16
+5%	2.93	1.50	2.19
+7.5%	3.16	1.55	2.69
+10%	3.22	1.53	3.01
All shifts	2.51 – 3.22	1.50 – 1.60	2.16 – 3.01
Limiting	**2.51**	**1.50**	**2.16**

8. References

1. Continuum Dynamics, Inc. (2008). "Stress Assessment of Browns Ferry Nuclear Unit 1 Steam Dryer with Tie-Bar Modifications, Rev. 2" C.D.I. Report No. 08-15P (Proprietary).

2. Continuum Dynamics, Inc. (2005). "Methodology to Determine Unsteady Pressure Loading on Components in Reactor Steam Domes (Rev. 6)." C.D.I. Report No. 04-09 (Proprietary).

3. Continuum Dynamics, Inc. (2008). "Acoustic and Low Frequency Hydrodynamic Loads at CLTP Power Level on Browns Ferry Nuclear Unit 2 Steam Dryer to 250 Hz with Noise Removed, Rev. 1" C.D.I. Report No. 08-05P (Proprietary).

4. Continuum Dynamics, Inc. (2008). "Flow-Induced Vibration in the Main Steam Lines at Browns Ferry Nuclear Units 1 and 2, With and Without Acoustic Side Branches, and Resulting Steam Dryer Loads," C.D.I. Report No. 08-14P (Proprietary).

5. Continuum Dynamics, Inc. (2008). "Stress Assessment of Browns Ferry Nuclear Unit 2 Steam Dryer, Rev. 1," C.D.I. Report No. 08-07P (Proprietary).

6. Continuum Dynamics, Inc. (2008). "Stress Assessments of Browns Ferry Nuclear Unit 2 Steam Dryer with Tie Bar and Hood Modifications, Rev. 0" C.D.I. Report No. 08-16P (Proprietary).

7. Continuum Dynamics, Inc. (2007). "Methodology to Predict Full Scale Steam Dryer Loads from In-Plant Measurements, with the Inclusion of a Low Frequency Hydrodynamic Contribution," C.D.I. Report No. 07-09P (Proprietary).

8. Structural Integrity Associates, Inc. (2006). "Main Steam Line 100% CLTP Strain Data Transmission." SIA Letter Report No. GSZ-06-017

9. ANSYS Release 10.0. URL http://www.ansys.com. Documentation: ANSYS 10.0 Complete User's Manual Set.

10. Continuum Dynamics, Inc. (2007). Response to NRC Request for Additional Information on the Hope Creek Generating Station, Extended Power Uprate, RAI No. 14.110

11. Continuum Dynamics, Inc. (2008). "Stress Assessment of Browns Ferry Nuclear Unit 1 Steam Dryer, Rev. 0," C.D.I. Report No. 08-06P (Proprietary).

12. Press, W. H., S. A. Teukolsky, et al. (1992). *Numerical Recipes*, Cambridge University Press.

13. O'Donnell W.J. (1973). "Effective Elastic Constants For the Bending of Thin Perforated Plates With Triangular and Square Penetration Patterns," ASME Journal of Engineering for Industry, Vol. 95, pp. 121-128.

14. Idel'chik, I E. and Fried, E. (1989). *Flow Resistance, a Design Guide for Engineers*, Taylor & Francis, Washington D.C., p 260.

15. DeSanto, D.F. (1981). "Added Mass and Hydrodynamic Damping of Perforated Plates Vibrating in Water," Journal of Pressure Vessel Technology, Vol. 103, p. 176-182.

16. Continuum Dynamics, Inc. (2007). "Dynamics of BWR Steam Dryer Components," C.D.I. Report No. 07-11P

17. U.S. Nuclear Regulatory Commission, (2007). Regulatory Guide 1.20 "Comprehensive Vibration Assessment Program for Reactor Internals During Preoperational and Initial Startup Testing," March 2007.

18. WRC Bulletin 432 (1998). "Fatigue Strength Reduction and Stress Concentration Factors For Welds In Pressure Vessels and Piping," WRC, NY, p.32

19. Pilkey W.D. (1997). *Peterson's Stress Concentration Factors*, 2nd ed., John Wiley, NY, p.139.

20. Lawrence F.V., Ho N.-J., Mazumdar P.K. (1981). "Predicting the Fatigue Resistance of Welds," Ann. Rev. Mater. Sci., vol. 11, pp. 401-425.

21. General Electric (GE) Nuclear Energy (2003). Supplement 1 to Service Information Letter (SIL) 644, "BWR/3 Steam Dryer Failure," September 5, 2003.

22. Tecplot 10 (2004). URL: http://www.tecplot.com. Documentation: *Tecplot* User's Manual Version 10 Tecplot, Inc. Bellevue, Washington October.

23. Structural Integrity Associates Calculation Package, 0006982.301, "Shell and Solid Sub-Model Finite Element Stress Comparison, Rev. 2" Oct. 17, 2008.

24. Continuum Dynamics, Inc., Response to NRC RAI EMCB 172, June 2008.

Appendix A. Submodel Analysis of Steam Dam / Gusset Junction Weld

[[

(3)]]

[[

(3)]]

[[

(3)]]

[[

(3)]]

[[

(3)]]

[[

(3)]]

[[

(3)]]

[[

(3)]]

[[

(3)]]

[[

(3)]]

[[

(3)]]

[[[3]]]

[[

[3]]]

[[

(3)]]

[[

(3)]]

[[

(3)]]

ENCLOSURE 5

TENNESSEE VALLEY AUTHORITY
BROWNS FERRY NUCLEAR PLANT (BFN)
UNITS 1, 2, AND 3

TECHNICAL SPECIFICATIONS (TS) CHANGES TS-431 AND TS-418
EXTENDED POWER UPRATE (EPU)

CDI AFFIDAVIT

Attached is the CDI affidavit for the proprietary information contained in Enclosures 1 and 2.

Continuum Dynamics, Inc.

(609) 538-0444 (609) 538-0464 fax 34 Lexington Avenue Ewing, NJ 08618-2302

AFFIDAVIT

Re: BROWNS FERRY NUCLEAR PLANT (BFN) – UNITS 1, 2, AND 3 – TECHNICAL SPECIFICATIONS (TS) CHANGES TS-418 AND TS-431 – EXTENDED POWER UPRATE (EPU) – SUPPLEMENTAL RESPONSE TO ROUNDS 19 AND 22 REQUEST FOR ADDITIONAL INFORMATION (RAI) REGARDING STEAM DRYERS (TAC NOS. MD5262, MD5263, AND MD5264); AND C.D.I. REPORT 08-20P "STRESS ASSESSMENT OF BROWNS FERRY NUCLEAR UNIT 2 STEAM DRYER WITH OUTER HOOD AND TIE-BAR REINFORCEMENTS," REVISION 0

I, Alan J. Bilanin, being duly sworn, depose and state as follows:

1. I hold the position of President and Senior Associate of Continuum Dynamics, Inc. (hereinafter referred to as C.D.I.), and I am authorized to make the request for withholding from Public Record the Information contained in the documents described in Paragraph 2. This Affidavit is submitted to the Nuclear Regulatory Commission (NRC) pursuant to 10 CFR 2.390(a)(4) based on the fact that the attached information consists of trade secret(s) of C.D.I. and that the NRC will receive the information from C.D.I. under privilege and in confidence.

2. The Information sought to be withheld, as transmitted to TVA Browns Ferry as attachment to C.D.I. Letter No. 08207 dated 14 November 2008, BROWNS FERRY NUCLEAR PLANT (BFN) – UNITS 1, 2, AND 3 – TECHNICAL SPECIFICATIONS (TS) CHANGES TS-418 AND TS-431 – EXTENDED POWER UPRATE (EPU) – SUPPLEMENTAL RESPONSE TO ROUNDS 19 AND 22 REQUEST FOR ADDITIONAL INFORMATION (RAI) REGARDING STEAM DRYERS (TAC NOS. MD5262, MD5263, AND MD5264); AND C.D.I. REPORT 08-20P "STRESS ASSESSMENT OF BROWNS FERRY NUCLEAR UNIT 2 STEAM DRYER WITH OUTER HOOD AND TIE-BAR REINFORCEMENTS," REVISION 0

3. The Information summarizes:

   (a) a process or method, including supporting data and analysis, where prevention of its use by C.D.I.'s competitors without license from C.D.I. constitutes a competitive advantage over other companies;

(b) Information which, if used by a competitor, would reduce his expenditure of resources or improve his competitive position in the design, manufacture, shipment, installation, assurance of quality, or licensing of a similar product;
(c) Information which discloses patentable subject matter for which it may be desirable to obtain patent protection.

The information sought to be withheld is considered to be proprietary for the reasons set forth in paragraphs 3(a), 3(b) and 3(c) above.

4. The Information has been held in confidence by C.D.I., its owner. The Information has consistently been held in confidence by C.D.I. and no public disclosure has been made and it is not available to the public. All disclosures to third parties, which have been limited, have been made pursuant to the terms and conditions contained in C.D.I.'s Nondisclosure Secrecy Agreement which must be fully executed prior to disclosure.

5. The Information is a type customarily held in confidence by C.D.I. and there is a rational basis therefore. The Information is a type, which C.D.I. considers trade secret and is held in confidence by C.D.I. because it constitutes a source of competitive advantage in the competition and performance of such work in the industry. Public disclosure of the Information is likely to cause substantial harm to C.D.I.'s competitive position and foreclose or reduce the availability of profit-making opportunities.

I declare under penalty of perjury that the foregoing affidavit and the matters stated therein are true and correct to be the best of my knowledge, information and belief.

Executed on this 14 day of NOVEMBER 2008.

Alan J. Bilanin
Continuum Dynamics, Inc.

Subscribed and sworn before me this day: November 14, 2008

Eileen P. Burmeister, Notary Public

EILEEN P. BURMEISTER
NOTARY PUBLIC OF NEW JERSEY
MY COMM. EXPIRES MAY 6, 2012